AFRL-AFOSR-VA-TR-2022-0070

Composite Soft Materials with Decentralized and Distributed Actuation

Mirkin, Chad
NORTHWESTERN UNIVERSITY
633 CLARK
EVANSTON, IL, 60208
USA

01/07/2022
Final Technical Report

Air Force Research Laboratory
Air Force Office of Scientific Research
Arlington, Virginia 22203
Air Force Materiel Command

REPORT DOCUMENTATION PAGE

PLEASE DO NOT RETURN YOUR FORM TO THE ABOVE ORGANIZATION.

1. REPORT DATE	2. REPORT TYPE	3. DATES COVERED	
20220107	Final	START DATE 20180915	END DATE 20210914

4. TITLE AND SUBTITLE
Composite Soft Materials with Decentralized and Distributed Actuation

5a. CONTRACT NUMBER	5b. GRANT NUMBER	5c. PROGRAM ELEMENT NUMBER
	FA9550-18-1-0493	
5d. PROJECT NUMBER	**5e. TASK NUMBER**	**5f. WORK UNIT NUMBER**

6. AUTHOR(S)
Chad Mirkin

7. PERFORMING ORGANIZATION NAME(S) AND ADDRESS(ES)
NORTHWESTERN UNIVERSITY
633 CLARK
EVANSTON, IL 60208
USA

8. PERFORMING ORGANIZATION REPORT NUMBER

9. SPONSORING/MONITORING AGENCY NAME(S) AND ADDRESS(ES)	10. SPONSOR/MONITOR'S ACRONYM(S)	11. SPONSOR/MONITOR'S REPORT NUMBER(S)
Air Force Office of Scientific Research 875 N. Randolph St. Room 3112 Arlington, VA 22203	AFRL/AFOSR RTB2	AFRL-AFOSR-VA-TR-2022-0070

12. DISTRIBUTION/AVAILABILITY STATEMENT
A Distribution Unlimited: PB Public Release

13. SUPPLEMENTARY NOTES

14. ABSTRACT
A long-standing goal of the nanoscience and nanoengineering communities is to actualize the ability to construct arbitrarily complex 2D and 3D ‘smart’ architectures with chemical and physical functionalities encoded directly into the materials at the micro- to nanoscale. In this project, Northwestern University (Mirkin Group) and TERA-print, LLC worked together to bring the prospect of engineering 3D nanostructures with limitless functionalization possibilities into reality. Beam pen lithography (BPL), invented in the Mirkin Group and commercialized by TERA-print, is uniquely positioned to engineer 3D functional materials with decentralized, spatially distributed actuation and control. BPL delivers structured and highly focused light to a substrate via a massively parallel array of pyramidal-shaped microprobes with nanoscopic apertures to enable the rapid generation of arbitrary patterns with diffraction unlimited, sub-300-nm resolution over the mesoscopic length scale. The simultaneous development of actuatable soft materials responsive to light and engineering solutions that allow BPL to act on such soft materials under all requisite environmental and thermodynamics states would, when combined, extend the limits of how complicated a 3D nanostructures shape can become and allow for the full scope of desired functionalities. The advances made by both teams over the last three years have brought the goal of facile printing of 2D and 3D ‘smart’ nanostructures with precisely controlled spatiotemporal functionalities much closer to reality. By combining a microfluidics BPL platform with environmental controls and fundamental research into soft material properties, the future scope of soft materials nano-engineering will expand for the development of novel mechanical and chemical interfaces with living tissues, smart materials with adaptable optical and electronic properties, and sensing devices.

15. SUBJECT TERMS

16. SECURITY CLASSIFICATION OF:			17. LIMITATION OF ABSTRACT	18. NUMBER OF PAGES
a. REPORT U	b. ABSTRACT U	c. THIS PAGE U	UU	30

19a. NAME OF RESPONSIBLE PERSON	19b. PHONE NUMBER *(Include area code)*
KATIE WISECARVER	426-9544

Cover Page
To: Dr. Samuel Stanton, samuel.c.stanton2.civ@mail.mil; Ms. Katie Wisecarver, katie.wisecarver@us.af.mil
Subject: Final Report
Contract/Grant Title: Composite Soft Materials with Decentralized and Distributed Actuation
Contract/Grant #: FA9550-18-1-0493
Reporting Period: 9/15/2018-9/14/2021

ACCOMPLISHMENTS

Research objectives:

Research Focus Area 1

- Synthesis and Characterization of Responsive and Actuatable Composite Hydrogels
- Synthesis and Photo-degradable/-Crosslinkable-Nucleic Acids Bonds in Hydrogels
- Examining Responsiveness of Hydrogels

Research Focus Area 2

- Development of a Nanofabrication Strategy to Rapidly Modify Local Physicochemical Properties and Functionality of Hydrogels under Controlled Environments
- Controlled Environment Capabilities
- Near-UV BPL Capabilities

Research Focus Area 3

- Design and Synthesis of Hydrogels with Distributed Actuation and Sensing
- Uni-layer Composite Systems with Distributed Properties
- Multi-layer Composite System with Distributed Properties
- Design of Actuatable Systems

Details of accomplishments:

Over the last three years, the Northwestern University (NU) team has 1) developed a post-polymerization functionalization method of tethering oligonucleotides to hydrogels, 2) evaluated a photocurable polymeric system which was subsequently utilized to build 2D architectures with submicron precision using BPL, and 3) fundamental studies to investigate the properties (i.e., mechanical behavior, biocompatibility) of the photocured material and its application in functional small molecule surface writing was explored. Additionally, BPL was combined with cross-linking photopolymerization and thiol-acrylate coupling chemistry to print biomolecule microarrays with ultrahigh resolution. By taking advantage of the rapid photo-induced polymerization reaction of multifunctional acrylates with thiol-modified target molecules, the NU and TERA-print teams were able to apply the fundamental advantage of BPL (ultrahigh print resolution and precision over a large printing area) to create finely controlled cross-linked polymer matrices with well-calibrated feature positions, heights, and diameters, which were incubated with proteins post-polymerization to create the final biomolecule microarray product.

Simultaneously, the TERA-print team developed and implemented elegant solutions to enable BPL printing of hydrogels under well controlled environmental and thermodynamic states. Specifically, TERA-print 1) developed and integrated environmental control systems to adjust temperature and relative humidity within the sample chamber, providing a method to finely control the hydration and gelation/physiochemical state of hydrogels during the patterning process; 2) designed and prototyped a microfluidics system to enable rapid exchange of reagents within the experimental chamber, enabling the printing of spatially distributed, disparate functionalities into soft materials; 3) demonstrated the successful use of the microfluidics system by exchanging hydrogel solutions in the experimental chamber in real-time to enable the construction of multi-material architectures while maintaining BPL's inherent resolution and print registry; 4) introduced BPL patterning with near-UV (365 nm) light to expand the spectrum of compatible photochemistries; 5) with technical advances and novel non-natural oligonucleotide chemistries

developed by NU, both teams highlighted the ability to engineer and pattern light-responsive colloidal crystals. The key goals of this project were met, and more details regarding 1) major activities; 2) specific objectives; 3) significant results or key outcomes (such as major findings, developments, or conclusions); and/or 4) other achievements are included in the Technical Update section below.

Dissemination of results:

The results of these efforts have been disseminated through various forms. Two peer-reviewed papers have been published that acknowledge this award. Furthermore, Mirkin gave more than 25 seminars (many of them virtual), including two distinguished lectureships: the Graham Lecture at the University of Virginia and the G. M. Kosolapoff Award Lecture at Auburn University. Mirkin was also awarded the ACS Division of Colloid and Surface Science Award for Outstanding Achievement in Nanoscience, the G. M. Kosolapoff Award (Auburn University and the Auburn Section of the American Chemical Society), the Royal Society of Chemistry de Gennes Prize, and the Acta Biomaterialia Gold Medal. Because of the collaboration with TERA-print, many of the inventions arising from this award are already being incorporated into the next generation of TERA-print nanofabrication technologies.

IMPACTS

Development of the principal discipline(s) of the project:

A long-standing goal of the nanoscience and nanoengineering communities is to actualize the ability to construct arbitrarily complex 2D and 3D 'smart' architectures with chemical and physical functionalities encoded directly into the materials at the micro- to nanoscale. Such advanced material engineering capabilities would open up the possibilities for precise spatiotemporal insertion of sensing and actuation modalities into complex material architectures, revolutionizing the entire fields of soft micro- and nanorobotics, bioengineering, and drug design and discovery, and more. Research and development efforts have been emphatically pursued to realize such 'smart' structures, from inkjet printing to soft lithography. However, these, and other, methods are not sufficient to create 3D structures with functionalization that is widespread, precise, and multi-functional for all conceivable 3D shapes and volumes.

In this project, Northwestern University (Mirkin Group) and TERA-print, LLC worked together to bring the prospect of engineering 3D nanostructures with limitless functionalization possibilities into reality. Beam pen lithography (BPL), invented in the Mirkin Group and commercialized by TERA-print, is uniquely positioned to engineer 3D functional materials with decentralized, spatially distributed actuation and control. BPL delivers structured and highly focused light to a substrate *via* a massively parallel array of pyramidal-shaped microprobes with nanoscopic apertures to enable the rapid generation of arbitrary patterns with diffraction unlimited, sub-300-nm resolution over the mesoscopic length scale. The simultaneous development of actuatable soft materials responsive to light and engineering solutions that allow BPL to act on such soft materials under all requisite environmental and thermodynamics states would, when combined, extend the limits of how complicated a 3D nanostructures shape can become and allow for the full scope of desired functionalities.

Other disciplines:

The advances made by both teams over the last three years have brought the goal of facile printing of 2D and 3D 'smart' nanostructures with precisely controlled spatiotemporal functionalities much closer to reality. By combining a microfluidics BPL platform with environmental controls and fundamental research into soft material properties, the future scope of soft materials nano-engineering will expand for the development of novel mechanical and chemical interfaces with living tissues, smart materials with adaptable optical and electronic properties, and sensing devices.

Describe the impact in this reporting period on the development of human resources

As a result of this project, several students have received advanced training in interdisciplinary research, including postdocs, graduate students, and staff scientists. One student has successfully defended their PhD. EunBi Oh received her PhD from NU and accepted a postdoctoral position with Professor Ryan Truby. Graduate student Namrata Ramani successfully passed her qualifying exam, a major milestone towards obtaining her PhD. Thus, this effort is making a substantial impact on increasing participation in the sciences and maintaining US competitiveness in STEM.

Describe the impact on teaching and educational experiences

This award has had a substantial impact on teaching and educational experiences at Northwestern. This project brings together one of the top research institutions in the nation (Northwestern) with an industrial collaborator (TERA-print), enhancing the experience, educational opportunities, and diverse backgrounds and perspectives. In addition, the interdisciplinary nature of the research enhances educational opportunities for researchers at the university and industrial level. This project brings together researchers with backgrounds in chemistry, engineering, and materials science. To achieve the project outcomes, they must all learn about each other's work and fields.

The Mirkin group is committed to engaging with students of all backgrounds and education levels. Exposure to nanolithography instruments, biology, chemistry, instrument development, and surface science are made available to students. This promotes a multidisciplinary educational environment that encourages collaborative learning from a diverse set of backgrounds. Mirkin has also had a substantial impact on education as director of the International Institute for Nanotechnology at Northwestern. Over 120 of his group's alumni hold faculty positions at top research institutions worldwide. Mirkin teaches nanochemistry concepts in his General Chemistry courses, and he is working to incorporate such lessons into textbooks so that they can reach wider audiences. He also gave a guest lecture in the Northwestern Kellogg School of Management Commercializing Innovations class.

Describe the impact in this reporting period on physical, institutional, and information resources that form infrastructure:

Nothing to report

Impact on society beyond science and technology:

Mirkin presented as a Distinguished Lecturer at the Kavli Nanoscience Institute at Caltech. Additionally, this year Mirkin presented at the GRC Connects event on the subject of "Innovation by Biomaterials" on International Women's Day 2021, highlighting the important work of women in the scientific community. This year, he also presented at two meetings pertaining to the progress

of the National Nanotechnology Initiative (NNI). Further, TERA-Fab instrumrents are already being used by researchers in seven countries on three continents in applications ranging from biosensing, microfluidics, and soft microrobotics. By expanding the capabilities of BPL, namely high-resolution printing and massively multiplexed optical exposures, to create biological and soft material chemistry on a single chip, this technology will gain significant interest and gain adoption from researchers in new industries, such as synthetic biology, tissue engineering, biotech and pharma, agriculture, and even molecular data storage.

CHANGES

Changes in approach

Nothing to report

Problems or delays

Nothing to report

Expenditure Impacts

Nothing to report

Significant changes in the use or care of human subjects, vertebrate animals and/or biohazards

Nothing to report

Changes to the primary place of performance from that originally proposed

Nothing to report

TECHNICAL UPDATES

Development of a Nanofabrication Strategy to Rapidly Modify Local Physicochemical Properties and Functionality of Hydrogels under Controlled Environments

Soft materials, i.e., hydrogels used in this project, are extremely sensitive to ambient conditions, such as temperature and humidity. Small variations in these parameters can drastically alter the thermodynamic state, physicochemical properties, and functionality of the fabricated active architectures. In addition, the construction of soft smart materials with multiple sensing and actuation functionalities requires the ability to assemble various modalities into composite architectures. The latter can be achieved, for example, by sequentially introducing inks of interest into the print bed *via* a fluidics system and polymerizing these materials in-registry using light. The development of these technical capabilities could enable new possibilities in soft robotics, smart materials, sensing, and tissue engineering, and, as such, was one of the main focuses of this project.

Over the course of the project, the TERA-print team has invented and prototyped a series of hardware upgrades for its commercial nanofabrication platform, TERA-Fab™ E series. Based on the beam pen lithography (BPL) technology it provides an unmatched set of nanofabrication capabilities to soft active materials. The team has introduced environmental control capabilities to control the thermodynamic state of the material being printed, developed the ability to rapidly exchange liquids and gases within the sample chamber for multi-material fabrication, and increased the accessible light wavelengths to broaden the spectrum of material chemistries that the system can activate and process.

Controlled Environment Capabilities

Introducing the ability to perform BPL experiments under controlled environmental conditions required re-thinking many aspects of the instrument. The following engineering challenges needed to be overcome: (*i*) a heating/cooling element needed to be integrated beneath the sample to allow for on-demand temperature adjustments of the sample without affecting nearby sensors and motors; (*ii*) a new, enclosed, air-tight printing chamber needed to be designed that allows for the real-time, leak-free exchange of reagents in the print bed, as well as supports for the tip/tilt motion of a BPL array and mm-scale vertical 3D builds; (*iii*) the operation of the fluidics system needed to be automated to allow for highly orchestrated exchange of inks, motion of motors, and photopolymerization with light into multi-material architectures; and (*iv*) an external, computer-controlled humidifier together with a humidity sensor needed to be introduced and programmed to operate in a PID feedback loop and maintain a desired ambient humidity in the experimental chamber with ±2% precision.

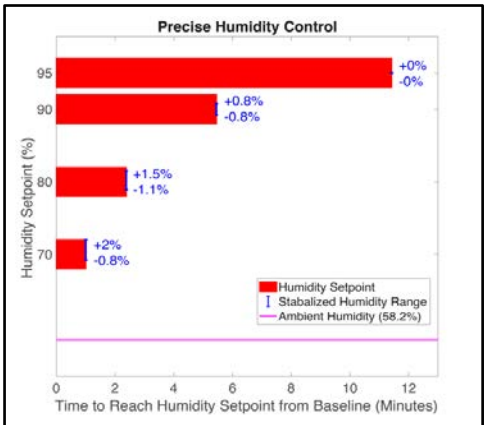

Figure 1. Humidity Control. x-axis corresponds to the time (min) required to raise the humidity from the ambient conditions (RH 58.2%). Error bars denote the humidity range achieved after the system stabilized for 3 min.

Humidity Control. We successfully introduced humidity control by connecting an external humidifier (w × d × h: 18 × 18 × 22 in; Asakuki, 100-HM001) to the BPL enclosure. The enclosure was modified to accept an adapter that allowed a water-resistant hose to run from the humidifier to the enclosure. Computer control of the humidifier was achieved using an Arduino board and a power relay in connection with an electrical feedback circuit that monitored the current humidity of the BPL instrument. Easy-to-use software was developed to quickly switch the humidifier between ON and OFF states, either based on the user's direct input or a user defined setpoint. In this way, the desired humidity can be defined, and the electrical PID feedback loop will operate to regulate the output of the humidifier to reach and maintain that setpoint. Figure 1 shows the relationship between the desired humidity setpoint and how long it takes to reach that setpoint from ambient humidity. In addition, it shows the stability of the humidifier to maintain the desired setpoint once it has been reached. This result demonstrates that with the optimized PID feedback loop, our system can achieve and maintain to within 2% the desired humidity in the print chamber and, as such, control the thermodynamic state of soft materials being processed.

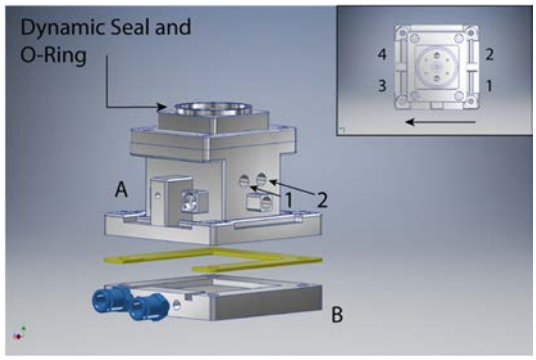

Figure 2. Temperature Control Apparatus. The thermocouple is sandwiched between the sample holder (A) and the aluminum bottom (B). Inset: Top view of the sample holder, denoting entrance apertures (1 and 2), exit apertures (3 and 4), and flow direction for fluidics.

Temperature Control. Temperature control and microfluidics control were partly achieved jointly through the re-design and construction of a new sample holder. **Figure 2** shows the latest

iteration of the sample holder design used in this project. A thin polyethylenimine (PEI) plastic layer is introduced between two aluminum elements to thermally decouple the top and bottom of the sample holder. When an electrical current is passed through a Peltier thermocouple, one side begins to heat up while the other side begins to cool down, depending on the direction and magnitude of the current. The temperature of the sample affixed directly atop of the sample holder can be regulated by changing the magnitude and direction of the electrical current passing through the thermocouple. Furthermore, we introduced water circulation through the bottom piece of the sample holder, which was designed to effectively remove excess heat generated by the system when the sample is cooled relative to ambient temperature (the water-cooling circuit is equipped with a radiator and a fan).

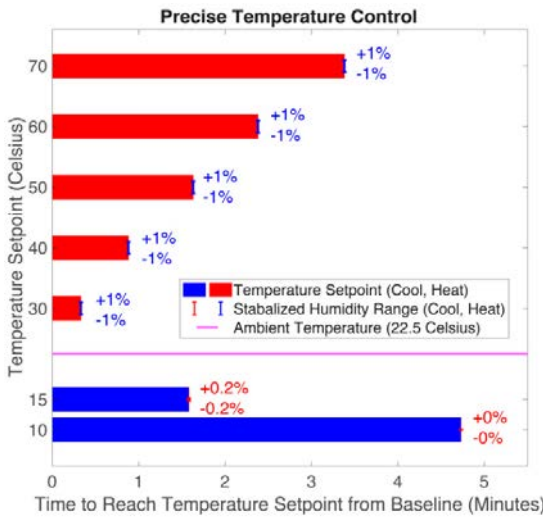

Figure 3. Temperature Control. x-axis corresponds to the time required to heat (red) or cool (blue) the sample from room temperature (22.5 °C). Error bars denote the temperature range achieved after the system stabilized for 7 min.

Control over the electrical current (i.e., temperature) was achieved *via* a feedback mechanism that includes regulator hardware (Laird, SH14-125-06) and a software implemented PID loop. This system enables a user to heat or cool the sample to any temperature within the 10 – 70°C range in less than 5 min and maintain the temperature within ±1 °C from the setpoint (**Figure 3**). Such precise and rapid temperature control provides a user with additional means to modulate the physicochemical state of soft materials during printing, potentially enabling access to new, previously unattainable structures and functionalities.

Microfluidics Control. The design and construction of the new, air-tight microfluidics sample holder is shown in **Figures 2** and **4**, respectively. The holder has two input and two output ports to ensure uniform distribution of liquid material over the sample. In addition, the sample holder features a vacuum channel and O-ring for affixing a sample, which is necessary to ensure an air-tight volume for the liquid to flow in and out without risk of seriously damaging other equipment (e.g., force sensors, piezo stages, etc.). Critically, the resolution and registry of printing are not affected by continuous application of a vacuum pressure of approximately -60 kPa, sufficient for affixing the sample (**Figure 5**).

The new sample holder in the BPL instrument was upgraded to create a fully sealed sample chamber for introducing soft materials between a substrate and a cover glass/BPL array. This was achieved by introducing a dynamic aluminum ring with a 2.25 mm travel range (**Figure 2, top**). The ring is actuated pneumatically by flowing air underneath v*ia* a Fluigent pressure pump (FLPG005 and LU-FEZ-02000). The air pressure lifts the ring and brings it into contact with a BPL array/glass, making a seal via a 1 mm wide O-ring. The overall chamber volume can be dynamically changed by adjusting the sample chamber position relative to the BPL array/glass, in conjunction with judiciously modulating the air pressure as needed. The total volume range was determined to be from ~300 µL (*initial print volume*) to ~1,440 µL (*maximum print volume*), and 1.2 bar of air pressure was demonstrated to deliver a seal without leaks from the sample chamber for liquid flow rates ranging from 100 – 1100 µL/min. This corresponded to an overall force of 900 – 2000 mN pushing down on the sample holder, well within the maximum load capacity of the motor controlling the vertical position of the sample (CONEX, TRB12CC).

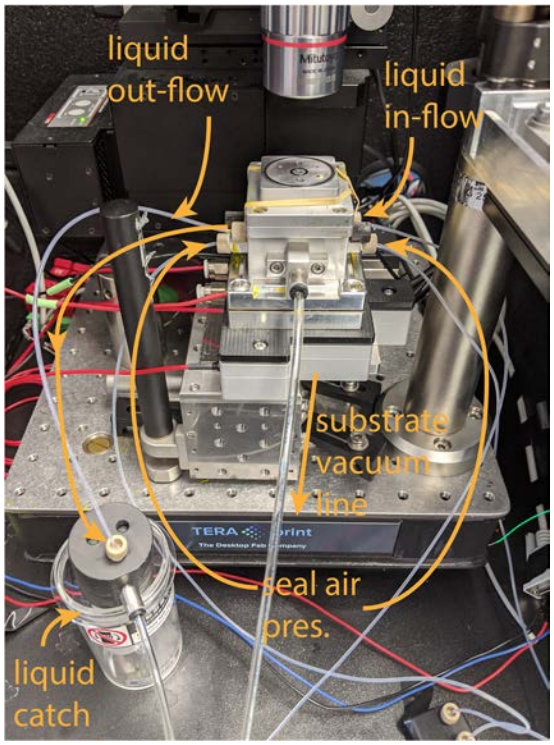

Figure 4. Microfluidics System. Experimental apparatus for testing fluidics design. Input and output ports are labeled consistent with that in Figure 2.

Actual flow control of the soft material (i.e., hydrogel) into the new fluidics sample holder was achieved using a Fluigent microfluidics flow system (Fluigent; FLPG005, LU-FEZ-02000, and MSW002). This system can flow soft materials into the chamber using pressurized air and can switch between materials on demand at any time over the course of a print. Unpolymerized material was flown out of the system using a vacuum line connected at the outlet ports (Parker; C190-12) and regulated via a vacuum pressure regulator (SMC; ITV0090-3UBS). Such an approach buttressed the accessible flow rates of 100 µL/min – 1100 µL/min and minimized the risk of pressure build up in the system and consequent leaks.

Taken together, these technical advances extend the capabilities of printing multiple soft materials at their controlled thermodynamic states in registry with high resolution, as shown in proof-of-principle experiments (**Figure 5**).

Near-UV BPL Capabilities

The first generation of the commercial BPL instrument featured two illumination sources with wavelengths of 405 nm and 532 nm. However, many photochemistries require illumination in the near-UV range (i.e., ~365 nm) for reactions to occur efficiently. The integration of near-UV illumination capabilities is not a trivial task and requires more than just changing the LED light source. The primary issue is that commonly used off the shelf optical components, including lenses, mirrors, and prisms, are optimized for the visible light spectrum (> 400 nm wavelength).

These elements absorb light in the near-UV range, and would, therefore, decrease the intensity of the transmitted light to the sample and heat up the DLP elements, potentially causing irreversible damage, if they were used with a near-UV LED. To mitigate these problems, we took a multi-pronged approach: (*i*) a number of mirrors were coated with aluminum to improve their reflectivity in the near-UV range; (*ii*) a custom lens was designed and manufactured to replace a pair of lenses in the light path to minimize the travel distance through the lenses and, thus, the intensity loss; (*iii*) a radiator was added to the DMD chip to provide passive cooling, and the volume of the radiator and the fan rotational velocity on the LED were increased to more effectively draw heat from the LED operating at the maximum power; (*iv*) the LED was overdriven at 10 A to achieve acceptable 365 nm light intensities and reaction rates. Additionally, the ability to drive the DMD in an '8-bit' mode, whereby the state of each micromirror of the DMD is modulated according to the value assigned to each micromirror (i.e., 0-255, the standard 8-bit values), was exploited to create an image of the DMD at the sample with even intensity throughout the image. This was done to ensure that all DMD micromirrors, and thereby all BPL micro-tips, presented the same intensity of near-UV on the substrate surface, resulting in print consistency and standardization across the entire printing area. By using a beam profiler (Edmund Optics) to collect images of the DMD projection and processing each image using MATLAB scripts, it was possible to iteratively 'correct' the DMD projection until uniformity was achieved such that the standard deviation of intensity over the whole image is ≤ 5% from the average. These modifications have allowed us to add the 365 nm illumination capabilities to the TERA-Fab™ E series repertoire, enhancing the modularity of the instrument's illumination offerings and providing access to the widest set of chemistries possible.

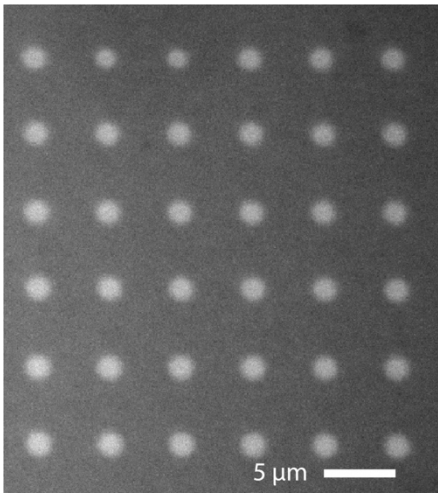

Figure 5. Printing Under Vacuum. Image of an etched 6 × 6 print made while the substrate was under vacuum (-20 kPa). Feature size and dot-to-dot distance are indistinguishable from a print with no vacuum applied.

Synthesis and Characterization of Responsive and Actuatable Composite Hydrogels

Over the course of this project, the NU team has developed novel hydrogel and soft matter materials with responsiveness and actuation that can be precisely calibrated and tuned using BPL technology. Developing novel polymeric materials and chemistries to manipulate their properties is a major part of this project and, more specifically,

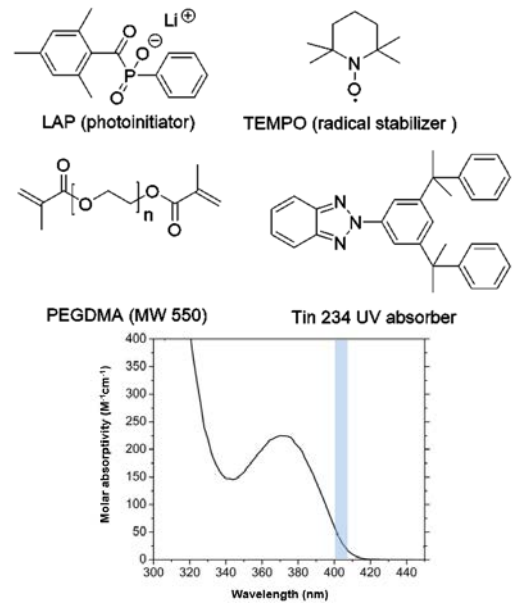

Figure 6. Chemical structure of the polymer ink (top). Absorption spectrum of lithium phenyl-2,4,6-trimethylbenzoylphosphinate (LAP) photoinitiator and the 405-nm LED light from the DMD (bottom).

working with many multi-faceted materials enables BPL to access a greater variety of actuation capabilities than other technologies. Functional polymeric materials constructed from photocurable acrylated monomers were synthesized and the polymerization kinetics between polymer stiffness and exposure dose were calibrated. Additionally, oligonucleotides were incorporated into a hydrogel backbone as a method for tuning the mechanical properties of the hydrogel structure.

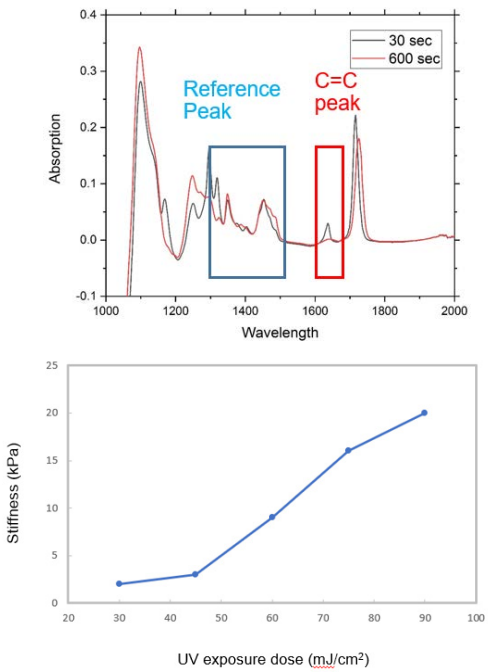

Figure 7. Acrylate monomer conversion upon UV light irradiation as measured by attenuated total reflection (ATR) measured (top). The evolution of the hydrogel stiffness as the function of the exposure dose (bottom).

3D functional polymeric materials for printing with beam pen-directed photopolymerization. Beam pen-regulated material printing (BPL) is utilized to fabricate stimuli-responsive digital 3D architectures via a photopolymerization methodology. The development of such highly controllable, smart materials revolutionizes a variety of research areas and applications in nanotechnology, biomedicine, microrobotics, and materials science and engineering. We developed a photocurable polymeric system and combined it with a DMD and BPL to construct 3D materials with sub-micron precision.

The photopolymerization system is synthesized using photocurable acrylated monomers. By tuning the functionality of the polymer ink (**Figure 6**), the chemical and physical properties of the material can be designed for specific applications. The kinetics and photoresponsiveness of the hydrogel photocuring are highly dependent on the properties of the photoinitiator. The absorption spectra of the photoinitiator as well as the emission of the DMD is shown in **Figure 6**. A UV absorber (Tin 234) and appropriate radical stabilizers (e.g., butylated hydroxytoluene and (2,2,6,6-tetramethylpiperidin-1-yl)oxyl (TEMPO)) were used to improve the fidelity of the photo-printed polymer architectures.

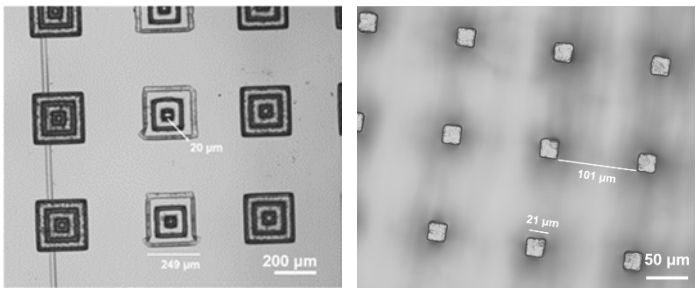

Figure 8. Optical images of the DMD light-patterned 2D hydrogel structure.

Beam pen-mediated 3D printing differentiates itself from other prevailing 3D printing techniques. For beam pen photocuring to be successfully performed, an understanding of the photopolymerization kinetics must be obtained in the context of certain experimental parameters (e.g., vertical printing rate, irradiation conditions). During photopolymerization, the consumption of polymer can be determined by monitoring the acrylate peak by Fourier transform infrared spectroscopy (FT-IR) (**Figure 7**). The IR reference peaks at 1420-1500 cm^{-1} and 1330-1370 cm^{-1}

were used as standard peaks to calculate the amount of acrylate. The remaining acrylate moiety can be controlled by the applied exposure dose, making it available for further modification and functionalization (e.g., DNA and proteins). The AFM experiments demonstrate that the photopolymerization of the hydrogel can be used to construct a variety of functional materials with tunable stiffness (moduli ranging from 2-25 kPa) (**Figure 7**).

With a fundamental understanding of the polymer ink, DMD was used to build 2D patterned structures from the acrylate system (**Figure 8**). Preliminary results demonstrate that 2D square features and simple patterns can be readily prepared by DMD-controlled photopolymerization. The resolution of the 2D patterned features is 5-10 μm, with a variation in height of 20-70 μm depending on the exposure conditions. Moving forward, we expect that by optimizing the polymer ink system will increase architecture fidelity to make it an appropriate curing system for beam pen-mediated printing.

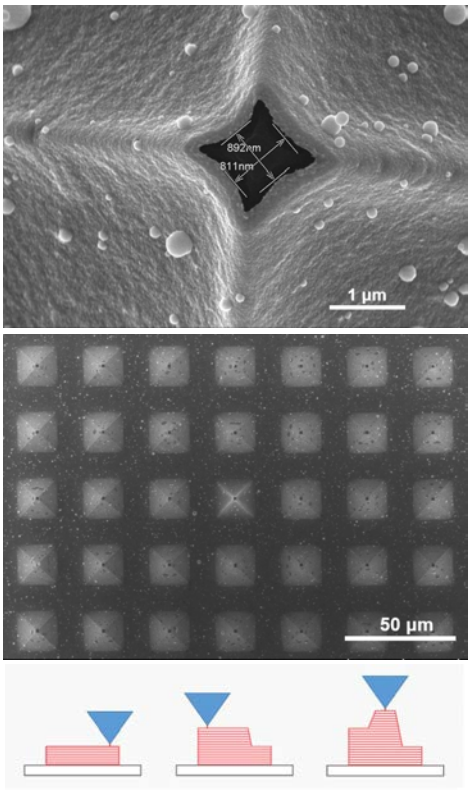

Figure 9. SEM image of a BPL pen array (top, middle). Schematic of layer-by-layer printing methodology in beam pen-regulated photopolymerization (bottom).

SEM images of the BPL pen array are shown in **Figure 9**. The size of the apertures on the pen array can be controlled from 400 nm to 2 μm. By controlling parameters such as the wavelength of light, exposure area, and exposure time, BPL can be used to build digital architectures with high spatiotemporal precision. Beam pen-regulated photopolymerization can be achieved by moving the substrate to control the photo-printing process, and the polymeric material is constructed in a layer-by-layer fashion (**Figure 9**).

In summary, this study focused on utilizing BPL as an efficient tool to develop a new 3D digital printing technique. Fundamental studies with the photocurable acrylate system were performed to investigate the photopolymerization kinetics and the mechanical properties of the photogenerated material. Preliminary DMD-controlled hydrogel patterning is demonstrated; however, further improvements in the polymer ink and the printing methodology are also required to fully achieve BPL-controlled 3D material printing. Later we show that by exploring new additives in the photocuring system stimuli-responsive (e.g., pH, light, or heat sensitive) 4D functional materials can be constructed.

Synthesis and Photo-degradable/ Crosslinkable-Nucleic Acids Bonds in Hydrogels

Stimuli-Responsive Nucleic Acid Crosslinks in Hydrogels. Oligonucleotides, including short strands of DNA, offer a highly tunable and programmable way of modulating the mechanical properties of soft matter. By spatially distributing oligonucleotide crosslinks in a controlled manner, local anisotropic responses within a hydrogel can be observed. A key component of this project deals with identifying and synthesizing a hydrogel platform that is amenable to chemical

functionalization. To develop such a highly tunable hydrogel system, a polyethylene glycol diacrylate (PEGdA) system with pendant functional acrylate groups was synthesized. The gel was polymerized on an acrylated glass slide with a 250 µm spacer. Next, a photochemical cross-linker, sulfosuccinimidyl 6-(4'-azido-2'-nitrophenylamino)hexanoate (Sulfo-SANPAH) was identified that could be used to chemically conjugate oligonucleotides to the hydrogel backbone (**Figure 10**). To attach the oligonucleotides to the PEGdA gel, the gel was incubated with the photochemical cross-linker overnight. Upon irradiation of the gel with 365-nm UV light, using a photomask, the linker was attached to the PEG backbone, leaving a sulfo-NHS ester to react with any primary amine. The gel was then incubated with an amine-functionalized T_{20} DNA strand with a Cy3.5 fluorophore overnight with shaking. Confocal micrographs revealed a localization of the fluorescence signal to the patterned areas (**Figure 11**).

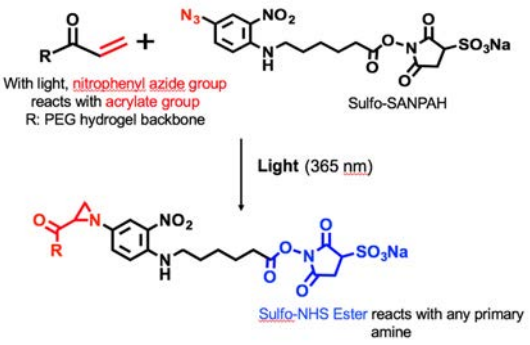

Figure 10. **S**ulfosuccinimidyl 6-(4'-azido-2'-nitrophenylamino)hexanoate (Sulfo-SANPAH) photochemistry. Using 365 nm UV-light, the azide can react with the acrylate, leaving the sulfo-NHS ester to conjugate with any primary amine.

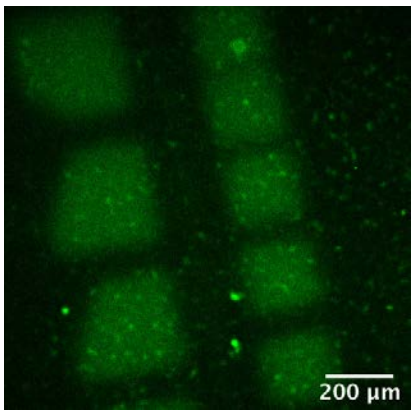

Figure 11. Confocal microscope images show patterns of localized fluorophore-labeled oligonucleotides made using a photomask and illumination at 365 nm.

Once it was shown that the oligonucleotides could be covalently conjugated to the gel, stimuli-responsive DNA was designed to change the mechanical properties of the hydrogel. I-motif DNA, a pH-sensitive oligonucleotide sequence that forms a secondary intercalated sequence under basic conditions or maintains an open form in acidic conditions, was synthesized (**Figure 12**). The i-motif strand was designed with amino modifiers on the 3' and 5' ends to perform crosslinking chemistry. Further, two sequences complementary to the ends of the i-motif sequence were designed to provide rigidity to the i-motif strand. The complementary strands contain fluorophore-labeled phosphoramidite bases (Cy3.5 and Cy5 coupled to the 5' and 3' ends, respectively). The fluorophores can be used to locate DNA strands within the hydrogel under the fluorescence mode of a confocal microscope. As the i-motif reversibly forms, the change in distance between the fluorophores can be tracked via distance-dependent Förster resonance

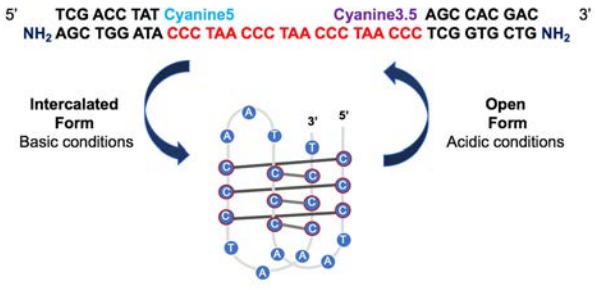

Figure 12. DNA sequence design and secondary i-motif structure.

energy transfer (FRET) measurements. Once synthesized, the strands were purified using high-performance liquid chromatography (HPLC) and characterized with matrix-assisted laser desorption ionization time-of-flight (MALDI-TOF) mass spectrometry to verify the correct sequence by mass.

Next, atomic force microscopy (AFM) was employed to measure stiffness changes in the material in the patterned areas when the i-motif is folded/unfolded. In addition, higher resolution and more complex features were printed using BPL. Finally, finite element models were used to model stress fields within the gel to predict how these materials change shape as a function of pH (*see below*).

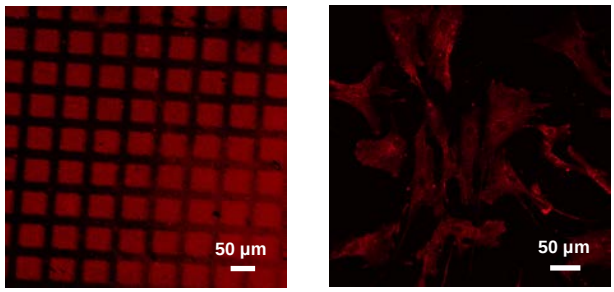

Figure 13. Fluorescence images of (a) a hydrogel patterned using a photomask and a 365 nm UV lamp and functionalized with fibronectin, which is labeled with AlexaFluoro 568 antibody, and (b) cells seeded and attached to the patterned hydrogels where vinculin is labeled with AlexaFluoro 633.

Examining Responsiveness of Hydrogels

Modulation of local chemistry of soft materials for biological studies. The chemistry of the PEGdA gels described previously was also used to construct soft materials with site-specific nanostructures, enabling biological studies. In addition to oligonucleotides, adhesion proteins, like fibronectin, can be incorporated into the gel to enhance molecular functionality. The sulfo-NHS ester from sulfo-SANPAH will react with primary amines in fibronectin. Using BPL, the attachment of fibronectin can then be precisely controlled and spatially decentralized on soft materials. The use of such soft, smart materials allows for the detection and acquisition of individual cells in a parallel manner. The manipulation of a single cell can also be performed at the nanoscale independently of the initial mechanical properties of the substrate.

In a proof-of-concept experiment, the PEGdA gels were incubated in sulfo-SANPAH overnight and exposed using 365 nm UV light and a pre-designed photomask. The gels were then rinsed with phosphate buffered saline (PBS) overnight and functionalized with fibronectin. To visualize the localization of fibronectin on the light-exposed areas, the gel was incubated in the fluorescently labeled antibody solution (**Figure 13a**). The cells were seeded on these hydrogels and stained for vinculin, which is a cytoskeletal protein found in the focal adhesions of cells (**Figure 13b**). To examine the compatibility of BPL with the gel system, a simple square pattern was made using a digital micromirror device (DMD) with the same light source (**Figure 14**).

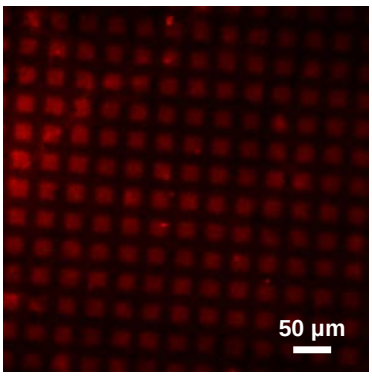

Figure 14. Image of a hydrogel patterned using a DMD system in a TERA-fab E series instrument. The square patterns indicate the areas that were exposed to light. Fibronectin conjugated to light-reacted sulfo-SANPAH and functionalized with antibody containing fluorescent molecules, Alexa Fluor 568.

Next, beam pen arrays were used to incorporate biological functionality into soft materials in a decentralized fashion from the nanoscale to the bulk. Adhesion proteins that are precisely distributed via beam pen arrays will enhance detection of individual cells for further bioanalysis. Using these actuatable hydrogels, fundamental biological questions pertaining to the physicochemical properties, such as substrate stiffness, cell shape, and extracellular matrix (ECM) domain size, affecting cellular behavior were answered (*see later sections*).

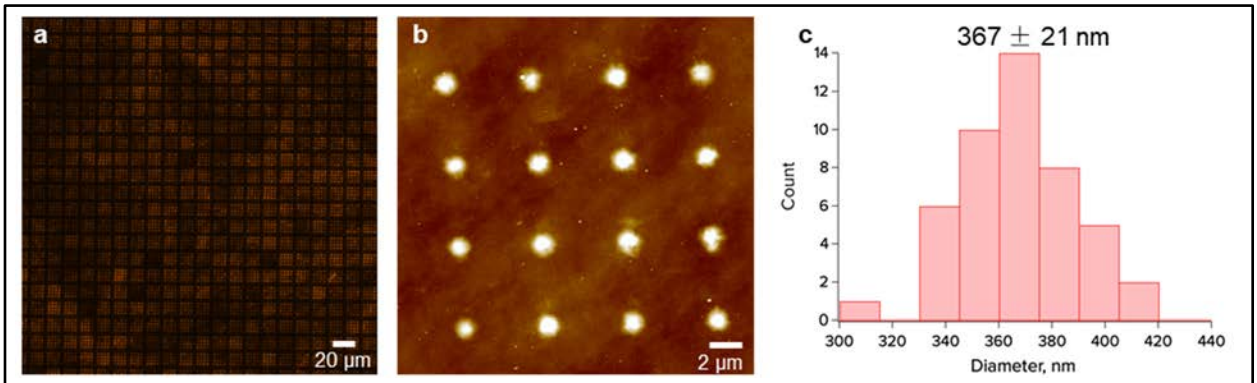

Figure 15. High-Resolution Printing of Hydrogels Using BPL. (a) Optical microscopy image of dot features of PEGDA patterned with BPL over a tens of square-millimeter area. (b) AFM image of hydrogel features in a pattern produced by a single BPL tip. (c) Histogram of feature diameter size obtained with AFM.

Design and Synthesis of Hydrogels with Distributed Actuation and Sensing Uni-Layer Composite Systems with Distributed Properties

Upon the introduction of the new technical capabilities to the BPL instrument, the NU and TERA-print teams joined forces to evaluate how these advances translate into new abilities in fabricating advanced functional soft material architectures. Our initial focus was on: (*i*) establishing the highest resolution with which we can print soft materials (i.e., hydrogels); (*ii*) demonstrating the ability to print multiple materials in registry; (*iii*) showing the modulation of local chemistry and mechanical properties in hydrogels; (*iv*) evaluating the platform's potential for 2.5D and 3D printing; and (*v*) showcasing the benefits of the environmental control capabilities by patterning colloidal crystal surfaces. These benchmarking and demonstration experiments were critical to establish the framework for the design of composite soft materials with distributed sensing and actuation properties that are feasible with the developed technology.

Printing Resolution. Although the potential of the BPL technology to pattern photoresists with sub-diffraction (< 250 nm resolution) was previously documented, printing soft materials such as hydrogels with high resolution is more challenging due to diffusion effects. To benchmark our resolution limits with hydrogels, we performed BPL experiments with two different hydrogel systems. One system included gelatin methacrylate (GelMA) with lithium phenyl-2,4,6-trimethylbenzoylphosphinate (LAP, Sigma-Aldrich) used as the photoinitiator, (2,2,6,6,-Tetramethylpiperidin-1-yl)oxyl (TEMPO, Sigma-Aldrich) as a free radical quencher, and phosphate buffered saline (PBS) as a solvent. The other system was poly(ethylene glycol) diacrylate (PEGDA) with TPO (diphenyl (2,4,6-trimethylbenzoyl)-phosphine oxide) used as a photoinitiator and dimethylformamide (DMF) as a solvent. These hydrogel formulations were photopolymerized into dot patterns using BPL by exposing the hydrogels to 405 nm light at an intensity of 180 mW/cm^2 for 0.5 – 1.5 s. The size of the features was established using optical

microscopy and validated using atomic force microscopy (AFM). **Figure 15** shows a representative PEGDA pattern with hydrogel features of < 400 nm in diameter.

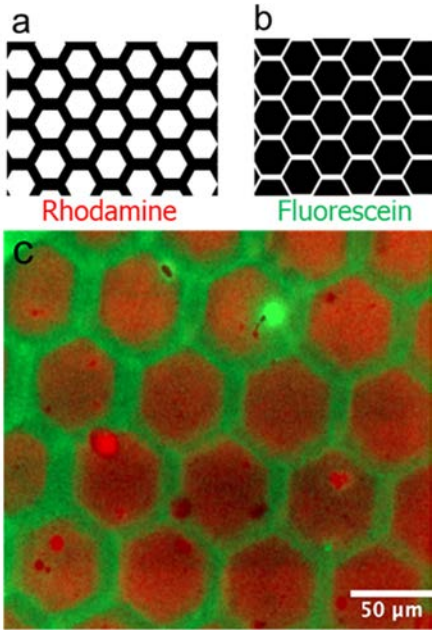

Figure 16. Multiple Hydrogel Compositions Printed In-Registry. DMD projection patterns for GelMA printing using (a) rhodamine and (b) fluorescein fluorophores. (c) The two patterns projected over the same area and imaged using confocal microscopy.

Printing In-Registry. In order to validate the potential of the newly developed fluidics system for the real-time *in situ* exchange of reagents in the sample chamber and printing multi-material architectures, we conceived an experiment, in which two GelMA hydrogel solutions doped with distinct methacrylated fluorophores (rhodamine B and fluorescein O-methacrylate) are sequentially introduced into the chamber and polymerized in complementary patterns. We first patterned a honeycomb array of hexagonal structures using rhodamine doped GelMA (**Figure 16a**), followed by extensive *in situ* (within the chamber) washing with warm water. We then introduced fluorescein doped GelMA and photopolymerized it into a bordering structure to complement the previous print (**Figure 16b**). The resulting composite structure was then washed and imaged using confocal microscopy (**Figure 16c**).

It is important to note that even though the in-registry printing resolution was ~10 µm, respectable for constructing composite architectures, it was not the focus of this demonstration and could be further improved by using BPL. This result provides a promising foundation for future applications involving the engineering of composite 2D and 3D layered structures with precise, spatially encoded chemical and mechanical sensing and actuation modalities.

Modulation of Mechanical Properties.

BPL can be used to control the local mechanical properties of soft materials. For example, a photo-responsive hydrogel can be exposed with light from the aperture at the apex of each pyramidal pen to modulate its cross-linking density, thus changing the stiffness of the gel. The degradation of a photodegradable PEG based hydrogel was initially validated using a DMD and 405 nm LED that is used to power BPL arrays. The hydrogels were irradiated, and the stiffness of the corresponding gels was then measured with AFM. An elasticity map of 10 µm × 10 µm square patterns

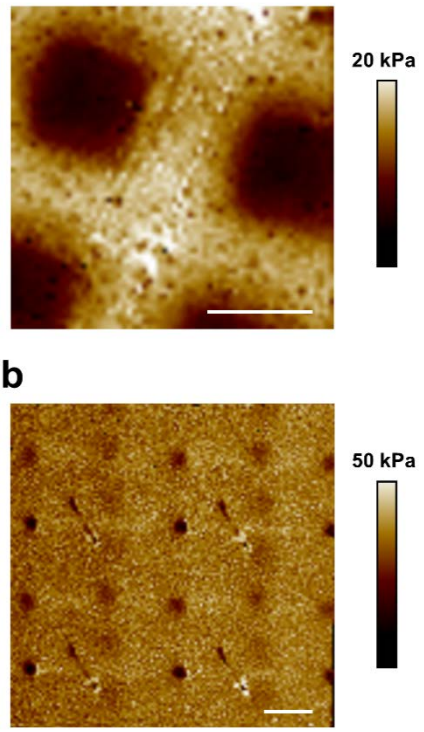

Figure 17. AFM images of patterned hydrogels using (a) DMD 10 µm x 10 µm squares and (b) BPL 1 µm radius circles. The darker regions indicate areas where the hydrogels were exposed to light and thus have decreased lower stiffness. Scale bar = 10 µm.

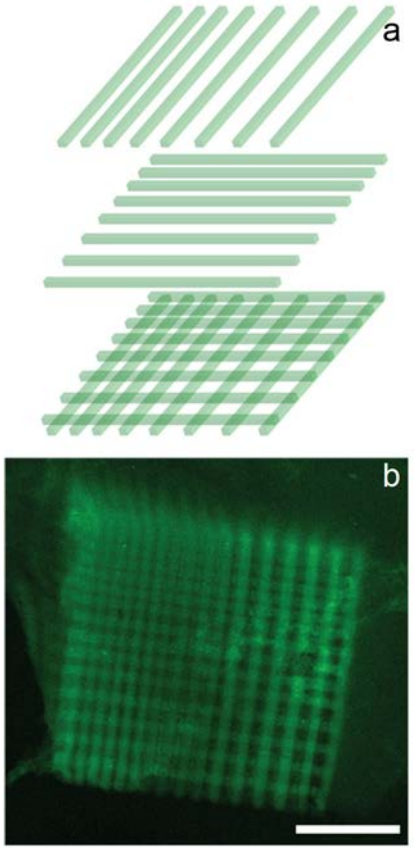

Figure 18. Layer-By-Layer DMD Printing. (a) Scheme of the 3D variable log pile concept to evaluate printing capabilities and (b) fluorescent image of the resulting print showing cross-stacked layers. Scale bar 100 µm.

obtained using AFM is shown in **Figure 17a**. After learning how to pattern hydrogels with a DMD, this knowledge was translated to the TERA-Fab and patterns were generated using BPL (**Figure 17b**). Here, the pattern size is limited by the aperture of the pen arrays; the smallest feature size achieved was 2 µm using a pen array with an average aperture size of 1.4 µm. We are currently working towards moving pen arrays in the *x* and *y* directions using a precise piezo controller to obtain more consistent patterns. These hydrogels with complex stiffness distributions can be used to study cellular behavior that could provide new insights in tissue engineering and regenerative medicine.

Multi-Layer Composite Systems with Distributed Properties

2.5D and 3D Printing. There are several ways to construct multi-layer architectures comprised of soft materials (i.e., hydrogels) with different sensing and actuation modalities. One such approach involves forming one layer of hydrogel, encoding a set of sensing and actuation functionalities into it, forming the next layer, encoding a different set of sensing and actuation functionalities into the second layer, and so on – one layer at a time. Alternatively, materials in the reaction chamber could be swapped in real-time and photopolymerized together in an additive manufacturing manner. The latter provides more flexibility and control over the accessible architectures and enables faster construction of more complex composite materials. This has motivated us to start exploring the potential of our platform for 3D printing hydrogel architectures.

Our first attempt relied on the use of the lower resolution DMD, and not BPL, mode for constructing a log pile structure out of GelMA. This latticed log pile design featured parallel rectangles of a consistent width and length separated by an increasing spacing and was printed as a basal layer before being rotated 90° and then printed again (**Figure 18a**). This procedure was repeated with the goal of producing a 3D structure. The structure was then dyed with fluorescein for imaging under a scanning light confocal microscope, showing the overlapping printed regions (**Figure 18b**). While this result was promising from the viewing window available, it was difficult to ascertain true 3-dimensionality from a confocal stack due to the diffusion limited nature of incubating a hydrogel in a fluorophore bath.

As such, the next refinement step will be to incorporate two different methacrylated fluorophores into the hydrogel mixture, in the same way it was done for printing two hydrogel compositions in registry, and alternate compositions as each new log-pile layer is printed.

Design of Actuatable Systems

Encoding of Chemical Functionality. BPL can also be used for encoding chemical functionality into 2D hydrogel architectures *via* a photopolymerization methodology. Here, acrylated

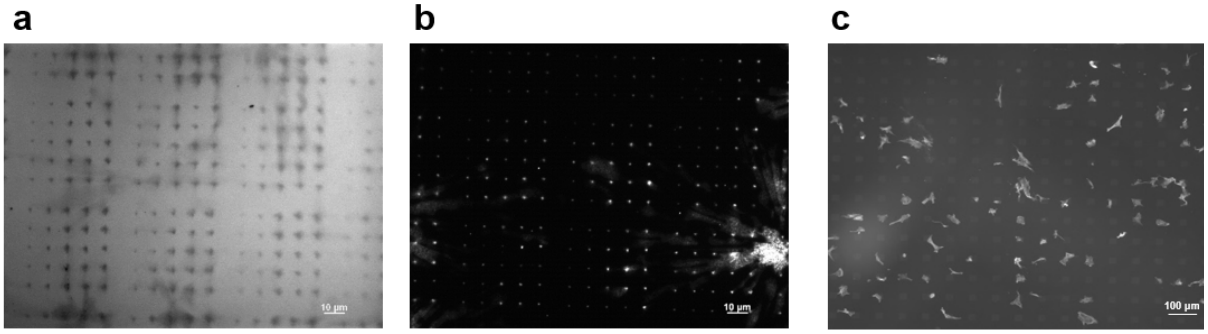

Figure 19. Encoding of Chemical Functionality. BPL controlled thiolayted material surface photo printing. (a) Optical image and (b) fluorescent image of SAMSA-SH dye within the PEGDA photopolymer. (c) Image of a fibroblast cell attachment study performed on the DMD printed, fibronectin functionalized PEGDA polymer.

photocurable polymeric systems were systemically investigated and combined with DMD and BPL printing systems to construct 2D functional materials with sub-micron precision. Additionally, we investigated the incorporation of functional small molecules into the photopolymers using a thiol modified fluorescein (SAMSA-SH), a practical challenge as thiolated functional molecules (e.g., dyes, nucleotides, proteins) can be covalently bonded to the PEGDA polymer network *via* thiol-acrylate "click" chemistry. Sub-micron patterns of PEGDA containing SAMSA-SH were successfully generated, as shown in **Figure 19a,b**, where the florescent image confirms the presence of dye within the crosslinked photopolymer. This demonstrates that BPL-regulated photopolymerization can be used to achieve high-resolution photopatterning of materials such as oligonucleotides, dyes, and proteins.

The BPL controlled printing of functional material 2D will open new avenues for a variety of applications and research including material sensing, as well as cell patterning and behavior studies. As a proof-of-concept, the features patterned with a thiolated, functional ink were used in a cell attachment study. MHA (6-mercaptohexanoic acid) was mixed with PEGDA and photocured under DMD exposure. The resulting 2D polymeric patterns (40 μm^2) were treated with fibronectin. The substrate was then washed with excess PBS to avoid non-specific cell binding. Cell attachment (fibroblast n1h3t3) on the patterned surface was successfully achieved (**Figure 19c**).

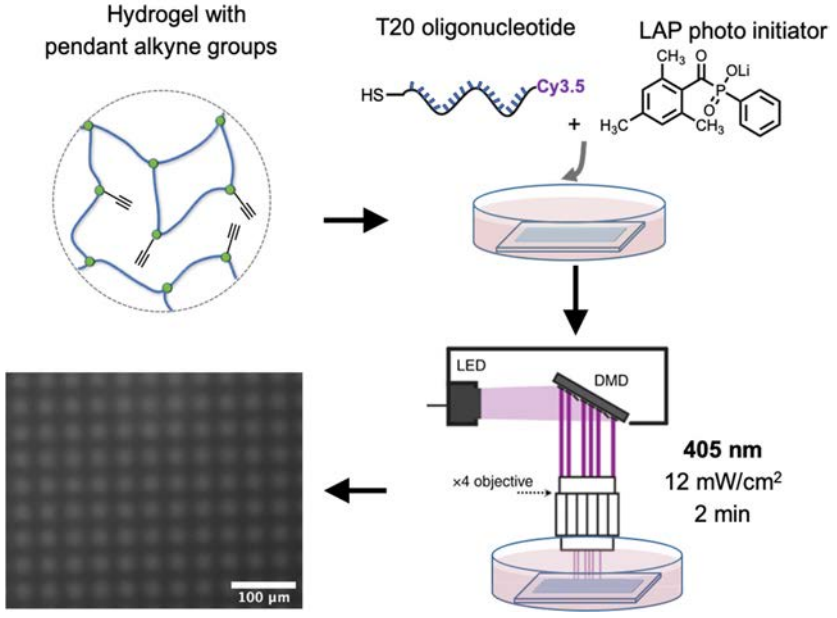

Figure 20. Oligonucleotide attachment workflow. Top left) hydrogel synthesized with pendant alkyne groups top right) Incubation of fluorophore labelled DNA and photo initiator bottom right) Photopatterning with digital micromirror device (DMD) bottom left) Optical microscope imaging of patterns.

However, the material composition and the photocuring methodology require modifications to increase the cell binding efficiency. In the future, beam pen controlled photopolymerization will be used to incorporate different biological functionalities into soft materials.

Spatially Encoding Stimuli-Responsive Nucleic Acids in Hydrogels. Oligonucleotides, including short strands of DNA, offer a programmable approach to design actuatable materials through the synthesis of sequences that form secondary structures as a response to light, pH, and chemical stimuli. By utilizing oligonucleotides as crosslinks in a polymer network, interchain connectivity can be reversibly modulated in a highly controlled fashion. Additionally, by spatially distributing oligonucleotide crosslinks in discrete domains within a hydrogel, local mechanical responses can be observed when a stimulus is applied.

Here, we explored a post-polymerization functionalization method to synthesize functional hydrogels with spatially patterned DNA domains. A key component of this project was first identifying and synthesizing a hydrogel platform that is amenable to photochemical functionalization as this will enable size and geometric control over the different domains. To this end, thiol-ene photochemistry was applied to this system, enabling the hydrogel to be functionalized with thiol terminated DNA in a light directed manner. This chemistry has been previous utilized in the patterning of proteins and other biomolecules as it is versatile, and has a high yield, rapid rate of reaction, and minimal side reactions.

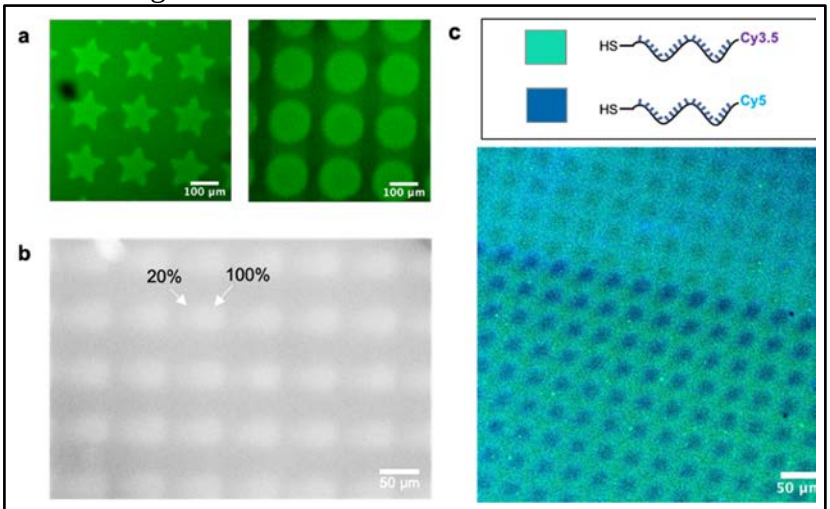

Figure 21. a) High fidelity geometric patterns are achieved via DMD control. b) Grayscale patterning is attained by varying LED source intensity, as seen with differing contrast between 20% intensity and 100% intensity features. c) Confocal microscope image of overlaid patterns with different fluorophore labelled DNA sequences.

To generate a system amenable to thiol-ene chemistry, a PEGDA system was copolymerized with propargyl acrylate, yielding a hydrogel with pendant functional alkyne groups (**Figure 20**). The gel was polymerized on an acrylated glass slide with a 250 µm spacer to ensure an even surface for patterning and was then incubated overnight in a solution of thiolated T20 oligonucleotide DNA with a cyanine3.5 fluorophore label. Next, a water-soluble photoinitiator, LAP, was added to the solution and allowed to diffuse into the hydrogel for 1 h. To covalently tether the DNA to the hydrogel network with light, a DMD with a 405 nm light source was used. The unreacted DNA was washed away, and the gels were imaged using fluorescent optical microscopy and confocal microscopy. The incubation time, light intensity, and exposure time were systematically studied to achieve optimal patterning conditions.

Once the patterning workflow was established, patterns of various geometries were prepared **(Figure 21a).** Confocal microscope images of star and circle patterns show sharp contrast between the patterned domains and background, suggesting DNA localization is limited to where the light is directed. Grayscale patterning was achieved by varying the LED intensity. The fluorescent optical microscope image in **Figure 21b** highlights that the fluorescence intensity of the patterned

features can be tuned by controlling the intensity of the light source while patterning. Patterning of multiple sequences was achieved through sequential incubation and irradiation steps. As a proof-of-concept, T20 DNA strands with different fluorophore labels, Cyanine 3.5 and Cyanine5, were patterned into a hydrogel sequentially (**Figure 21c**). Through alignment of patterned regions, microscale DNA domains of alternating sequence were arranged next to each other.

The next step in this study is to design stimuli-responsive oligonucleotide sequences that can modulate the mechanical properties of individual domains. These sequences can modulate crosslink density of the polymer network through hybridization interactions and the formation of secondary structures. By using the methodology developed for patterning multiple sequences, the effect of orthogonal triggers on domains of different stimuli-responsive oligonucleotide sequences was explored.

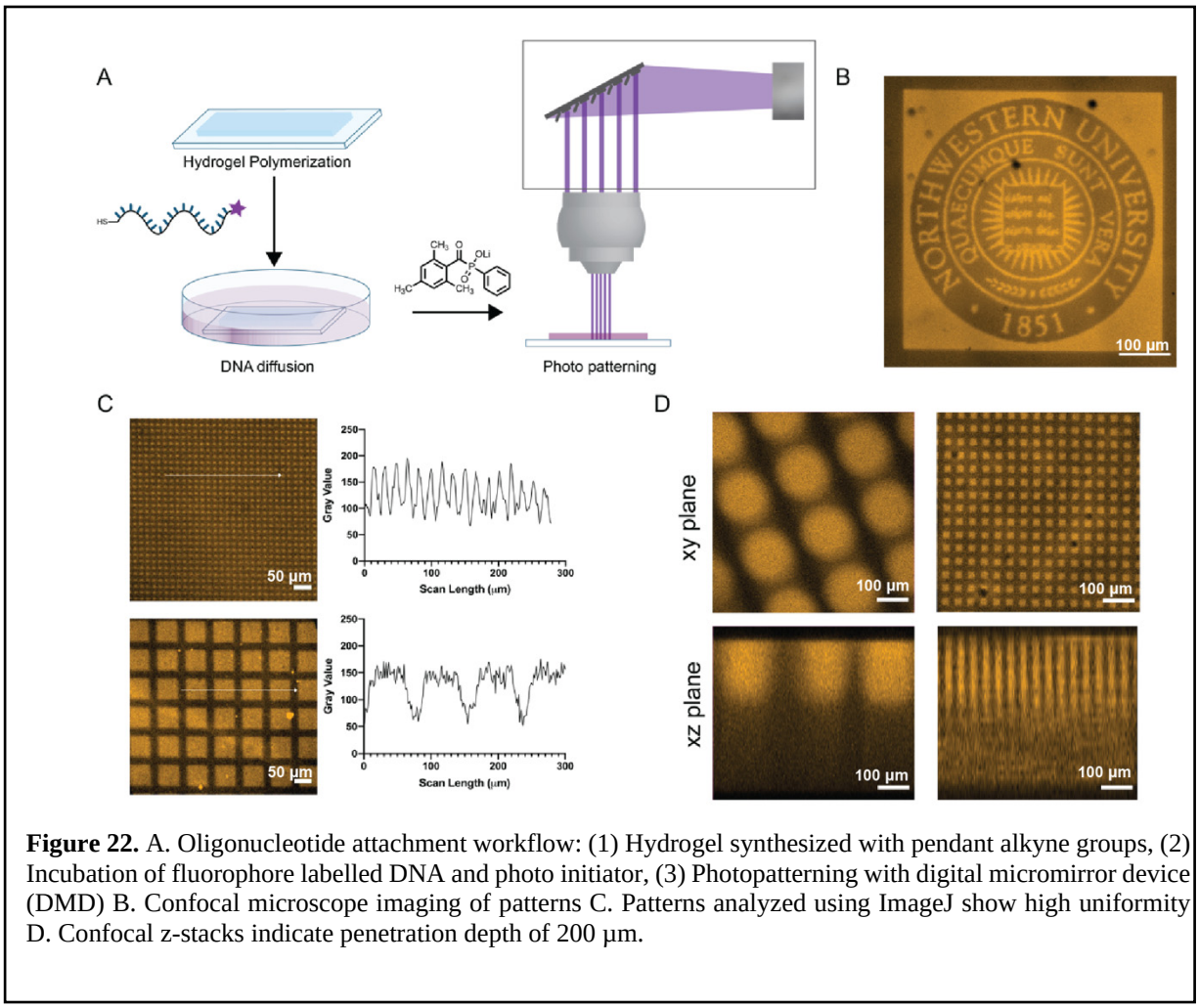

Figure 22. A. Oligonucleotide attachment workflow: (1) Hydrogel synthesized with pendant alkyne groups, (2) Incubation of fluorophore labelled DNA and photo initiator, (3) Photopatterning with digital micromirror device (DMD) B. Confocal microscope imaging of patterns C. Patterns analyzed using ImageJ show high uniformity D. Confocal z-stacks indicate penetration depth of 200 µm.

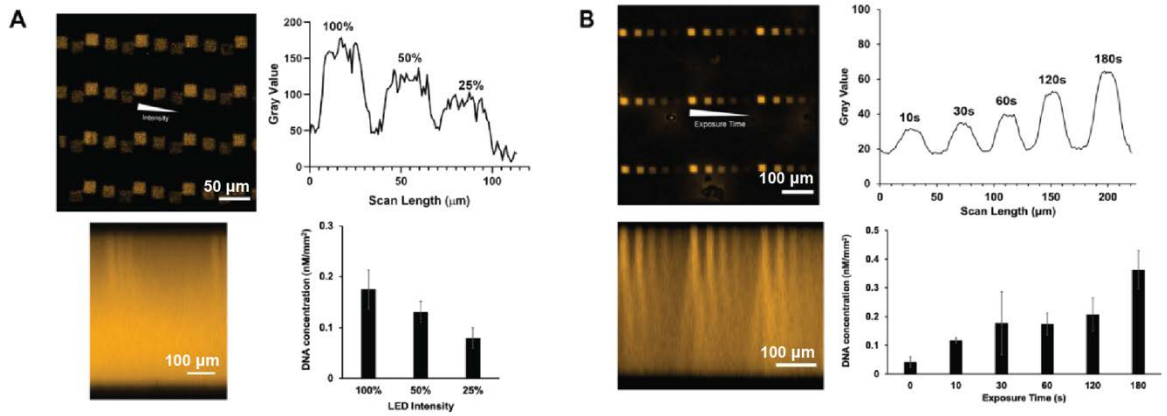

Figure 23. Confocal micrographs, z-stacks, line profiles and DNA quantification studies for (A) varying LED intensity and (B) Light exposure time.

The unreacted DNA was washed away and the gels were imaged using fluorescent optical microscopy and confocal microscopy **(Figure 22B**). A key advantage of using a DMD system is that uniform features can pe patterned over large areas, as shown in **(Figure 22C).** The variables of incubation time, light intensity, and exposure time were systematically studied to achieve optimal patterning conditions. DNA surface concentration was shown to be controlled by both light intensity and exposure time, enabling the patterning of gradient and discrete features of arbitrary geometry **(Figure 23)**. Z-stack analysis showed that functionalization in the z-direction varied with exposure time and not light intensity. To characterize DNA functionalization, patterned gels of varying exposure time and light intensity were degraded using 0.1 M NaOH and Cy3.5 fluorescence was measured using a plate reader. A calibration curve of known concentration of Cy3.5 T20 was used to correlate Cy3.5 fluorescence to DNA concentration. Measured concentration values followed similar trends as the image analysis of patterned features.

Patterning of multiple sequences was developed through sequential incubation and irradiation steps. As a proof-of-concept, T20 DNA strand, a 20-base anchor-DNA sequence with a Cyanine 3 fluorophore labels, were patterned into a hydrogel sequentially (**Figure 24A**). Through alignment of patterned regions, microscale DNA domains of alternating sequence were arranged next to each other. DNA hybridization between a patterned anchor strand and its complement was observed. When the Cyanine5 labelled complement to the anchor-DNA was added to the multi-sequence gel, fluorescence in the Cy5 channel was only colocalized with the complementary sequence.

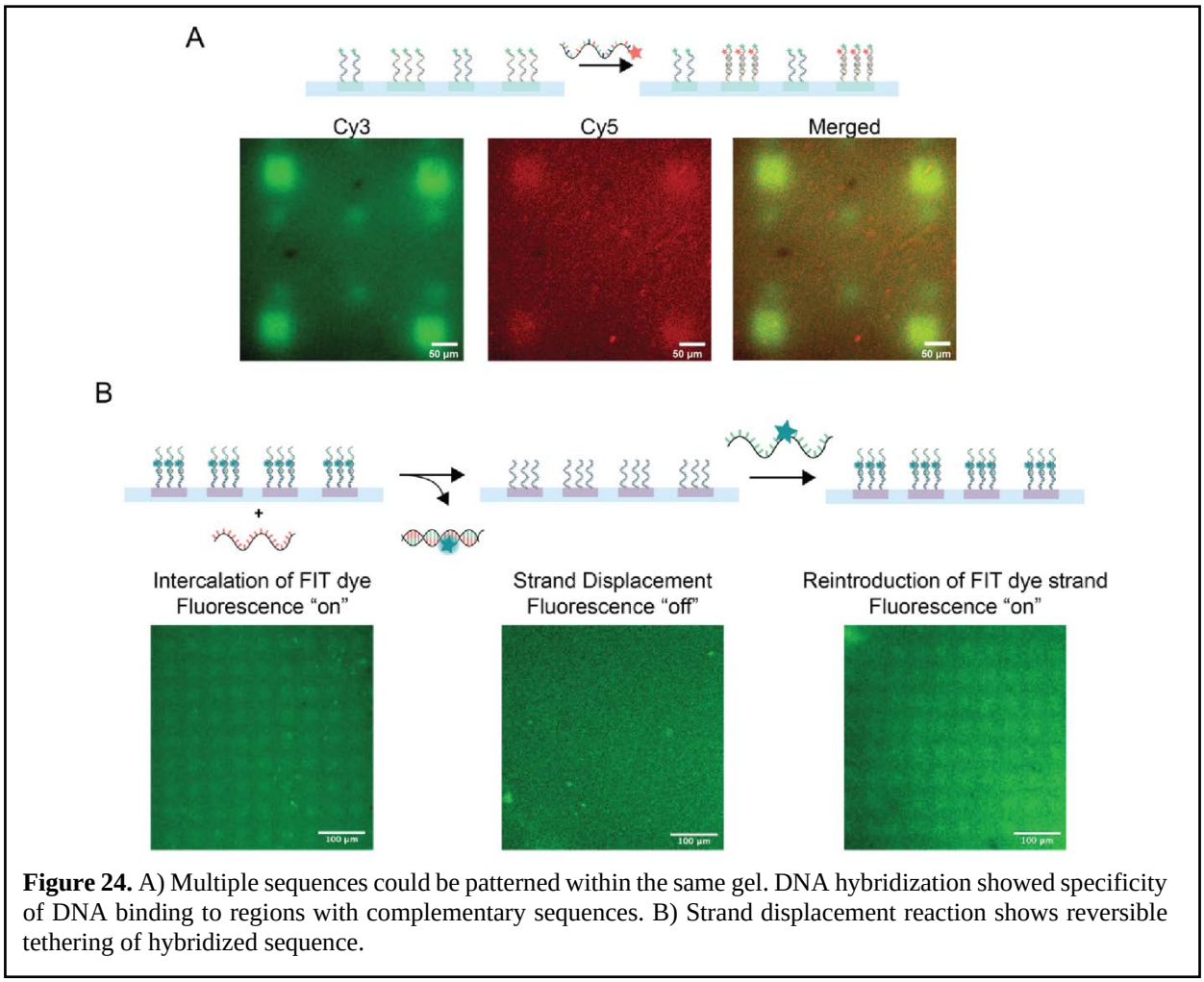

Figure 24. A) Multiple sequences could be patterned within the same gel. DNA hybridization showed specificity of DNA binding to regions with complementary sequences. B) Strand displacement reaction shows reversible tethering of hybridized sequence.

To test if anchored DNA could be displaced using a strand displacement reaction, a complementary sequence (strand B) to an anchored DNA sequence (strand A) was designed, containing an 8 base overhang region. We hypothesized that in the presence of a complementary sequence containing increased complementarity (strand C), it would be thermodynamically favorable for the hybridized sequence to de-duplex with the anchored strand and bind to its full complement. To monitor this strand displacement reaction, strand B was functionalized with a forced intercalator dye, thiazole orange (TO). This dye fluoresces only upon forced intercalation in the oligonucleotide duplex, by restricting rotation around its methine bridge. We observed fluorescence turn on when strand B was hybridized to strand A and turn off upon introduction of

strand C, suggesting successful displacement. Additionally, we observed that fluorescence could be recovered when reintroducing strand B to the system, suggesting that this displacement is reversible **(Figure 24B)**.

Finally, an aptamer-DNA construct was designed to tether proteins to the hydrogel matrix. The model aptamer, thrombin binding aptamer (TBA), was selected due to its well characterized binding to the serine protease thrombin. To achieve functionalization of the aptamer a three-strand construct was utilized. First, a Cy3 fluorophore labelled sequence was patterned in the hydrogel. Next, a sequence containing the TBA was hybridized to the patterned sequence and a Black Hole Quencher labelled sequence, such that the quencher could reduce fluorescence of the fluorophore, and the sequence partially blocked the aptamer region of the sequence. Upon introduction of thrombin and folding of the aptamer, the quencher strand could be displaced, and fluorescence recovery was observed **(Figure 25)**.

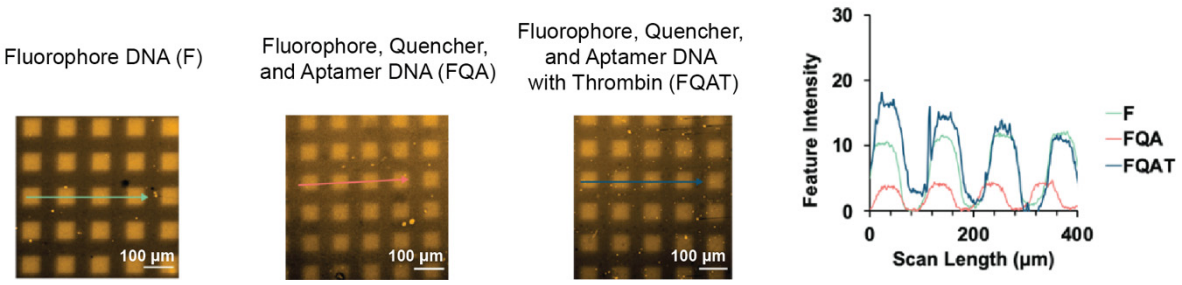

Figure 25. Thrombin binding aptamer with a fluorophore-quencher reporting construct was patterned to tether thrombin to the hydrogel. In the presence of thrombin, the aptamer sequences folds, displacing the quencher DNA strand. Thrombin binding to the aptamer can then be observed through recovery of the fluorescence signal.

Printing Temperature and pH Sensitive Materials. The implementation of stimuli responsive polymer/hydrogel in beam pen mediated printing enables the construction of soft material with distributed sensing and actuation properties. The temperature/ pH-sensitive poly(N-isopropylacrylamide) (pNIPAM) material was utilized as the ink and printed with BPL to fabricate stimuli responsive soft materials. Here, N-isopropylacrylamide (NIPAM) was copolymerized with

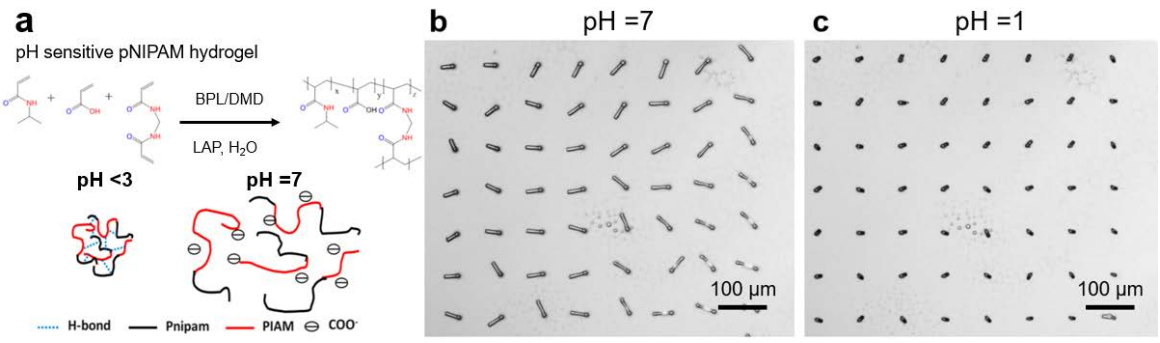

Figure 26. Photopatterned pH responsive hydrogel. (a) The chemical formulation of the pH sensitive pNIPAM hydrogel and the pH activation mechanism. Optical images of the DMD printed pNIPAM hydrogel in (b) pH 7 buffer and (c) a pH 1 acid solution where the hydrogel is contracted. The pNIAM polymer is composed of 20% NPIM, 20% MA, and 2% crosslinker. It was photocured with 405 nm light through a DMD. The morphology transformation is reversible.

acrylic acid (MA) and a di-acrylamide crosslinker to form the pH actuatable hydrogel (**Figure 26a)**. The polymer precursor was printed as 10 µm × 10 µm pillars via irradiation with 405 nm light through a DMD (**Figure 26b**). To create an acidic environment (pH=1), 0.1 M sulfonic acid was added. This induced a morphology transformation as the pNIPAM hydrogel contracted (**Figure 26a,c**). Importantly, the macroscopic changes are reversible, and the system returns to its initial state upon the displacement of the acid with PBS buffer. By tuning the composition of the pNIPAM, light can be used to pattern a series of "smart" polymers which can respond to various stimuli, including heat, pH, ionic strength, light, and magnetic and electric fields. The combination of pNIPAM with BPL printed PEGDA or GelMA would lead to the generation of soft materials with distributed sensing and actuation properties.

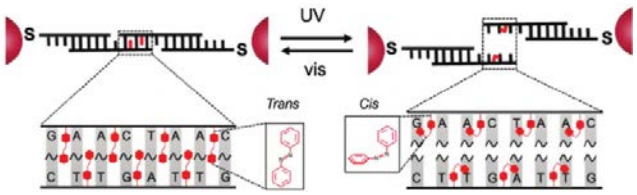

Figure 27. UV-Induced Disassembly of SNA Based Colloidal Crystals. Using UV/visible light cleaves/repairs strands on a SNA material. UV/visible light causes a reversible isomerization, whereby the trans position repairs DNA and the cis position cleaves DNA.

Patterning Colloidal Crystal Surfaces. Colloidal crystals form the basis for engineering novel optical and electronic elements, magnetic storage devices, and sensors.[1-3] There is, however, an unmet need for rapid, flexible, yet versatile methods to assemble complex colloidal crystal architectures with structural and functional characteristics precisely fine-tuned throughout the lattice. Our early proof-of-principle experiments suggest that the upgraded BPL platform along with the novel design of the colloidal crystals based on non-natural oligonucleotides could address this issue.

A promising method for assembling colloidal crystals into precise 2D and 3D structures is to graft metal (e.g., Au) nanoparticles with oligonucleotides and take advantage of sequence-specific hybridization.[4] The incorporation of azobenzene moieties, which can undergo reversable conformational transformations upon the exposure to UV (365 nm) and visible (460 nm) light, into the oligonucleotide links opens up the possibility of constructing light-responsive colloidal crystals (**Figure 27**). The light induced azobenzene conformational changes can introduce steric perturbations and trigger local dehybridization of oligonucleotide strands. The energy cost of light-induced conformational changes and the energy barrier of dehybridization can be precisely tuned by adjusting the sequence of the oligonucleotides, temperature at which the system is kept, and the number of incorporated azobenzene moieties. As such, this novel colloidal crystal system allows for temperature-controlled and light-directed erase and assembly of colloidal units from and into the crystal lattice, respectively.

To demonstrate the validity of this approach, a colloidal crystal lattice was first formed on a substrate out of gold nanoparticles (10-30 nm in diameter) interconnected with light-responsive DNA. The system was then heated close to its melting temperature (within 5 °C) to lower the energy barrier of dehybridization, followed by projecting a pattern with near-UV illumination to erase gold nanoparticles from the lattice in a precise, site-specific manner, leaving behind a 2D thin film colloidal crystal structure of a desired design.

Successful photopatterns of a crystalline thin film are shown in **Figure 28**. The upper left-hand side of the figure shows near-UV illumination being focused onto a substrate for DNA cleavage, reflecting off a DMD such that only the desired pattern is focused onto the substrate, thereby

resulting in DNA cleavage according to the desired pattern. Additionally, **Figure 28** also shows two successful DNA cleavage experiments, one of them is the Northwestern University seal (upper right-hand side) and the other one is the Northwestern University mascot (center bottom). The portions of the print that show up as lighter contrast, according to our microscopy measurements, are those parts of the DNA that have been cleaved away from the gold nanoparticle thin film. Scale bars in these images clearly show that the size of these features can be made as small as 15 μm over an ~ 600 μm scale, and finer microscope images (**Figure 28,** bottom left- and right-hand, respectively) clearly show the successful removal of light-sensitive DNA and their corresponding gold nanoparticles. It is worth noting that this feasibility study focused on validating the approach and used a lower resolution DMD patterning mode, but all the processes developed are compatible with our higher resolution BPL patterning mode.

Thus, this novel light-responsive chemistry based on non-natural oligonucleotides taken together with the newly developed technical capabilities of the BPL technology enables new opportunities for the design and fabrication of previously inaccessible active soft material structures and devices.

Facile Synthesis of Ultrahigh-Resolution Protein Micropatterns. Here, BPL is combined with cross-linking photopolymerization and thiol-acrylate coupling chemistry to provide a new, unparalleled means for printing biomolecular microarrays with ultrahigh resolution. Conventional strategies for producing functional bioactive microarrays (i.e., linear polymer synthesis) yield highly controllable polymer growth. However, relatively long reaction times (generally over 10 minutes) are required and chain-length limitations, due to the deactivation or embedding of the initiating ends, exist. In contrast, the BPL-based photoinduced cross-linking reaction of multifunctional acrylates proceeds more rapidly (in a few seconds) and thiol-modified target molecules (i.e., biotin and 6-mercaptohexanoic acid, MHA) can be incorporated simultaneously into the cross-linked network *via* thiol-acrylate coupling reactions (**Figure 29**). Furthermore, high-resolution protein microarrays (i.e., of streptavidin and/or fibronectin) can be achieved subsequently *via* streptavidin-biotin and MHA-fibronectin coupling reactions. By precisely controlling the UV dosage *via* the modulation of exposure time (seconds) and contact force (milli-newtons), BPL affords exquisite control over the photoreaction conditions on the substrate, thus making the photopolymerization and thiol-acrylate reactions highly tunable. This nanolithographic method enables the fabrication of nanoscale functional polymer

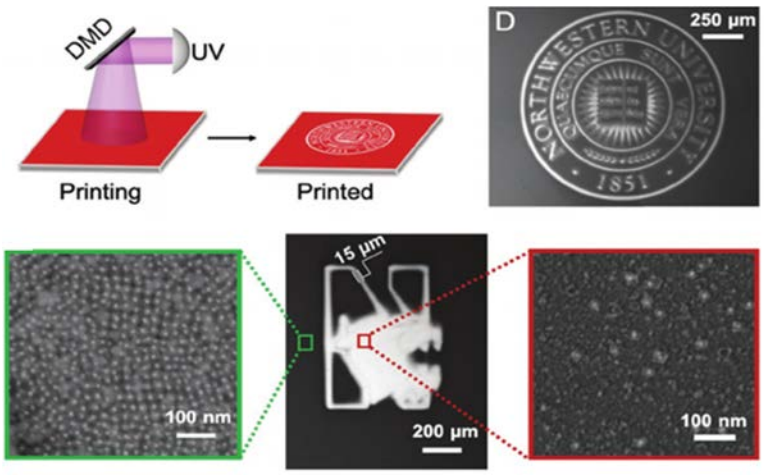

Figure 28. Photopatterning of crystalline thin films Using UV light and a DMD, a precise, arbitrary pattern can be focused onto a substrate covered with a thin film of photo-cleavable DNA. Prints were made on the cm scale with features as small as 15 μm. The green outlined image shows areas where photo-cleaving did not take place, and the red outlined image shows areas where photo-cleaving successfully took place as desired.

features (resolution < 300 nm) over large printing areas (3.84 mm × 5.12 mm), making these protein micropatterns adaptable for numerous applications. The BPL-printed bioactive polymers exhibit high protein binding affinity, and the amount of immobilized protein can be controlled based on photopolymer growth. Lastly, the addressability of the individual BPL probes allows the generation of arbitrary arrangements of 2D features while maintaining sub-diffraction resolution.

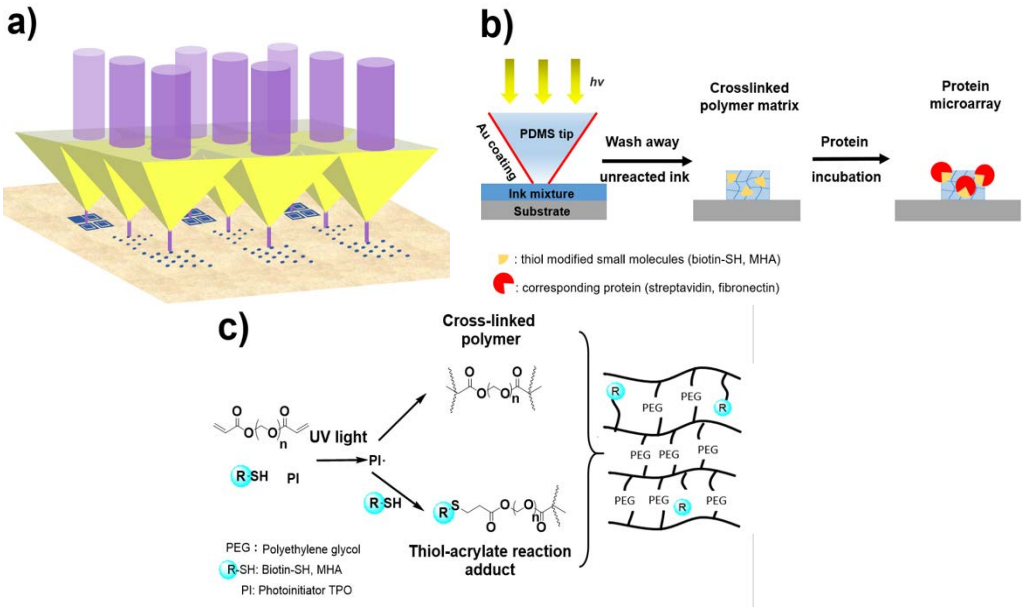

Figure 29. **(a)** Schematic of BPL-controlled, high-resolution printing on a surface. UV light passing through the apertures of the pyramid-like pens locally exposes the pre-polymer ink material, and the photoreaction progress is precisely controlled to form arbitrary patterns. **(b)** Schematic of BPL-controlled photopolymer printing and protein immobilization. **(c)** Reaction scheme of BPL-induced cross-linked network formation. UV light emitted from the tips during BPL induces the cleavage of photoinitiator diphenyl(2,4,6-trimethylbenzoyl) phosphine oxide (TPO) to release radical species for (i) initiating the homopolymerization of poly(ethylene glycol) diacrylate (PEGDA) and forming a cross-linked network as a scaffold, (ii) simultaneously triggering a radical-mediated thiol-acrylate coupling reaction and (iii) incorporating target binding, thiolated molecules (e.g., thiol-PEG-biotin, MHA) into the polymer matrix.

In a typical experiment, a TPO, PEGDA, and a thiol-PEG-biotin photopolymerization system was used and subsequently fluorescently labeled streptavidin was employed to create ultra-high resolution protein patterns. Due to its high stability and binding specificity, thiol-PEG-biotin was implemented as the target-binding species during lithographic printing. Before BPL printing, the gold surface was passivated using poly (ethylene glycol) methyl ether thiol (PEG) to minimize the non-specific binding of proteins (or cells) to the non-patterned areas.[5] A pre-polymer ink composed of TPO, PEGDA, and thiol-PEG-biotin (0.2 g/L, 21.2 g/L, and 1 g/L, respectively) was dissolved in NN-dimethylformamide (DMF) and then spin-coated onto the PEG-treated gold surface to form a uniform pre-polymer layer. The BPL pen array was prepared and mounted on a scanning probe system, equipped with hardware and software that allows advanced control over the patterning process (i.e., contact force in mN), exposure time, light intensity, and feature spacing). Illumination via BPL initiates the photo cross-linking of the PEGDA by repeatedly bringing the pen arrays into contact with the ink material on the surface (405 nm UV light, 90 mW/cm^2, dwell times: 0.2 to 3 s, printing force: 200 to 1,500 mN). After BPL printing, the surfaces were subsequently washed with acetone, ethanol, and Nanopure water to remove unreacted ink.

When an exposure time of 0.5 s was used, uniform 4 × 4 dot features (average diameter of 367 ± 21 nm) were patterned on the TPO, PEGDA, and thiol-PEG-biotin mixture. (**Figure 30a**). This biotin/polymer microarray was incubated in a PBS solution of fluorescently labeled streptavidin (20 µg/mL, 30 minutes), and the resultant protein pattern was evaluated using confocal microscopy (**Figure 30b**). As expected, the amount of attached streptavidin increases as concentration of thiol-PEG-biotin is increased from 0.02 mM to 3.12 mM (in DMF) within the polymer network (as the thiol-PEG-biotin concentration in DMF is increased from 0.02 mM to 3.12 mM).

BPL can be used to spatiotemporally control not only the morphologies of the features composed of polymers and thiolated moieties, but also the attachment of the corresponding binding proteins through the tuning of the UV exposure conditions. Using an ink material composed of TPO, PEGDA, and thiol-PEG-biotin (0.2 g/L, 21.2 g/mL, and 1g/mL in DMF, respectively), 10 × 10 gradient polymer features were printed using exposure times ranging from 0.2 s to 2 s (**Figure**

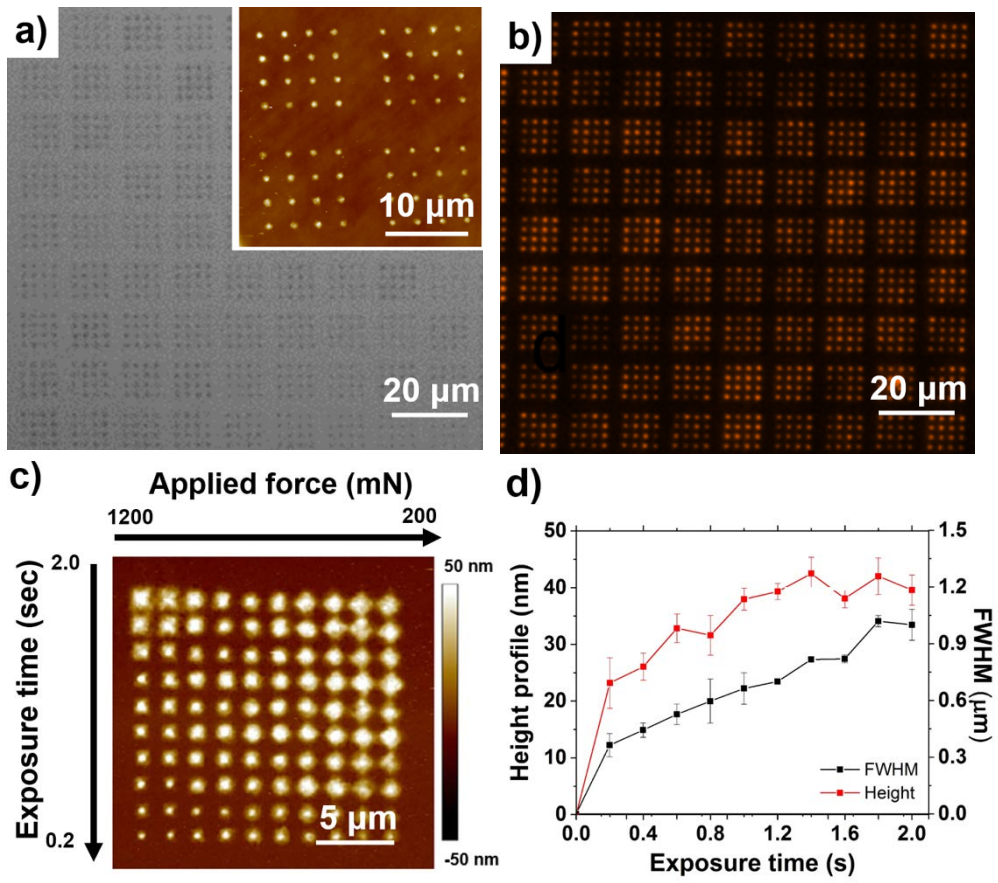

Figure 30. (a) Optical microscopy image of BPL-printed biotin containing cross-linked polymer patterns showing a representative area of ~10,000 duplicates of 4 × 4 dot features, using 0.5 s of 90 mW/cm^2 UV exposure and 800 mN of applied force. The inset shows an AFM image of the polymer pattern, and the average feature diameter was measured to be 367 ± 21 nm. (b) A fluorescence microscopy image of a biotin-containing array treated with fluorescently labeled streptavidin (streptavidin−Cy3), showing uniform immobilization of the protein on a BPL-printed pattern. (c) AFM image of BPL-printed 10 × 10 cross-linked polymer features, using dwell times (y-axis) of 0.2, 0.4, 0.6, 0.8, 1.2, 1.4, 1.6, 1.8, 2.0 s and printing forces of 200, 300, 400, 500, 600, 700, 800, 900, 1000, 1100, 1200 mN. (d) The evolution of the feature height and full width at half maximum (FWHM) of the BPL-printed polymer as a function of exposure time at a printing force of 1,200 mN.

31a). Based on the aforementioned morphology-control experiment (**Figure 30c**), a moderate printing force of 900 mN was applied here to acquire efficient control over the printed features. The normalized fluorescence intensity, calculated as the peak fluorescence divided by the baseline fluorescence, was used to quantify the amount of protein attachment. The normalized fluorescence intensity, calculated as the peak fluorescence divided by the baseline fluorescence, was used to understand the amount of protein attachment. After sufficient solvent wash and fluorescent protein treatment, a gradient of streptavidin patterns was obtained with normalized fluorescence intensity increasing from 2.4 ± 0.2 to 10.0 ± 0.7 with increasing UV exposure time was observed (**Figure 31b**). These data indicate that BPL can be used to precisely control the amount of immobilized protein within each printed feature. This feature makes the presented biopatterning technique attractive and enabling for many applications in functional biochips synthesis, antibody/peptide detection and screening, and cell biological studies.

In addition to biotin/streptavidin arrays, other types of protein nanoscale patterns can also be achieved using the appropriate thiol-binding species in this lithographic system. As a proof-of-concept, rhodamine-labeled fibronectin was immobilized on BPL-printed PEGDA/6-mercaptohexanoic acid (MHA) polymer patterns. First, the surface was passivated with PEG, and then TPO, PEGDA, and MHA (0.2 g/L, 21.2 g/L, and 0.8 g/L, respectively) were mixed as a pre-polymer ink and spin-coated on a gold substrate before BPL printing (force 900 mN, exposure time 0.8 s). After removing the unreacted ink and incubating with fluorescently tagged fibronectin, high-resolution fibronectin features with an average diameter of 810 ± 40 nm were generated and analyzed using confocal microscopy (**Figure 31c**). Fibronectin is an extracellular matrix (ECM) protein that is often used for the immobilization of cells on a surface. Indeed, single cells were attached to the individual micropatterns. However, in some cases, multiple cells attached to the individual micropatterns, and non-specific binding was observed.

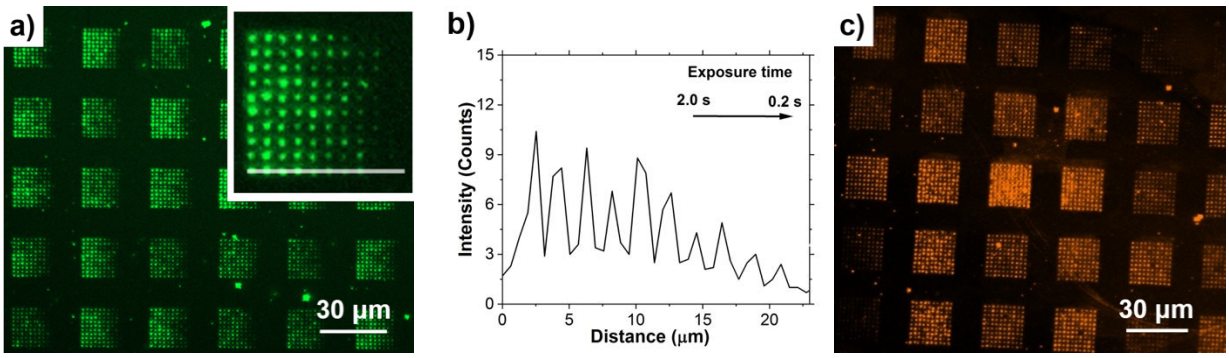

Figure 31. (a) Fluorescence image of a fluorescently labeled streptavidin (Streptavidin−Cy3) array printed on the pattern prepared using BPL with a constant force of 900 mN and illumination times of 0.2, 0.4, 0.6, 0.8, 1.0, 1.2, 1.4, 1.6, 1.8, and 2.0 s (increasing from right to left). The inset shows a 10 × 10 gradient array printed by a single pen. (b) Normalized fluorescence intensity profile of the features printed with different exposure times indicated by the white line in (a). (c) Fluorescence microscopy image of MHA-containing polymer pattern treated with fluorescently labeled fibronectin (rhodamine fibronectin), showing the attachment of fibronectin on the BPL-printed micropattern.

Previous reports describe how polymer pen lithography (PPL) can be used to pattern fibronectin to control focal adhesions and influence stem cell fate.[6] However, PPL cannot be used to modulate the micropattern design created by each pen and adjust protein density between or within the micropatterns as can be done with BPL. Furthermore, other studies point out that the implementation of PEG in biomaterials prolongs the circulation of proteins and peptides without compromising their bioactivity.[7] So, advantageously, this system could be used to control the 3D morphology of a polymer-based fibronectin pattern as well as its mechanical properties, serving as a tool for the preparation of arbitrary bioactive arrays that mimic the cellular microenvironment for the study and control of cell motility, differentiation, and organization.[8]

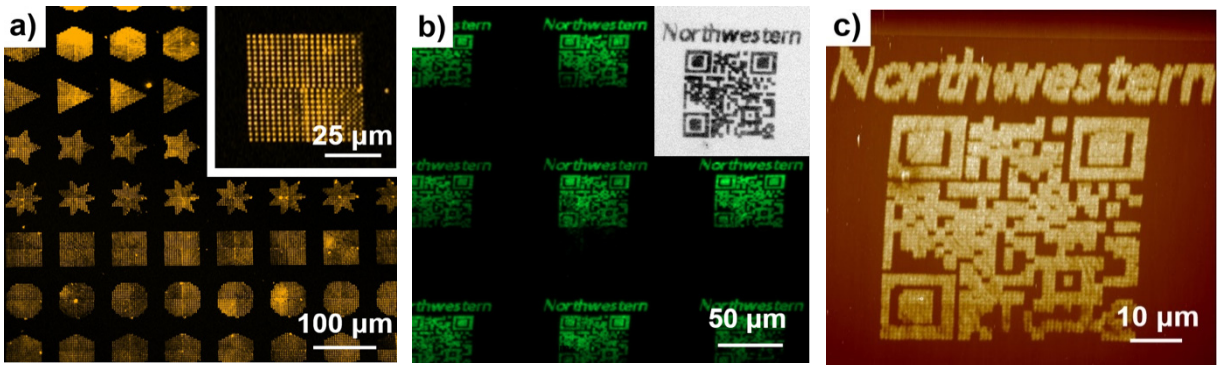

Figure 32. (a) Fluorescence microscopy image of fluorescently labeled streptavidin (streptavidin−Cy3) arrays of varied shapes (e.g., triangle, square, hexagon) printed by BPL. Inset shows a square pattern formed by dot features printed using a single tip. (b) Fluorescence microscopy image of "QR code" patterns generated after treatment with fluorescently labeled streptavidin. Inset shows the optical microscopy image of "QR code" printed by a single tip. (c) AFM image of the polymer pattern printed by an individual tip showing a continuous pattern formed by a pixel size of 830 ± 70 nm.

Conventional contact printing techniques, which are limited by directing cantilevers, are most often used to generate simple dot or line features in a restricted printing area. In contrast, BPL allows one to make arbitrary patterns using massively parallel and individually addressable pens. As a proof-of-concept, fluorescently tagged streptavidin microarrays with different pattern designs (e.g., triangles, squares, and hexagons, consisting of dot features with an average diameter of 750 ± 50 nm) were fabricated using actuated BPL. A pre-polymer ink, composed of TPO, PEGDA, and thiol-PEG-biotin, was photopolymerized within 50 × 50 µm regions using BPL (force 900 mN, dwell time 0.8 s, exposure intensity 72 mW/cm^2). After the removal of the unreacted ink, the system was incubated with Cy3-labeled streptavidin, and the protein patterns were developed (**Figure 32a**). Moreover, the BPL tool's advanced software automatically synchronizes the precise piezo movement of the sample relative to the BPL tip array, projected light pattern at each piezo position, and the light exposure once a desired image to be patterned is uploaded. As a result, BPL allows one to arbitrarily generate continuous features and therefore print micropatterns with more complicated designs. For example, a QR code to the Mirkin group website (https://mirkin-group.northwestern.edu/) with a size of 50 × 50 µm^2 was printed (**Figure 32b**). The resulting pattern was evaluated by AFM, and a continuous polymer pattern was formed with an individual pixel size of 830 ± 70 nm (**Figure 32c**).

Concluding Remarks

The research efforts and results presented here by Northwestern University (Mirkin Group) and TERA-print, LLC are the culmination of a multi-year investment to realize the ability to create arbitrability complicated, spatiotemporally actuated, 2D and 3D 'smart' nanostructures with physical and chemical functionalities dispersed throughout said structures. By using TERA-print's BPL technology, we were able to synthesize various soft-material structures with functionalities that were both nanoscopic in precision and as widespread as the whole mesoscopic structure. By adapting the technology to include a microfluidics sample holder with the ability to precisely control temperature, humidity, and near-UV light exposure, the TERA-print team provided a complete solution to enable TERA-Fab BPL technology to access and functionalize as wide a variety of soft material chemistries as possible,. The NU team used the solutions engineered by TERA-print to explore, modify, and construct 2D and 3D actuated nanostructures, accessing materials ranging from a post-polymerization functionalization method of tethering oligonucleotides to hydrogels, evaluating a photocurable polymeric system which was subsequently utilized to build 2D architectures with submicron precision, and investigating the properties of the photocured material and its application in functional small molecule surface writing was explored. Additionally, the NU team combined cross-linking photopolymerization and thiol-acrylate coupling chemistry to print biomolecule microarrays with ultrahigh resolution, and both teams highlighted the ability to engineer and pattern light-responsive colloidal crystals. Overall, the technical advantages of BPL (high-throughput, nanoscale precision, feature size and geometry modulated by light exposure and, tip-on-substrate force, etc.) were shown to be highly advantageous to synthesize nanostructures with the wide variety of chemical and physical functionalities presented in this report. Critically, the combined research efforts of Northwestern University and TERA-print, LLC have brought the goal of widespread access to facile printing of 2D and 3D 'smart' nanostructures with precisely controlled spatiotemporal functionalities much closer to realization, demonstrating that BPL TERA-Fab technology is not only well-suited to the immediate research challenges addressed in this report, but is integral for further progress to take place in the field of multi-functional nano-fabrication.

References

1. Urban, J. J., Talapin, D. V., Shevchenko, E. V., Kagan, C. R. & Murray, C. B. Synergism in binary nanocrystal superlattices leads to enhanced p-type conductivity in self-assembled PbTe/Ag2Te thin films. *Nature Materials* **6**, 115-121, doi:10.1038/nmat1826 (2007).
2. Auyeung, E. *et al.* Controlling Structure and Porosity in Catalytic Nanoparticle Superlattices with DNA. *Journal of the American Chemical Society* **137**, 1658-1662, doi:10.1021/ja512116p (2015).
3. Chen, J. *et al.* Collective Dipolar Interactions in Self-Assembled Magnetic Binary Nanocrystal Superlattice Membranes. *Nano Letters* **10**, 5103-5108, doi:10.1021/nl103568q (2010).
4. Zhu, J. *et al.* Light-Responsive Colloidal Crystals Engineered with DNA. *Advanced Materials* **32**, 1906600, doi:10.1002/adma.201906600 (2020).
5. Chandradoss, S. D. *et al.* Surface Passivation for Single-molecule Protein Studies. *JoVE*, e50549, doi:10.3791/50549 (2014).

6. Giam, L. R. *et al.* Scanning probe-enabled nanocombinatorics define the relationship between fibronectin feature size and stem cell fate. *Proceedings of the National Academy of Sciences* **109**, 4377, doi:10.1073/pnas.1201086109 (2012).
7. Lu, X., Perera, T. H., Aria, A. B. & Callahan, L. A. S. Polyethylene glycol in spinal cord injury repair: a critical review. *J Exp Pharmacol* **10**, 37-49, doi:10.2147/JEP.S148944 (2018).
8. Wu, J. *et al.* Binding characteristics between polyethylene glycol (PEG) and proteins in aqueous solution. *Journal of Materials Chemistry B* **2**, 2983-2992, doi:10.1039/C4TB00253A (2014).
9. Huo, F. *et al.* Beam pen lithography. *Nature Nanotechnology* **2010**, 637-640, doi:10.1038/nnano.2010.161.

SUPPORTED PERSONNEL

Prof. Chad Mirkin (2% Academic months, 2% summer months, PI, NU)
Dr. Xinpeng Zhang (25%, postdoctoral fellow, NU)
Dr. Alex Anderson (31%, postdoctoral fellow, NU)
Namrata Ramani (50%, graduate student, NU)
EunBi Oh (29%, graduate student, NU)
Dr. Andrey Ivankin (49.91%, TERA-print, CTO)
Dr. Shaowei Ding (24.33%, TERA-print, Research Scientists)
Dr. Kyle Justus (12.32%, TERA-print, Research Scientists)
Dr. Will Hutson (79.84%, TERA-print, Research Engineer)
Jared Magoline (14.63%, TERA-print, Research Scientists)

Cover Page
To: Dr. Samuel Stanton, samuel.c.stanton2.civ@mail.mil; Ms. Katie Wisecarver, katie.wisecarver@us.af.mil
Subject: Final Report
Contract/Grant Title: Composite Soft Materials with Decentralized and Distributed Actuation
Contract/Grant #: FA9550-18-1-0493
Reporting Period: 9/15/2018-9/14/2021

ACCOMPLISHMENTS

Research objectives:

Research Focus Area 1

- Synthesis and Characterization of Responsive and Actuatable Composite Hydrogels
- Synthesis and Photo-degradable/-Crosslinkable-Nucleic Acids Bonds in Hydrogels
- Examining Responsiveness of Hydrogels

Research Focus Area 2

- Development of a Nanofabrication Strategy to Rapidly Modify Local Physicochemical Properties and Functionality of Hydrogels under Controlled Environments
- Controlled Environment Capabilities
- Near-UV BPL Capabilities

Research Focus Area 3

- Design and Synthesis of Hydrogels with Distributed Actuation and Sensing
- Uni-layer Composite Systems with Distributed Properties
- Multi-layer Composite System with Distributed Properties
- Design of Actuatable Systems

Details of accomplishments:

Over the last three years, the Northwestern University (NU) team has 1) developed a post-polymerization functionalization method of tethering oligonucleotides to hydrogels, 2) evaluated a photocurable polymeric system which was subsequently utilized to build 2D architectures with submicron precision using BPL, and 3) fundamental studies to investigate the properties (i.e., mechanical behavior, biocompatibility) of the photocured material and its application in functional small molecule surface writing was explored. Additionally, BPL was combined with cross-linking photopolymerization and thiol-acrylate coupling chemistry to print biomolecule microarrays with ultrahigh resolution. By taking advantage of the rapid photo-induced polymerization reaction of multifunctional acrylates with thiol-modified target molecules, the NU and TERA-print teams were able to apply the fundamental advantage of BPL (ultrahigh print resolution and precision over a large printing area) to create finely controlled cross-linked polymer matrices with well-calibrated feature positions, heights, and diameters, which were incubated with proteins post-polymerization to create the final biomolecule microarray product.

Simultaneously, the TERA-print team developed and implemented elegant solutions to enable BPL printing of hydrogels under well controlled environmental and thermodynamic states. Specifically, TERA-print 1) developed and integrated environmental control systems to adjust temperature and relative humidity within the sample chamber, providing a method to finely control the hydration and gelation/physiochemical state of hydrogels during the patterning process; 2) designed and prototyped a microfluidics system to enable rapid exchange of reagents within the experimental chamber, enabling the printing of spatially distributed, disparate functionalities into soft materials; 3) demonstrated the successful use of the microfluidics system by exchanging hydrogel solutions in the experimental chamber in real-time to enable the construction of multi-material architectures while maintaining BPL's inherent resolution and print registry; 4) introduced BPL patterning with near-UV (365 nm) light to expand the spectrum of compatible photochemistries; 5) with technical advances and novel non-natural oligonucleotide chemistries

developed by NU, both teams highlighted the ability to engineer and pattern light-responsive colloidal crystals. The key goals of this project were met, and more details regarding 1) major activities; 2) specific objectives; 3) significant results or key outcomes (such as major findings, developments, or conclusions); and/or 4) other achievements are included in the Technical Update section below.

Dissemination of results:

The results of these efforts have been disseminated through various forms. Two peer-reviewed papers have been published that acknowledge this award. Furthermore, Mirkin gave more than 25 seminars (many of them virtual), including two distinguished lectureships: the Graham Lecture at the University of Virginia and the G. M. Kosolapoff Award Lecture at Auburn University. Mirkin was also awarded the ACS Division of Colloid and Surface Science Award for Outstanding Achievement in Nanoscience, the G. M. Kosolapoff Award (Auburn University and the Auburn Section of the American Chemical Society), the Royal Society of Chemistry de Gennes Prize, and the Acta Biomaterialia Gold Medal. Because of the collaboration with TERA-print, many of the inventions arising from this award are already being incorporated into the next generation of TERA-print nanofabrication technologies.

IMPACTS

Development of the principal discipline(s) of the project:

A long-standing goal of the nanoscience and nanoengineering communities is to actualize the ability to construct arbitrarily complex 2D and 3D 'smart' architectures with chemical and physical functionalities encoded directly into the materials at the micro- to nanoscale. Such advanced material engineering capabilities would open up the possibilities for precise spatiotemporal insertion of sensing and actuation modalities into complex material architectures, revolutionizing the entire fields of soft micro- and nanorobotics, bioengineering, and drug design and discovery, and more. Research and development efforts have been emphatically pursued to realize such 'smart' structures, from inkjet printing to soft lithography. However, these, and other, methods are not sufficient to create 3D structures with functionalization that is widespread, precise, and multi-functional for all conceivable 3D shapes and volumes.

In this project, Northwestern University (Mirkin Group) and TERA-print, LLC worked together to bring the prospect of engineering 3D nanostructures with limitless functionalization possibilities into reality. Beam pen lithography (BPL), invented in the Mirkin Group and commercialized by TERA-print, is uniquely positioned to engineer 3D functional materials with decentralized, spatially distributed actuation and control. BPL delivers structured and highly focused light to a substrate *via* a massively parallel array of pyramidal-shaped microprobes with nanoscopic apertures to enable the rapid generation of arbitrary patterns with diffraction unlimited, sub-300-nm resolution over the mesoscopic length scale. The simultaneous development of actuatable soft materials responsive to light and engineering solutions that allow BPL to act on such soft materials under all requisite environmental and thermodynamics states would, when combined, extend the limits of how complicated a 3D nanostructures shape can become and allow for the full scope of desired functionalities.

Other disciplines:

The advances made by both teams over the last three years have brought the goal of facile printing of 2D and 3D 'smart' nanostructures with precisely controlled spatiotemporal functionalities much closer to reality. By combining a microfluidics BPL platform with environmental controls and fundamental research into soft material properties, the future scope of soft materials nano-engineering will expand for the development of novel mechanical and chemical interfaces with living tissues, smart materials with adaptable optical and electronic properties, and sensing devices.

Describe the impact in this reporting period on the development of human resources

As a result of this project, several students have received advanced training in interdisciplinary research, including postdocs, graduate students, and staff scientists. One student has successfully defended their PhD. EunBi Oh received her PhD from NU and accepted a postdoctoral position with Professor Ryan Truby. Graduate student Namrata Ramani successfully passed her qualifying exam, a major milestone towards obtaining her PhD. Thus, this effort is making a substantial impact on increasing participation in the sciences and maintaining US competitiveness in STEM.

Describe the impact on teaching and educational experiences

This award has had a substantial impact on teaching and educational experiences at Northwestern. This project brings together one of the top research institutions in the nation (Northwestern) with an industrial collaborator (TERA-print), enhancing the experience, educational opportunities, and diverse backgrounds and perspectives. In addition, the interdisciplinary nature of the research enhances educational opportunities for researchers at the university and industrial level. This project brings together researchers with backgrounds in chemistry, engineering, and materials science. To achieve the project outcomes, they must all learn about each other's work and fields.

The Mirkin group is committed to engaging with students of all backgrounds and education levels. Exposure to nanolithography instruments, biology, chemistry, instrument development, and surface science are made available to students. This promotes a multidisciplinary educational environment that encourages collaborative learning from a diverse set of backgrounds. Mirkin has also had a substantial impact on education as director of the International Institute for Nanotechnology at Northwestern. Over 120 of his group's alumni hold faculty positions at top research institutions worldwide. Mirkin teaches nanochemistry concepts in his General Chemistry courses, and he is working to incorporate such lessons into textbooks so that they can reach wider audiences. He also gave a guest lecture in the Northwestern Kellogg School of Management Commercializing Innovations class.

Describe the impact in this reporting period on physical, institutional, and information resources that form infrastructure:

Nothing to report

Impact on society beyond science and technology:

Mirkin presented as a Distinguished Lecturer at the Kavli Nanoscience Institute at Caltech. Additionally, this year Mirkin presented at the GRC Connects event on the subject of "Innovation by Biomaterials" on International Women's Day 2021, highlighting the important work of women in the scientific community. This year, he also presented at two meetings pertaining to the progress

of the National Nanotechnology Initiative (NNI). Further, TERA-Fab instrumrents are already being used by researchers in seven countries on three continents in applications ranging from biosensing, microfluidics, and soft microrobotics. By expanding the capabilities of BPL, namely high-resolution printing and massively multiplexed optical exposures, to create biological and soft material chemistry on a single chip, this technology will gain significant interest and gain adoption from researchers in new industries, such as synthetic biology, tissue engineering, biotech and pharma, agriculture, and even molecular data storage.

CHANGES

Changes in approach

Nothing to report

Problems or delays

Nothing to report

Expenditure Impacts

Nothing to report

Significant changes in the use or care of human subjects, vertebrate animals and/or biohazards

Nothing to report

Changes to the primary place of performance from that originally proposed

Nothing to report

TECHNICAL UPDATES

Development of a Nanofabrication Strategy to Rapidly Modify Local Physicochemical Properties and Functionality of Hydrogels under Controlled Environments

Soft materials, i.e., hydrogels used in this project, are extremely sensitive to ambient conditions, such as temperature and humidity. Small variations in these parameters can drastically alter the thermodynamic state, physicochemical properties, and functionality of the fabricated active architectures. In addition, the construction of soft smart materials with multiple sensing and actuation functionalities requires the ability to assemble various modalities into composite architectures. The latter can be achieved, for example, by sequentially introducing inks of interest into the print bed *via* a fluidics system and polymerizing these materials in-registry using light. The development of these technical capabilities could enable new possibilities in soft robotics, smart materials, sensing, and tissue engineering, and, as such, was one of the main focuses of this project.

Over the course of the project, the TERA-print team has invented and prototyped a series of hardware upgrades for its commercial nanofabrication platform, TERA-Fab™ E series. Based on the beam pen lithography (BPL) technology it provides an unmatched set of nanofabrication capabilities to soft active materials. The team has introduced environmental control capabilities to control the thermodynamic state of the material being printed, developed the ability to rapidly exchange liquids and gases within the sample chamber for multi-material fabrication, and increased the accessible light wavelengths to broaden the spectrum of material chemistries that the system can activate and process.

Controlled Environment Capabilities

Introducing the ability to perform BPL experiments under controlled environmental conditions required re-thinking many aspects of the instrument. The following engineering challenges needed to be overcome: (*i*) a heating/cooling element needed to be integrated beneath the sample to allow for on-demand temperature adjustments of the sample without affecting nearby sensors and motors; (*ii*) a new, enclosed, air-tight printing chamber needed to be designed that allows for the real-time, leak-free exchange of reagents in the print bed, as well as supports for the tip/tilt motion of a BPL array and mm-scale vertical 3D builds; (*iii*) the operation of the fluidics system needed to be automated to allow for highly orchestrated exchange of inks, motion of motors, and photopolymerization with light into multi-material architectures; and (*iv*) an external, computer-controlled humidifier together with a humidity sensor needed to be introduced and programmed to operate in a PID feedback loop and maintain a desired ambient humidity in the experimental chamber with ±2% precision.

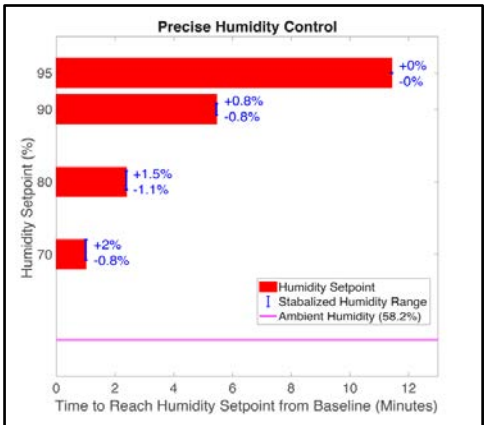

Figure 1. Humidity Control. x-axis corresponds to the time (min) required to raise the humidity from the ambient conditions (RH 58.2%). Error bars denote the humidity range achieved after the system stabilized for 3 min.

Humidity Control. We successfully introduced humidity control by connecting an external humidifier (w × d × h: 18 × 18 × 22 in; Asakuki, 100-HM001) to the BPL enclosure. The enclosure was modified to accept an adapter that allowed a water-resistant hose to run from the humidifier to the enclosure. Computer control of the humidifier was achieved using an Arduino board and a power relay in connection with an electrical feedback circuit that monitored the current humidity of the BPL instrument. Easy-to-use software was developed to quickly switch the humidifier between ON and OFF states, either based on the user's direct input or a user defined setpoint. In this way, the desired humidity can be defined, and the electrical PID feedback loop will operate to regulate the output of the humidifier to reach and maintain that setpoint. Figure 1 shows the relationship between the desired humidity setpoint and how long it takes to reach that setpoint from ambient humidity. In addition, it shows the stability of the humidifier to maintain the desired setpoint once it has been reached. This result demonstrates that with the optimized PID feedback loop, our system can achieve and maintain to within 2% the desired humidity in the print chamber and, as such, control the thermodynamic state of soft materials being processed.

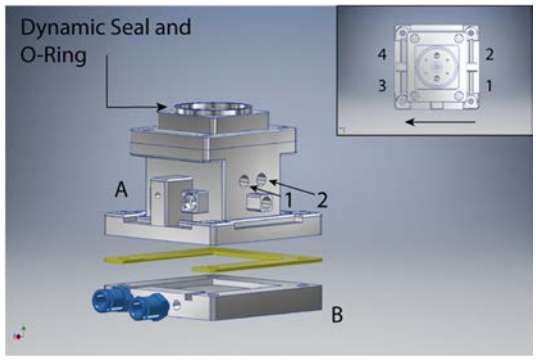

Figure 2. Temperature Control Apparatus. The thermocouple is sandwiched between the sample holder (A) and the aluminum bottom (B). Inset: Top view of the sample holder, denoting entrance apertures (1 and 2), exit apertures (3 and 4), and flow direction for fluidics.

Temperature Control. Temperature control and microfluidics control were partly achieved jointly through the re-design and construction of a new sample holder. **Figure 2** shows the latest

iteration of the sample holder design used in this project. A thin polyethylenimine (PEI) plastic layer is introduced between two aluminum elements to thermally decouple the top and bottom of the sample holder. When an electrical current is passed through a Peltier thermocouple, one side begins to heat up while the other side begins to cool down, depending on the direction and magnitude of the current. The temperature of the sample affixed directly atop of the sample holder can be regulated by changing the magnitude and direction of the electrical current passing through the thermocouple. Furthermore, we introduced water circulation through the bottom piece of the sample holder, which was designed to effectively remove excess heat generated by the system when the sample is cooled relative to ambient temperature (the water-cooling circuit is equipped with a radiator and a fan).

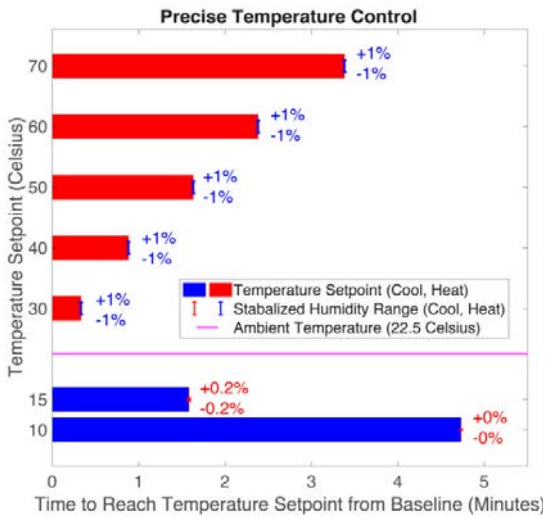

Figure 3. Temperature Control. x-axis corresponds to the time required to heat (red) or cool (blue) the sample from room temperature (22.5 °C). Error bars denote the temperature range achieved after the system stabilized for 7 min.

Control over the electrical current (i.e., temperature) was achieved *via* a feedback mechanism that includes regulator hardware (Laird, SH14-125-06) and a software implemented PID loop. This system enables a user to heat or cool the sample to any temperature within the 10 – 70°C range in less than 5 min and maintain the temperature within ±1 °C from the setpoint (**Figure 3**). Such precise and rapid temperature control provides a user with additional means to modulate the physicochemical state of soft materials during printing, potentially enabling access to new, previously unattainable structures and functionalities.

Microfluidics Control. The design and construction of the new, air-tight microfluidics sample holder is shown in **Figures 2** and **4**, respectively. The holder has two input and two output ports to ensure uniform distribution of liquid material over the sample. In addition, the sample holder features a vacuum channel and O-ring for affixing a sample, which is necessary to ensure an air-tight volume for the liquid to flow in and out without risk of seriously damaging other equipment (e.g., force sensors, piezo stages, etc.). Critically, the resolution and registry of printing are not affected by continuous application of a vacuum pressure of approximately -60 kPa, sufficient for affixing the sample (**Figure 5**).

The new sample holder in the BPL instrument was upgraded to create a fully sealed sample chamber for introducing soft materials between a substrate and a cover glass/BPL array. This was achieved by introducing a dynamic aluminum ring with a 2.25 mm travel range (**Figure 2, top**). The ring is actuated pneumatically by flowing air underneath v*ia* a Fluigent pressure pump (FLPG005 and LU-FEZ-02000). The air pressure lifts the ring and brings it into contact with a BPL array/glass, making a seal via a 1 mm wide O-ring. The overall chamber volume can be dynamically changed by adjusting the sample chamber position relative to the BPL array/glass, in conjunction with judiciously modulating the air pressure as needed. The total volume range was determined to be from ~300 µL (*initial print volume*) to ~1,440 µL (*maximum print volume*), and 1.2 bar of air pressure was demonstrated to deliver a seal without leaks from the sample chamber for liquid flow rates ranging from 100 – 1100 µL/min. This corresponded to an overall force of 900 – 2000 mN pushing down on the sample holder, well within the maximum load capacity of the motor controlling the vertical position of the sample (CONEX, TRB12CC).

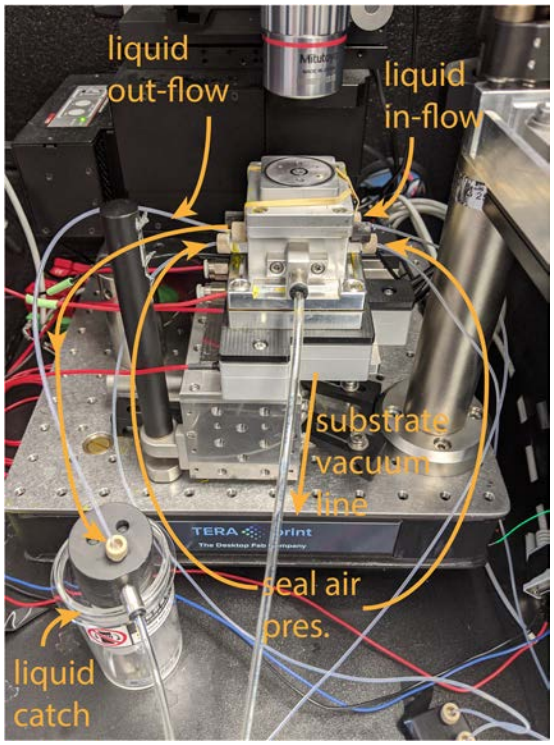

Figure 4. Microfluidics System. Experimental apparatus for testing fluidics design. Input and output ports are labeled consistent with that in Figure 2.

Actual flow control of the soft material (i.e., hydrogel) into the new fluidics sample holder was achieved using a Fluigent microfluidics flow system (Fluigent; FLPG005, LU-FEZ-02000, and MSW002). This system can flow soft materials into the chamber using pressurized air and can switch between materials on demand at any time over the course of a print. Unpolymerized material was flown out of the system using a vacuum line connected at the outlet ports (Parker; C190-12) and regulated via a vacuum pressure regulator (SMC; ITV0090-3UBS). Such an approach buttressed the accessible flow rates of 100 µL/min – 1100 µL/min and minimized the risk of pressure build up in the system and consequent leaks.

Taken together, these technical advances extend the capabilities of printing multiple soft materials at their controlled thermodynamic states in registry with high resolution, as shown in proof-of-principle experiments (**Figure 5**).

Near-UV BPL Capabilities

The first generation of the commercial BPL instrument featured two illumination sources with wavelengths of 405 nm and 532 nm. However, many photochemistries require illumination in the near-UV range (i.e., ~365 nm) for reactions to occur efficiently. The integration of near-UV illumination capabilities is not a trivial task and requires more than just changing the LED light source. The primary issue is that commonly used off the shelf optical components, including lenses, mirrors, and prisms, are optimized for the visible light spectrum (> 400 nm wavelength).

These elements absorb light in the near-UV range, and would, therefore, decrease the intensity of the transmitted light to the sample and heat up the DLP elements, potentially causing irreversible damage, if they were used with a near-UV LED. To mitigate these problems, we took a multi-pronged approach: (*i*) a number of mirrors were coated with aluminum to improve their reflectivity in the near-UV range; (*ii*) a custom lens was designed and manufactured to replace a pair of lenses in the light path to minimize the travel distance through the lenses and, thus, the intensity loss; (*iii*) a radiator was added to the DMD chip to provide passive cooling, and the volume of the radiator and the fan rotational velocity on the LED were increased to more effectively draw heat from the LED operating at the maximum power; (*iv*) the LED was overdriven at 10 A to achieve acceptable 365 nm light intensities and reaction rates. Additionally, the ability to drive the DMD in an '8-bit' mode, whereby the state of each micromirror of the DMD is modulated according to the value assigned to each micromirror (i.e., 0-255, the standard 8-bit values), was exploited to create an image of the DMD at the sample with even intensity throughout the image. This was done to ensure that all DMD micromirrors, and thereby all BPL micro-tips, presented the same intensity of near-UV on the substrate surface, resulting in print consistency and standardization across the entire printing area. By using a beam profiler (Edmund Optics) to collect images of the DMD projection and processing each image using MATLAB scripts, it was possible to iteratively 'correct' the DMD projection until uniformity was achieved such that the standard deviation of intensity over the whole image is ≤ 5% from the average. These modifications have allowed us to add the 365 nm illumination capabilities to the TERA-Fab™ E series repertoire, enhancing the modularity of the instrument's illumination offerings and providing access to the widest set of chemistries possible.

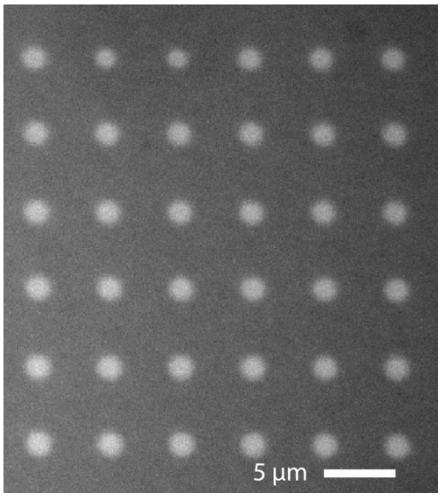

Figure 5. Printing Under Vacuum. Image of an etched 6 × 6 print made while the substrate was under vacuum (-20 kPa). Feature size and dot-to-dot distance are indistinguishable from a print with no vacuum applied.

Synthesis and Characterization of Responsive and Actuatable Composite Hydrogels

Over the course of this project, the NU team has developed novel hydrogel and soft matter materials with responsiveness and actuation that can be precisely calibrated and tuned using BPL technology. Developing novel polymeric materials and chemistries to manipulate their properties is a major part of this project and, more specifically,

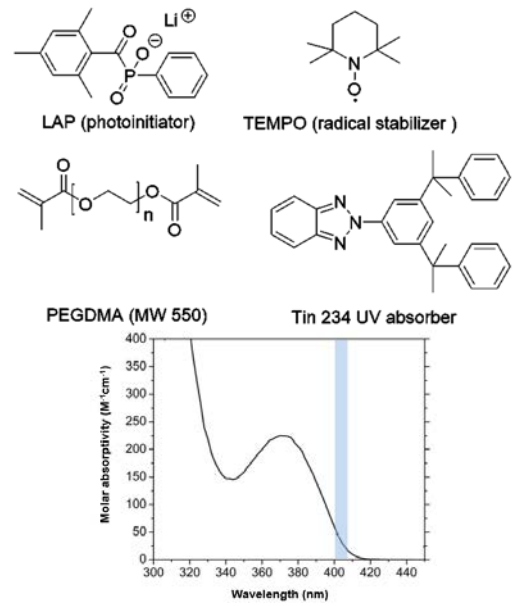

Figure 6. Chemical structure of the polymer ink (top). Absorption spectrum of lithium phenyl-2,4,6-trimethylbenzoylphosphinate (LAP) photoinitiator and the 405-nm LED light from the DMD (bottom).

working with many multi-faceted materials enables BPL to access a greater variety of actuation capabilities than other technologies. Functional polymeric materials constructed from photocurable acrylated monomers were synthesized and the polymerization kinetics between polymer stiffness and exposure dose were calibrated. Additionally, oligonucleotides were incorporated into a hydrogel backbone as a method for tuning the mechanical properties of the hydrogel structure.

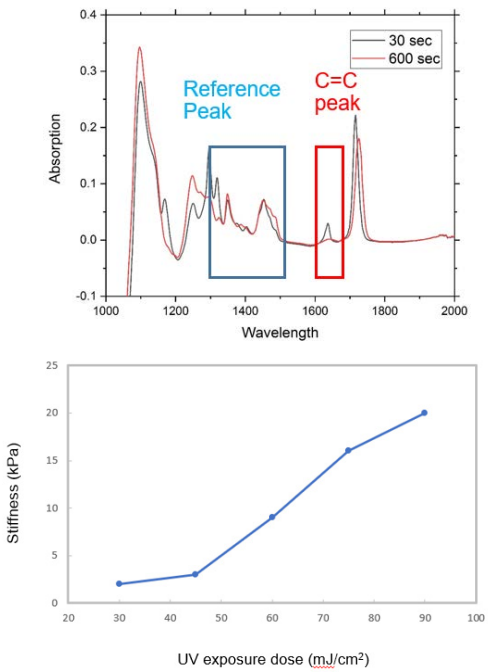

Figure 7. Acrylate monomer conversion upon UV light irradiation as measured by attenuated total reflection (ATR) measured (top). The evolution of the hydrogel stiffness as the function of the exposure dose (bottom).

3D functional polymeric materials for printing with beam pen-directed photopolymerization. Beam pen-regulated material printing (BPL) is utilized to fabricate stimuli-responsive digital 3D architectures via a photopolymerization methodology. The development of such highly controllable, smart materials revolutionizes a variety of research areas and applications in nanotechnology, biomedicine, microrobotics, and materials science and engineering. We developed a photocurable polymeric system and combined it with a DMD and BPL to construct 3D materials with sub-micron precision.

The photopolymerization system is synthesized using photocurable acrylated monomers. By tuning the functionality of the polymer ink (**Figure 6**), the chemical and physical properties of the material can be designed for specific applications. The kinetics and photoresponsiveness of the hydrogel photocuring are highly dependent on the properties of the photoinitiator. The absorption spectra of the photoinitiator as well as the emission of the DMD is shown in **Figure 6**. A UV absorber (Tin 234) and appropriate radical stabilizers (e.g., butylated hydroxytoluene and (2,2,6,6-tetramethylpiperidin-1-yl)oxyl (TEMPO)) were used to improve the fidelity of the photo-printed polymer architectures.

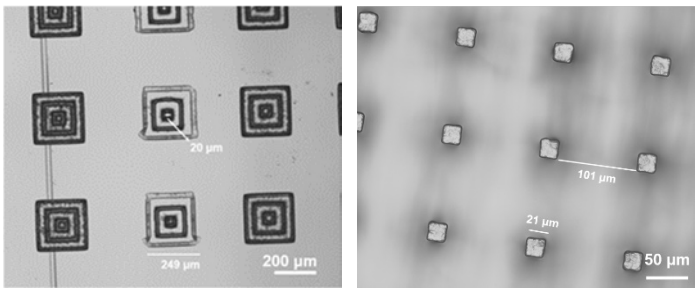

Figure 8. Optical images of the DMD light-patterned 2D hydrogel structure.

Beam pen-mediated 3D printing differentiates itself from other prevailing 3D printing techniques. For beam pen photocuring to be successfully performed, an understanding of the photopolymerization kinetics must be obtained in the context of certain experimental parameters (e.g., vertical printing rate, irradiation conditions). During photopolymerization, the consumption of polymer can be determined by monitoring the acrylate peak by Fourier transform infrared spectroscopy (FT-IR) (**Figure 7**). The IR reference peaks at 1420-1500 cm^{-1} and 1330-1370 cm^{-1}

were used as standard peaks to calculate the amount of acrylate. The remaining acrylate moiety can be controlled by the applied exposure dose, making it available for further modification and functionalization (e.g., DNA and proteins). The AFM experiments demonstrate that the photopolymerization of the hydrogel can be used to construct a variety of functional materials with tunable stiffness (moduli ranging from 2-25 kPa) (**Figure 7**).

With a fundamental understanding of the polymer ink, DMD was used to build 2D patterned structures from the acrylate system (**Figure 8**). Preliminary results demonstrate that 2D square features and simple patterns can be readily prepared by DMD-controlled photopolymerization. The resolution of the 2D patterned features is 5-10 μm, with a variation in height of 20-70 μm depending on the exposure conditions. Moving forward, we expect that by optimizing the polymer ink system will increase architecture fidelity to make it an appropriate curing system for beam pen-mediated printing.

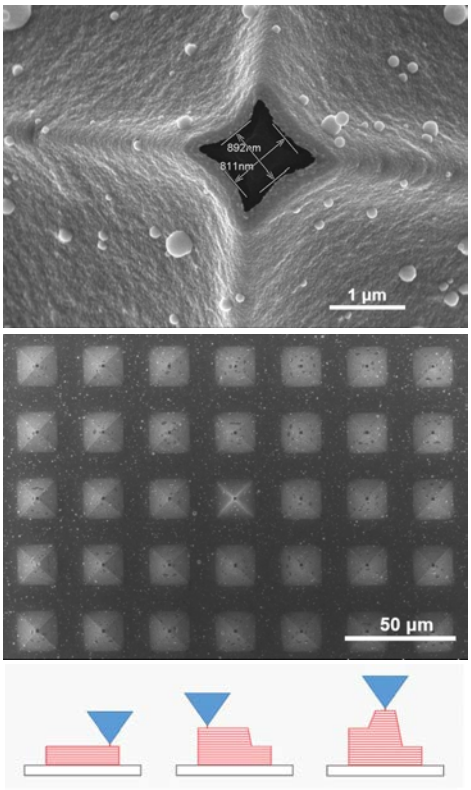

Figure 9. SEM image of a BPL pen array (top, middle). Schematic of layer-by-layer printing methodology in beam pen-regulated photopolymerization (bottom).

SEM images of the BPL pen array are shown in **Figure 9**. The size of the apertures on the pen array can be controlled from 400 nm to 2 μm. By controlling parameters such as the wavelength of light, exposure area, and exposure time, BPL can be used to build digital architectures with high spatiotemporal precision. Beam pen-regulated photopolymerization can be achieved by moving the substrate to control the photo-printing process, and the polymeric material is constructed in a layer-by-layer fashion (**Figure 9**).

In summary, this study focused on utilizing BPL as an efficient tool to develop a new 3D digital printing technique. Fundamental studies with the photocurable acrylate system were performed to investigate the photopolymerization kinetics and the mechanical properties of the photogenerated material. Preliminary DMD-controlled hydrogel patterning is demonstrated; however, further improvements in the polymer ink and the printing methodology are also required to fully achieve BPL-controlled 3D material printing. Later we show that by exploring new additives in the photocuring system stimuli-responsive (e.g., pH, light, or heat sensitive) 4D functional materials can be constructed.

Synthesis and Photo-degradable/ Crosslinkable-Nucleic Acids Bonds in Hydrogels

Stimuli-Responsive Nucleic Acid Crosslinks in Hydrogels. Oligonucleotides, including short strands of DNA, offer a highly tunable and programmable way of modulating the mechanical properties of soft matter. By spatially distributing oligonucleotide crosslinks in a controlled manner, local anisotropic responses within a hydrogel can be observed. A key component of this project deals with identifying and synthesizing a hydrogel platform that is amenable to chemical

functionalization. To develop such a highly tunable hydrogel system, a polyethylene glycol diacrylate (PEGdA) system with pendant functional acrylate groups was synthesized. The gel was polymerized on an acrylated glass slide with a 250 µm spacer. Next, a photochemical cross-linker, sulfosuccinimidyl 6-(4'-azido-2'-nitrophenylamino)hexanoate (Sulfo-SANPAH) was identified that could be used to chemically conjugate oligonucleotides to the hydrogel backbone (**Figure 10**). To attach the oligonucleotides to the PEGdA gel, the gel was incubated with the photochemical cross-linker overnight. Upon irradiation of the gel with 365-nm UV light, using a photomask, the linker was attached to the PEG backbone, leaving a sulfo-NHS ester to react with any primary amine. The gel was then incubated with an amine-functionalized T_{20} DNA strand with a Cy3.5 fluorophore overnight with shaking. Confocal micrographs revealed a localization of the fluorescence signal to the patterned areas (**Figure 11**).

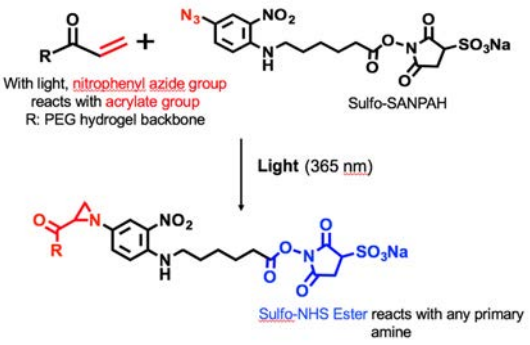

Figure 10. **S**ulfosuccinimidyl 6-(4'-azido-2'-nitrophenylamino)hexanoate (Sulfo-SANPAH) photochemistry. Using 365 nm UV-light, the azide can react with the acrylate, leaving the sulfo-NHS ester to conjugate with any primary amine.

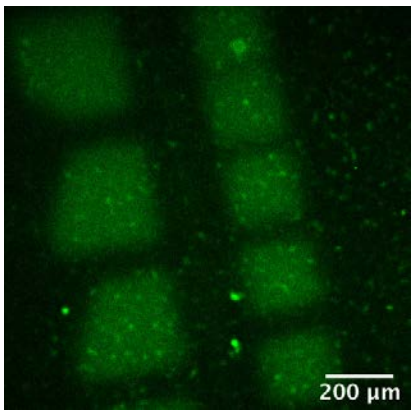

Figure 11. Confocal microscope images show patterns of localized fluorophore-labeled oligonucleotides made using a photomask and illumination at 365 nm.

Once it was shown that the oligonucleotides could be covalently conjugated to the gel, stimuli-responsive DNA was designed to change the mechanical properties of the hydrogel. I-motif DNA, a pH-sensitive oligonucleotide sequence that forms a secondary intercalated sequence under basic conditions or maintains an open form in acidic conditions, was synthesized (**Figure 12**). The i-motif strand was designed with amino modifiers on the 3' and 5' ends to perform crosslinking chemistry. Further, two sequences complementary to the ends of the i-motif sequence were designed to provide rigidity to the i-motif strand. The complementary strands contain fluorophore-labeled phosphoramidite bases (Cy3.5 and Cy5 coupled to the 5' and 3' ends, respectively). The fluorophores can be used to locate DNA strands within the hydrogel under the fluorescence mode of a confocal microscope. As the i-motif reversibly forms, the change in distance between the fluorophores can be tracked via distance-dependent Förster resonance

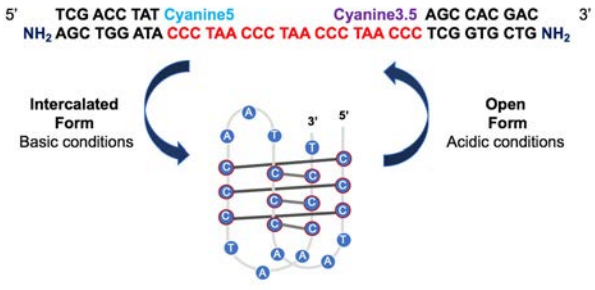

Figure 12. DNA sequence design and secondary i-motif structure.

energy transfer (FRET) measurements. Once synthesized, the strands were purified using high-performance liquid chromatography (HPLC) and characterized with matrix-assisted laser desorption ionization time-of-flight (MALDI-TOF) mass spectrometry to verify the correct sequence by mass.

Next, atomic force microscopy (AFM) was employed to measure stiffness changes in the material in the patterned areas when the i-motif is folded/unfolded. In addition, higher resolution and more complex features were printed using BPL. Finally, finite element models were used to model stress fields within the gel to predict how these materials change shape as a function of pH (*see below*).

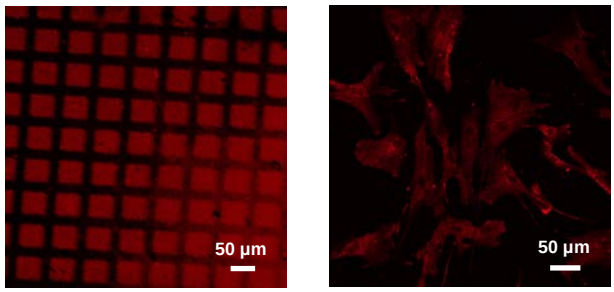

Figure 13. Fluorescence images of (a) a hydrogel patterned using a photomask and a 365 nm UV lamp and functionalized with fibronectin, which is labeled with AlexaFluoro 568 antibody, and (b) cells seeded and attached to the patterned hydrogels where vinculin is labeled with AlexaFluoro 633.

Examining Responsiveness of Hydrogels

Modulation of local chemistry of soft materials for biological studies. The chemistry of the PEGdA gels described previously was also used to construct soft materials with site-specific nanostructures, enabling biological studies. In addition to oligonucleotides, adhesion proteins, like fibronectin, can be incorporated into the gel to enhance molecular functionality. The sulfo-NHS ester from sulfo-SANPAH will react with primary amines in fibronectin. Using BPL, the attachment of fibronectin can then be precisely controlled and spatially decentralized on soft materials. The use of such soft, smart materials allows for the detection and acquisition of individual cells in a parallel manner. The manipulation of a single cell can also be performed at the nanoscale independently of the initial mechanical properties of the substrate.

In a proof-of-concept experiment, the PEGdA gels were incubated in sulfo-SANPAH overnight and exposed using 365 nm UV light and a pre-designed photomask. The gels were then rinsed with phosphate buffered saline (PBS) overnight and functionalized with fibronectin. To visualize the localization of fibronectin on the light-exposed areas, the gel was incubated in the fluorescently labeled antibody solution (**Figure 13a**). The cells were seeded on these hydrogels and stained for vinculin, which is a cytoskeletal protein found in the focal adhesions of cells (**Figure 13b**). To examine the compatibility of BPL with the gel system, a simple square pattern was made using a digital micromirror device (DMD) with the same light source (**Figure 14**).

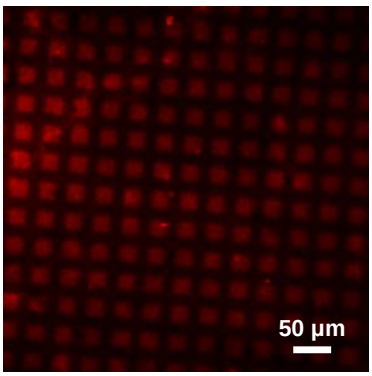

Figure 14. Image of a hydrogel patterned using a DMD system in a TERA-fab E series instrument. The square patterns indicate the areas that were exposed to light. Fibronectin conjugated to light-reacted sulfo-SANPAH and functionalized with antibody containing fluorescent molecules, Alexa Fluor 568.

Next, beam pen arrays were used to incorporate biological functionality into soft materials in a decentralized fashion from the nanoscale to the bulk. Adhesion proteins that are precisely distributed via beam pen arrays will enhance detection of individual cells for further bioanalysis. Using these actuatable hydrogels, fundamental biological questions pertaining to the physicochemical properties, such as substrate stiffness, cell shape, and extracellular matrix (ECM) domain size, affecting cellular behavior were answered (*see later sections*).

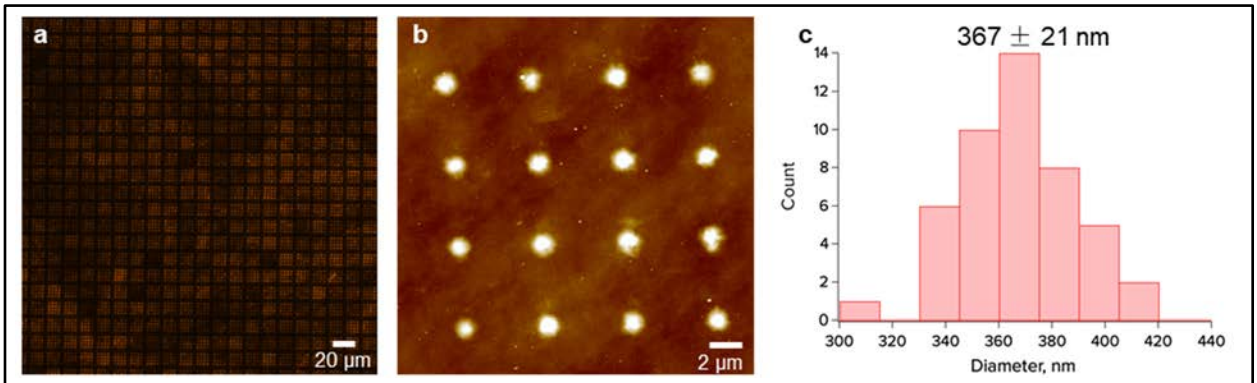

Figure 15. High-Resolution Printing of Hydrogels Using BPL. (a) Optical microscopy image of dot features of PEGDA patterned with BPL over a tens of square-millimeter area. (b) AFM image of hydrogel features in a pattern produced by a single BPL tip. (c) Histogram of feature diameter size obtained with AFM.

Design and Synthesis of Hydrogels with Distributed Actuation and Sensing Uni-Layer Composite Systems with Distributed Properties

Upon the introduction of the new technical capabilities to the BPL instrument, the NU and TERA-print teams joined forces to evaluate how these advances translate into new abilities in fabricating advanced functional soft material architectures. Our initial focus was on: (*i*) establishing the highest resolution with which we can print soft materials (i.e., hydrogels); (*ii*) demonstrating the ability to print multiple materials in registry; (*iii*) showing the modulation of local chemistry and mechanical properties in hydrogels; (*iv*) evaluating the platform's potential for 2.5D and 3D printing; and (*v*) showcasing the benefits of the environmental control capabilities by patterning colloidal crystal surfaces. These benchmarking and demonstration experiments were critical to establish the framework for the design of composite soft materials with distributed sensing and actuation properties that are feasible with the developed technology.

Printing Resolution. Although the potential of the BPL technology to pattern photoresists with sub-diffraction (< 250 nm resolution) was previously documented, printing soft materials such as hydrogels with high resolution is more challenging due to diffusion effects. To benchmark our resolution limits with hydrogels, we performed BPL experiments with two different hydrogel systems. One system included gelatin methacrylate (GelMA) with lithium phenyl-2,4,6-trimethylbenzoylphosphinate (LAP, Sigma-Aldrich) used as the photoinitiator, (2,2,6,6,-Tetramethylpiperidin-1-yl)oxyl (TEMPO, Sigma-Aldrich) as a free radical quencher, and phosphate buffered saline (PBS) as a solvent. The other system was poly(ethylene glycol) diacrylate (PEGDA) with TPO (diphenyl (2,4,6-trimethylbenzoyl)-phosphine oxide) used as a photoinitiator and dimethylformamide (DMF) as a solvent. These hydrogel formulations were photopolymerized into dot patterns using BPL by exposing the hydrogels to 405 nm light at an intensity of 180 mW/cm^2 for 0.5 – 1.5 s. The size of the features was established using optical

microscopy and validated using atomic force microscopy (AFM). **Figure 15** shows a representative PEGDA pattern with hydrogel features of < 400 nm in diameter.

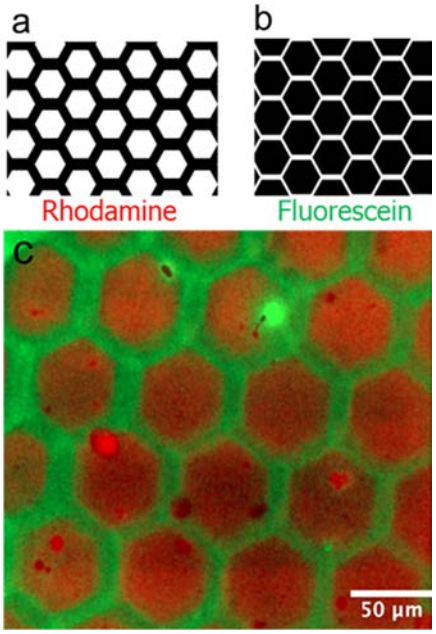

Figure 16. Multiple Hydrogel Compositions Printed In-Registry. DMD projection patterns for GelMA printing using (a) rhodamine and (b) fluorescein fluorophores. (c) The two patterns projected over the same area and imaged using confocal microscopy.

Printing In-Registry. In order to validate the potential of the newly developed fluidics system for the real-time *in situ* exchange of reagents in the sample chamber and printing multi-material architectures, we conceived an experiment, in which two GelMA hydrogel solutions doped with distinct methacrylated fluorophores (rhodamine B and fluorescein O-methacrylate) are sequentially introduced into the chamber and polymerized in complementary patterns. We first patterned a honeycomb array of hexagonal structures using rhodamine doped GelMA (**Figure 16a**), followed by extensive *in situ* (within the chamber) washing with warm water. We then introduced fluorescein doped GelMA and photopolymerized it into a bordering structure to complement the previous print (**Figure 16b**). The resulting composite structure was then washed and imaged using confocal microscopy (**Figure 16c**).

It is important to note that even though the in-registry printing resolution was ~10 µm, respectable for constructing composite architectures, it was not the focus of this demonstration and could be further improved by using BPL. This result provides a promising foundation for future applications involving the engineering of composite 2D and 3D layered structures with precise, spatially encoded chemical and mechanical sensing and actuation modalities.

Modulation of Mechanical Properties.

BPL can be used to control the local mechanical properties of soft materials. For example, a photo-responsive hydrogel can be exposed with light from the aperture at the apex of each pyramidal pen to modulate its cross-linking density, thus changing the stiffness of the gel. The degradation of a photodegradable PEG based hydrogel was initially validated using a DMD and 405 nm LED that is used to power BPL arrays. The hydrogels were irradiated, and the stiffness of the corresponding gels was then measured with AFM. An elasticity map of 10 µm × 10 µm square patterns

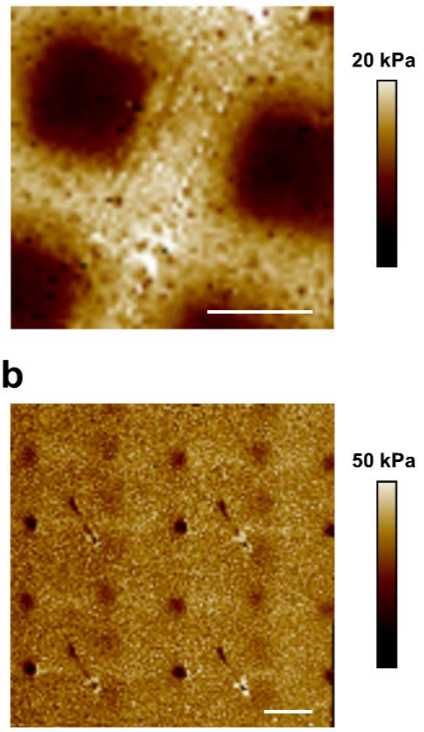

Figure 17. AFM images of patterned hydrogels using (a) DMD 10 µm x 10 µm squares and (b) BPL 1 µm radius circles. The darker regions indicate areas where the hydrogels were exposed to light and thus have decreased lower stiffness. Scale bar = 10 µm.

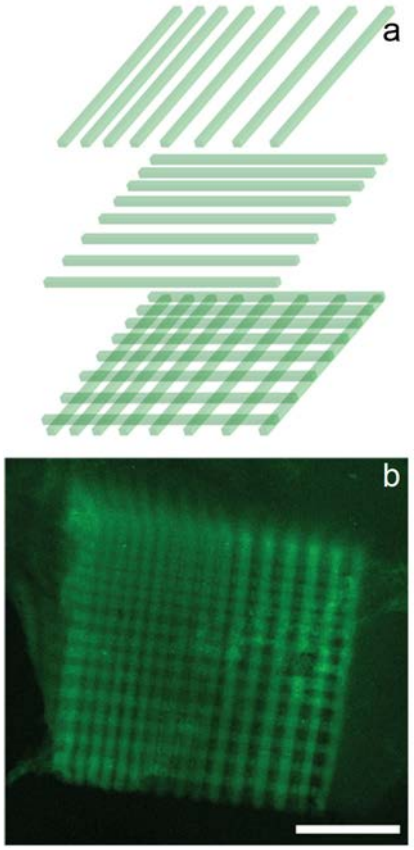

Figure 18. Layer-By-Layer DMD Printing. (a) Scheme of the 3D variable log pile concept to evaluate printing capabilities and (b) fluorescent image of the resulting print showing cross-stacked layers. Scale bar 100 µm.

obtained using AFM is shown in **Figure 17a**. After learning how to pattern hydrogels with a DMD, this knowledge was translated to the TERA-Fab and patterns were generated using BPL (**Figure 17b**). Here, the pattern size is limited by the aperture of the pen arrays; the smallest feature size achieved was 2 µm using a pen array with an average aperture size of 1.4 µm. We are currently working towards moving pen arrays in the *x* and *y* directions using a precise piezo controller to obtain more consistent patterns. These hydrogels with complex stiffness distributions can be used to study cellular behavior that could provide new insights in tissue engineering and regenerative medicine.

Multi-Layer Composite Systems with Distributed Properties

2.5D and 3D Printing. There are several ways to construct multi-layer architectures comprised of soft materials (i.e., hydrogels) with different sensing and actuation modalities. One such approach involves forming one layer of hydrogel, encoding a set of sensing and actuation functionalities into it, forming the next layer, encoding a different set of sensing and actuation functionalities into the second layer, and so on – one layer at a time. Alternatively, materials in the reaction chamber could be swapped in real-time and photopolymerized together in an additive manufacturing manner. The latter provides more flexibility and control over the accessible architectures and enables faster construction of more complex composite materials. This has motivated us to start exploring the potential of our platform for 3D printing hydrogel architectures.

Our first attempt relied on the use of the lower resolution DMD, and not BPL, mode for constructing a log pile structure out of GelMA. This latticed log pile design featured parallel rectangles of a consistent width and length separated by an increasing spacing and was printed as a basal layer before being rotated 90° and then printed again (**Figure 18a**). This procedure was repeated with the goal of producing a 3D structure. The structure was then dyed with fluorescein for imaging under a scanning light confocal microscope, showing the overlapping printed regions (**Figure 18b**). While this result was promising from the viewing window available, it was difficult to ascertain true 3-dimensionality from a confocal stack due to the diffusion limited nature of incubating a hydrogel in a fluorophore bath.

As such, the next refinement step will be to incorporate two different methacrylated fluorophores into the hydrogel mixture, in the same way it was done for printing two hydrogel compositions in registry, and alternate compositions as each new log-pile layer is printed.

Design of Actuatable Systems

Encoding of Chemical Functionality. BPL can also be used for encoding chemical functionality into 2D hydrogel architectures *via* a photopolymerization methodology. Here, acrylated

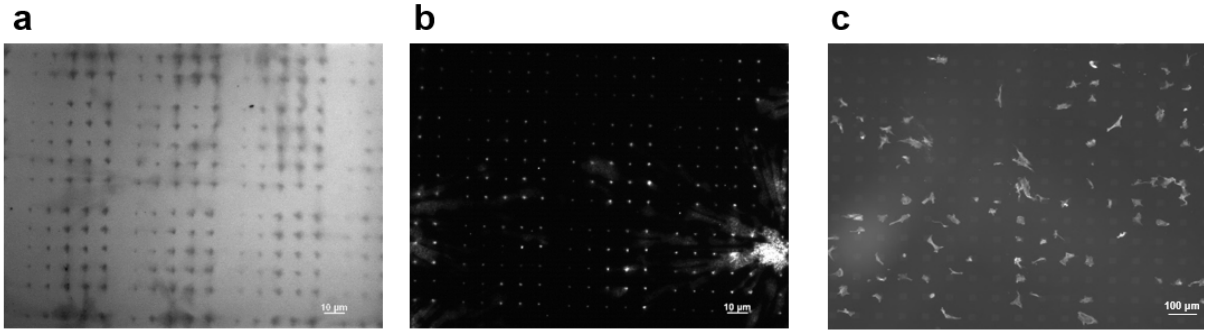

Figure 19. Encoding of Chemical Functionality. BPL controlled thiolayted material surface photo printing. (a) Optical image and (b) fluorescent image of SAMSA-SH dye within the PEGDA photopolymer. (c) Image of a fibroblast cell attachment study performed on the DMD printed, fibronectin functionalized PEGDA polymer.

photocurable polymeric systems were systemically investigated and combined with DMD and BPL printing systems to construct 2D functional materials with sub-micron precision. Additionally, we investigated the incorporation of functional small molecules into the photopolymers using a thiol modified fluorescein (SAMSA-SH), a practical challenge as thiolated functional molecules (e.g., dyes, nucleotides, proteins) can be covalently bonded to the PEGDA polymer network *via* thiol-acrylate "click" chemistry. Sub-micron patterns of PEGDA containing SAMSA-SH were successfully generated, as shown in **Figure 19a,b**, where the florescent image confirms the presence of dye within the crosslinked photopolymer. This demonstrates that BPL-regulated photopolymerization can be used to achieve high-resolution photopatterning of materials such as oligonucleotides, dyes, and proteins.

The BPL controlled printing of functional material 2D will open new avenues for a variety of applications and research including material sensing, as well as cell patterning and behavior studies. As a proof-of-concept, the features patterned with a thiolated, functional ink were used in a cell attachment study. MHA (6-mercaptohexanoic acid) was mixed with PEGDA and photocured under DMD exposure. The resulting 2D polymeric patterns (40 μm^2) were treated with fibronectin. The substrate was then washed with excess PBS to avoid non-specific cell binding. Cell attachment (fibroblast n1h3t3) on the patterned surface was successfully achieved (**Figure 19c**).

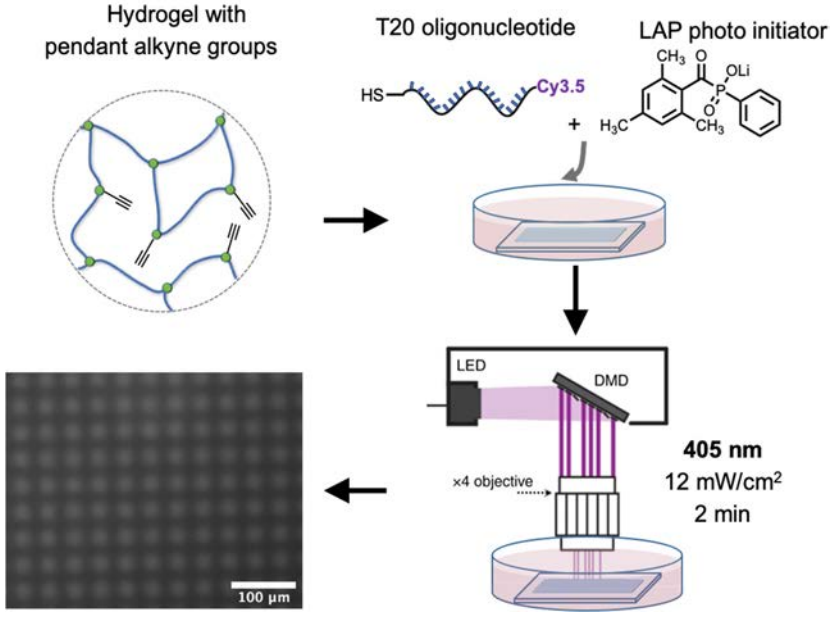

Figure 20. Oligonucleotide attachment workflow. Top left) hydrogel synthesized with pendant alkyne groups top right) Incubation of fluorophore labelled DNA and photo initiator bottom right) Photopatterning with digital micromirror device (DMD) bottom left) Optical microscope imaging of patterns.

However, the material composition and the photocuring methodology require modifications to increase the cell binding efficiency. In the future, beam pen controlled photopolymerization will be used to incorporate different biological functionalities into soft materials.

Spatially Encoding Stimuli-Responsive Nucleic Acids in Hydrogels. Oligonucleotides, including short strands of DNA, offer a programmable approach to design actuatable materials through the synthesis of sequences that form secondary structures as a response to light, pH, and chemical stimuli. By utilizing oligonucleotides as crosslinks in a polymer network, interchain connectivity can be reversibly modulated in a highly controlled fashion. Additionally, by spatially distributing oligonucleotide crosslinks in discrete domains within a hydrogel, local mechanical responses can be observed when a stimulus is applied.

Here, we explored a post-polymerization functionalization method to synthesize functional hydrogels with spatially patterned DNA domains. A key component of this project was first identifying and synthesizing a hydrogel platform that is amenable to photochemical functionalization as this will enable size and geometric control over the different domains. To this end, thiol-ene photochemistry was applied to this system, enabling the hydrogel to be functionalized with thiol terminated DNA in a light directed manner. This chemistry has been previous utilized in the patterning of proteins and other biomolecules as it is versatile, and has a high yield, rapid rate of reaction, and minimal side reactions.

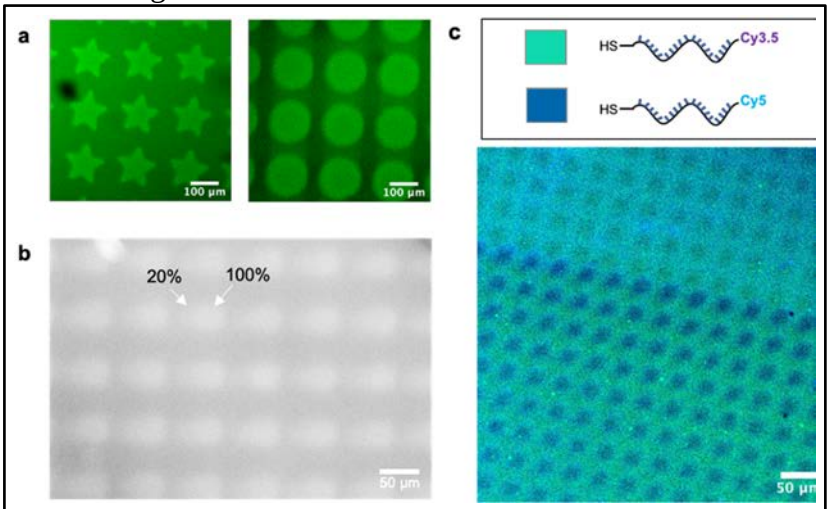

Figure 21. a) High fidelity geometric patterns are achieved via DMD control. b) Grayscale patterning is attained by varying LED source intensity, as seen with differing contrast between 20% intensity and 100% intensity features. c) Confocal microscope image of overlaid patterns with different fluorophore labelled DNA sequences.

To generate a system amenable to thiol-ene chemistry, a PEGDA system was copolymerized with propargyl acrylate, yielding a hydrogel with pendant functional alkyne groups (**Figure 20**). The gel was polymerized on an acrylated glass slide with a 250 µm spacer to ensure an even surface for patterning and was then incubated overnight in a solution of thiolated T20 oligonucleotide DNA with a cyanine3.5 fluorophore label. Next, a water-soluble photoinitiator, LAP, was added to the solution and allowed to diffuse into the hydrogel for 1 h. To covalently tether the DNA to the hydrogel network with light, a DMD with a 405 nm light source was used. The unreacted DNA was washed away, and the gels were imaged using fluorescent optical microscopy and confocal microscopy. The incubation time, light intensity, and exposure time were systematically studied to achieve optimal patterning conditions.

Once the patterning workflow was established, patterns of various geometries were prepared **(Figure 21a).** Confocal microscope images of star and circle patterns show sharp contrast between the patterned domains and background, suggesting DNA localization is limited to where the light is directed. Grayscale patterning was achieved by varying the LED intensity. The fluorescent optical microscope image in **Figure 21b** highlights that the fluorescence intensity of the patterned

features can be tuned by controlling the intensity of the light source while patterning. Patterning of multiple sequences was achieved through sequential incubation and irradiation steps. As a proof-of-concept, T20 DNA strands with different fluorophore labels, Cyanine 3.5 and Cyanine5, were patterned into a hydrogel sequentially (**Figure 21c**). Through alignment of patterned regions, microscale DNA domains of alternating sequence were arranged next to each other.

The next step in this study is to design stimuli-responsive oligonucleotide sequences that can modulate the mechanical properties of individual domains. These sequences can modulate crosslink density of the polymer network through hybridization interactions and the formation of secondary structures. By using the methodology developed for patterning multiple sequences, the effect of orthogonal triggers on domains of different stimuli-responsive oligonucleotide sequences was explored.

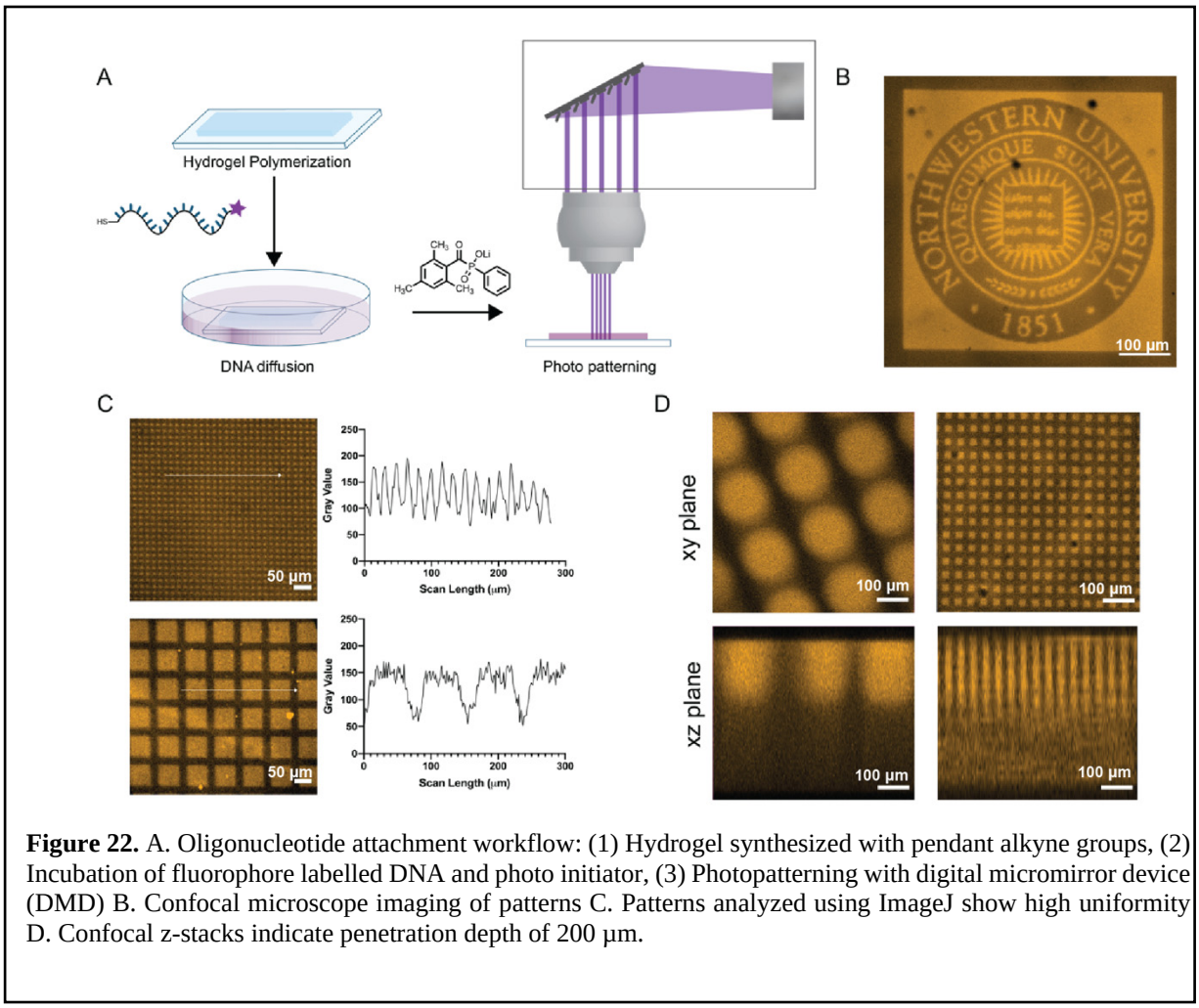

Figure 22. A. Oligonucleotide attachment workflow: (1) Hydrogel synthesized with pendant alkyne groups, (2) Incubation of fluorophore labelled DNA and photo initiator, (3) Photopatterning with digital micromirror device (DMD) B. Confocal microscope imaging of patterns C. Patterns analyzed using ImageJ show high uniformity D. Confocal z-stacks indicate penetration depth of 200 µm.

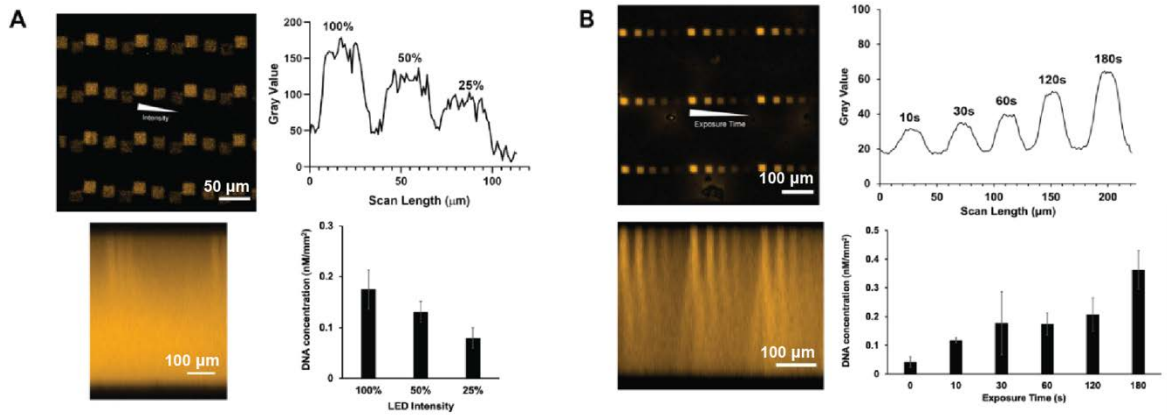

Figure 23. Confocal micrographs, z-stacks, line profiles and DNA quantification studies for (A) varying LED intensity and (B) Light exposure time.

The unreacted DNA was washed away and the gels were imaged using fluorescent optical microscopy and confocal microscopy **(Figure 22B**). A key advantage of using a DMD system is that uniform features can pe patterned over large areas, as shown in **(Figure 22C).** The variables of incubation time, light intensity, and exposure time were systematically studied to achieve optimal patterning conditions. DNA surface concentration was shown to be controlled by both light intensity and exposure time, enabling the patterning of gradient and discrete features of arbitrary geometry **(Figure 23)**. Z-stack analysis showed that functionalization in the z-direction varied with exposure time and not light intensity. To characterize DNA functionalization, patterned gels of varying exposure time and light intensity were degraded using 0.1 M NaOH and Cy3.5 fluorescence was measured using a plate reader. A calibration curve of known concentration of Cy3.5 T20 was used to correlate Cy3.5 fluorescence to DNA concentration. Measured concentration values followed similar trends as the image analysis of patterned features.

Patterning of multiple sequences was developed through sequential incubation and irradiation steps. As a proof-of-concept, T20 DNA strand, a 20-base anchor-DNA sequence with a Cyanine 3 fluorophore labels, were patterned into a hydrogel sequentially (**Figure 24A**). Through alignment of patterned regions, microscale DNA domains of alternating sequence were arranged next to each other. DNA hybridization between a patterned anchor strand and its complement was observed. When the Cyanine5 labelled complement to the anchor-DNA was added to the multi-sequence gel, fluorescence in the Cy5 channel was only colocalized with the complementary sequence.

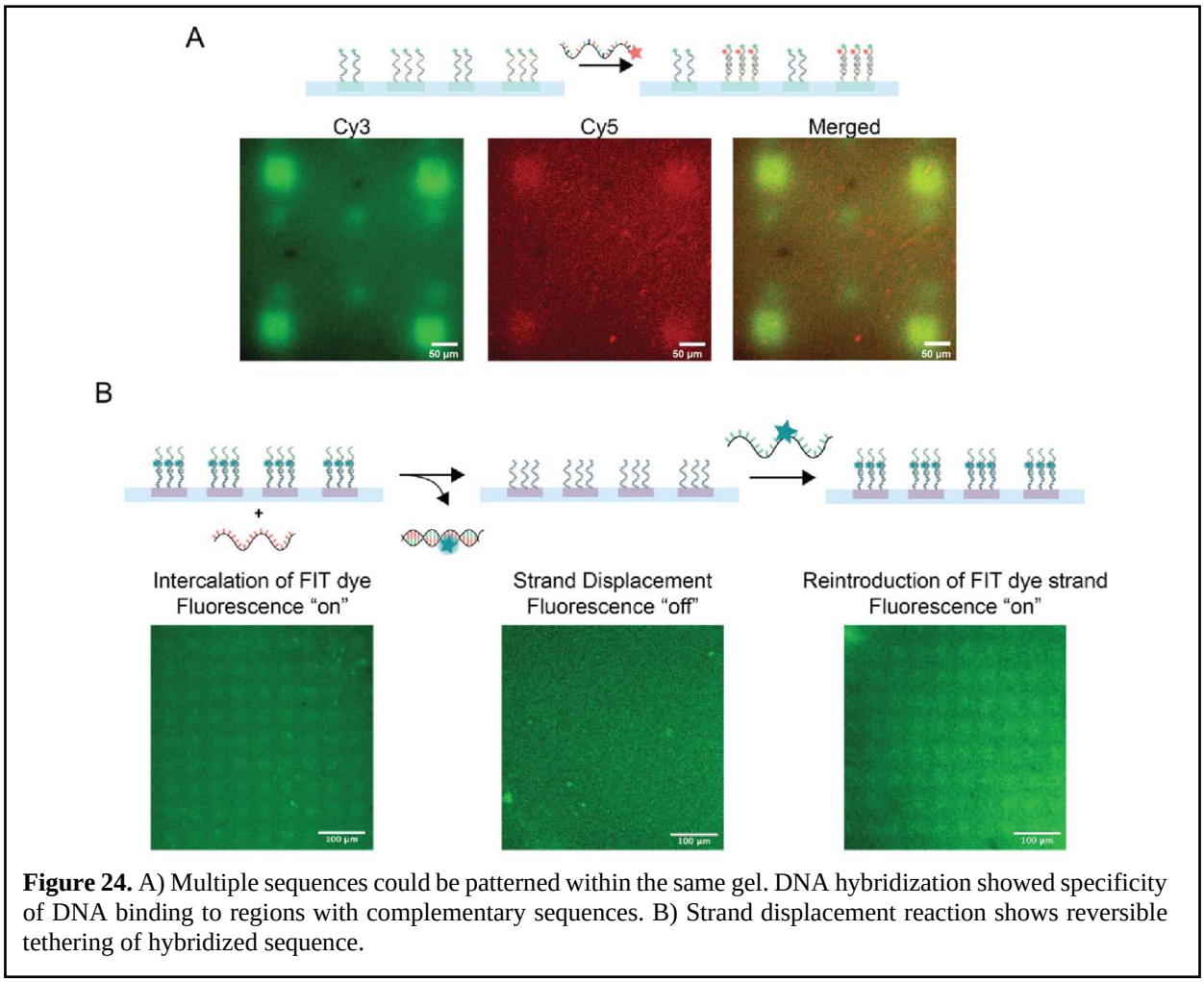

Figure 24. A) Multiple sequences could be patterned within the same gel. DNA hybridization showed specificity of DNA binding to regions with complementary sequences. B) Strand displacement reaction shows reversible tethering of hybridized sequence.

To test if anchored DNA could be displaced using a strand displacement reaction, a complementary sequence (strand B) to an anchored DNA sequence (strand A) was designed, containing an 8 base overhang region. We hypothesized that in the presence of a complementary sequence containing increased complementarity (strand C), it would be thermodynamically favorable for the hybridized sequence to de-duplex with the anchored strand and bind to its full complement. To monitor this strand displacement reaction, strand B was functionalized with a forced intercalator dye, thiazole orange (TO). This dye fluoresces only upon forced intercalation in the oligonucleotide duplex, by restricting rotation around its methine bridge. We observed fluorescence turn on when strand B was hybridized to strand A and turn off upon introduction of

strand C, suggesting successful displacement. Additionally, we observed that fluorescence could be recovered when reintroducing strand B to the system, suggesting that this displacement is reversible **(Figure 24B)**.

Finally, an aptamer-DNA construct was designed to tether proteins to the hydrogel matrix. The model aptamer, thrombin binding aptamer (TBA), was selected due to its well characterized binding to the serine protease thrombin. To achieve functionalization of the aptamer a three-strand construct was utilized. First, a Cy3 fluorophore labelled sequence was patterned in the hydrogel. Next, a sequence containing the TBA was hybridized to the patterned sequence and a Black Hole Quencher labelled sequence, such that the quencher could reduce fluorescence of the fluorophore, and the sequence partially blocked the aptamer region of the sequence. Upon introduction of thrombin and folding of the aptamer, the quencher strand could be displaced, and fluorescence recovery was observed **(Figure 25)**.

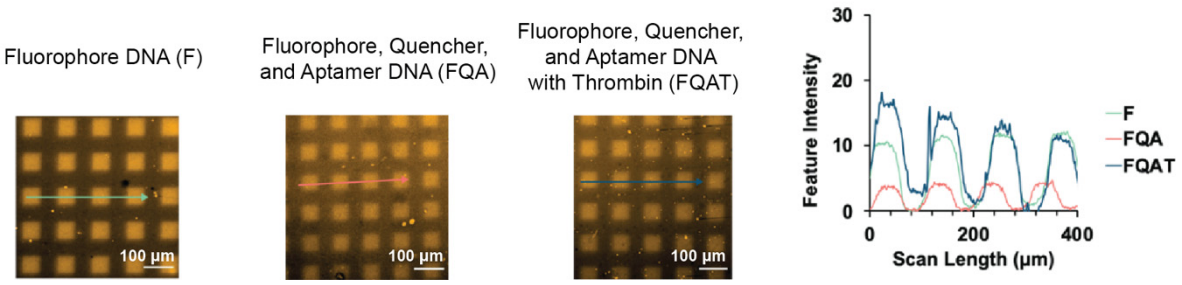

Figure 25. Thrombin binding aptamer with a fluorophore-quencher reporting construct was patterned to tether thrombin to the hydrogel. In the presence of thrombin, the aptamer sequences folds, displacing the quencher DNA strand. Thrombin binding to the aptamer can then be observed through recovery of the fluorescence signal.

Printing Temperature and pH Sensitive Materials. The implementation of stimuli responsive polymer/hydrogel in beam pen mediated printing enables the construction of soft material with distributed sensing and actuation properties. The temperature/ pH-sensitive poly(N-isopropylacrylamide) (pNIPAM) material was utilized as the ink and printed with BPL to fabricate stimuli responsive soft materials. Here, N-isopropylacrylamide (NIPAM) was copolymerized with

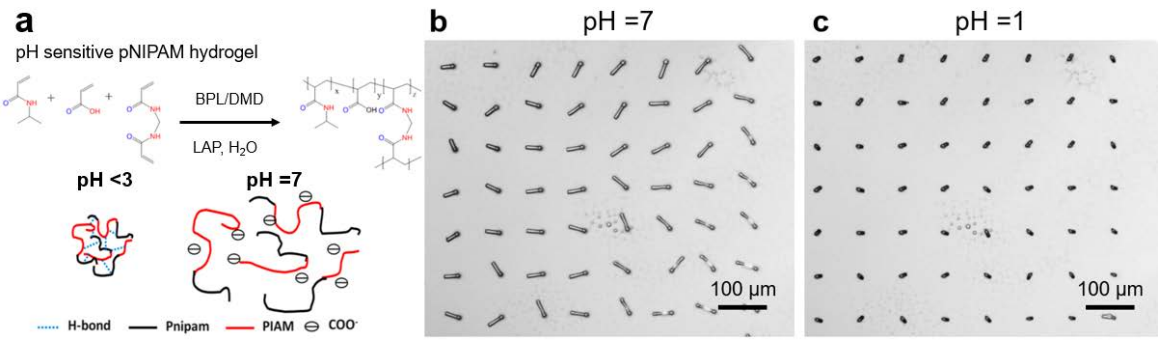

Figure 26. Photopatterned pH responsive hydrogel. (a) The chemical formulation of the pH sensitive pNIPAM hydrogel and the pH activation mechanism. Optical images of the DMD printed pNIPAM hydrogel in (b) pH 7 buffer and (c) a pH 1 acid solution where the hydrogel is contracted. The pNIAM polymer is composed of 20% NPIM, 20% MA, and 2% crosslinker. It was photocured with 405 nm light through a DMD. The morphology transformation is reversible.

acrylic acid (MA) and a di-acrylamide crosslinker to form the pH actuatable hydrogel (**Figure 26a)**. The polymer precursor was printed as 10 µm × 10 µm pillars via irradiation with 405 nm light through a DMD (**Figure 26b**). To create an acidic environment (pH=1), 0.1 M sulfonic acid was added. This induced a morphology transformation as the pNIPAM hydrogel contracted (**Figure 26a,c**). Importantly, the macroscopic changes are reversible, and the system returns to its initial state upon the displacement of the acid with PBS buffer. By tuning the composition of the pNIPAM, light can be used to pattern a series of "smart" polymers which can respond to various stimuli, including heat, pH, ionic strength, light, and magnetic and electric fields. The combination of pNIPAM with BPL printed PEGDA or GelMA would lead to the generation of soft materials with distributed sensing and actuation properties.

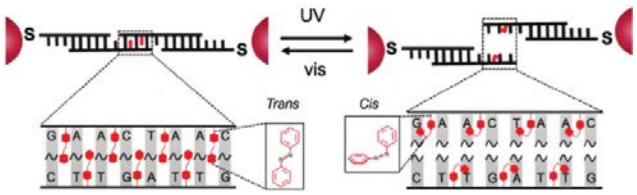

Figure 27. UV-Induced Disassembly of SNA Based Colloidal Crystals. Using UV/visible light cleaves/repairs strands on a SNA material. UV/visible light causes a reversible isomerization, whereby the trans position repairs DNA and the cis position cleaves DNA.

Patterning Colloidal Crystal Surfaces. Colloidal crystals form the basis for engineering novel optical and electronic elements, magnetic storage devices, and sensors.[1-3] There is, however, an unmet need for rapid, flexible, yet versatile methods to assemble complex colloidal crystal architectures with structural and functional characteristics precisely fine-tuned throughout the lattice. Our early proof-of-principle experiments suggest that the upgraded BPL platform along with the novel design of the colloidal crystals based on non-natural oligonucleotides could address this issue.

A promising method for assembling colloidal crystals into precise 2D and 3D structures is to graft metal (e.g., Au) nanoparticles with oligonucleotides and take advantage of sequence-specific hybridization.[4] The incorporation of azobenzene moieties, which can undergo reversable conformational transformations upon the exposure to UV (365 nm) and visible (460 nm) light, into the oligonucleotide links opens up the possibility of constructing light-responsive colloidal crystals (**Figure 27**). The light induced azobenzene conformational changes can introduce steric perturbations and trigger local dehybridization of oligonucleotide strands. The energy cost of light-induced conformational changes and the energy barrier of dehybridization can be precisely tuned by adjusting the sequence of the oligonucleotides, temperature at which the system is kept, and the number of incorporated azobenzene moieties. As such, this novel colloidal crystal system allows for temperature-controlled and light-directed erase and assembly of colloidal units from and into the crystal lattice, respectively.

To demonstrate the validity of this approach, a colloidal crystal lattice was first formed on a substrate out of gold nanoparticles (10-30 nm in diameter) interconnected with light-responsive DNA. The system was then heated close to its melting temperature (within 5 °C) to lower the energy barrier of dehybridization, followed by projecting a pattern with near-UV illumination to erase gold nanoparticles from the lattice in a precise, site-specific manner, leaving behind a 2D thin film colloidal crystal structure of a desired design.

Successful photopatterns of a crystalline thin film are shown in **Figure 28**. The upper left-hand side of the figure shows near-UV illumination being focused onto a substrate for DNA cleavage, reflecting off a DMD such that only the desired pattern is focused onto the substrate, thereby

resulting in DNA cleavage according to the desired pattern. Additionally, **Figure 28** also shows two successful DNA cleavage experiments, one of them is the Northwestern University seal (upper right-hand side) and the other one is the Northwestern University mascot (center bottom). The portions of the print that show up as lighter contrast, according to our microscopy measurements, are those parts of the DNA that have been cleaved away from the gold nanoparticle thin film. Scale bars in these images clearly show that the size of these features can be made as small as 15 μm over an ~ 600 μm scale, and finer microscope images (**Figure 28,** bottom left- and right-hand, respectively) clearly show the successful removal of light-sensitive DNA and their corresponding gold nanoparticles. It is worth noting that this feasibility study focused on validating the approach and used a lower resolution DMD patterning mode, but all the processes developed are compatible with our higher resolution BPL patterning mode.

Thus, this novel light-responsive chemistry based on non-natural oligonucleotides taken together with the newly developed technical capabilities of the BPL technology enables new opportunities for the design and fabrication of previously inaccessible active soft material structures and devices.

Facile Synthesis of Ultrahigh-Resolution Protein Micropatterns. Here, BPL is combined with cross-linking photopolymerization and thiol-acrylate coupling chemistry to provide a new, unparalleled means for printing biomolecular microarrays with ultrahigh resolution. Conventional strategies for producing functional bioactive microarrays (i.e., linear polymer synthesis) yield highly controllable polymer growth. However, relatively long reaction times (generally over 10 minutes) are required and chain-length limitations, due to the deactivation or embedding of the initiating ends, exist. In contrast, the BPL-based photoinduced cross-linking reaction of multifunctional acrylates proceeds more rapidly (in a few seconds) and thiol-modified target molecules (i.e., biotin and 6-mercaptohexanoic acid, MHA) can be incorporated simultaneously into the cross-linked network *via* thiol-acrylate coupling reactions (**Figure 29**). Furthermore, high-resolution protein microarrays (i.e., of streptavidin and/or fibronectin) can be achieved subsequently *via* streptavidin-biotin and MHA-fibronectin coupling reactions. By precisely controlling the UV dosage *via* the modulation of exposure time (seconds) and contact force (milli-newtons), BPL affords exquisite control over the photoreaction conditions on the substrate, thus making the photopolymerization and thiol-acrylate reactions highly tunable. This nanolithographic method enables the fabrication of nanoscale functional polymer

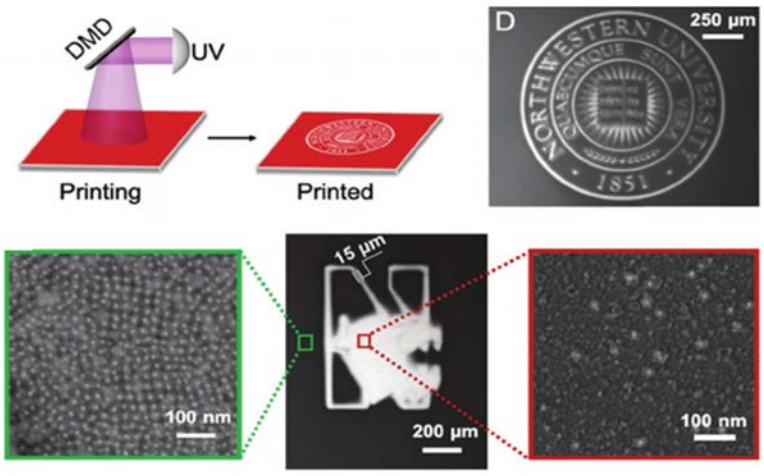

Figure 28. Photopatterning of crystalline thin films Using UV light and a DMD, a precise, arbitrary pattern can be focused onto a substrate covered with a thin film of photo-cleavable DNA. Prints were made on the cm scale with features as small as 15 μm. The green outlined image shows areas where photo-cleaving did not take place, and the red outlined image shows areas where photo-cleaving successfully took place as desired.

features (resolution < 300 nm) over large printing areas (3.84 mm × 5.12 mm), making these protein micropatterns adaptable for numerous applications. The BPL-printed bioactive polymers exhibit high protein binding affinity, and the amount of immobilized protein can be controlled based on photopolymer growth. Lastly, the addressability of the individual BPL probes allows the generation of arbitrary arrangements of 2D features while maintaining sub-diffraction resolution.

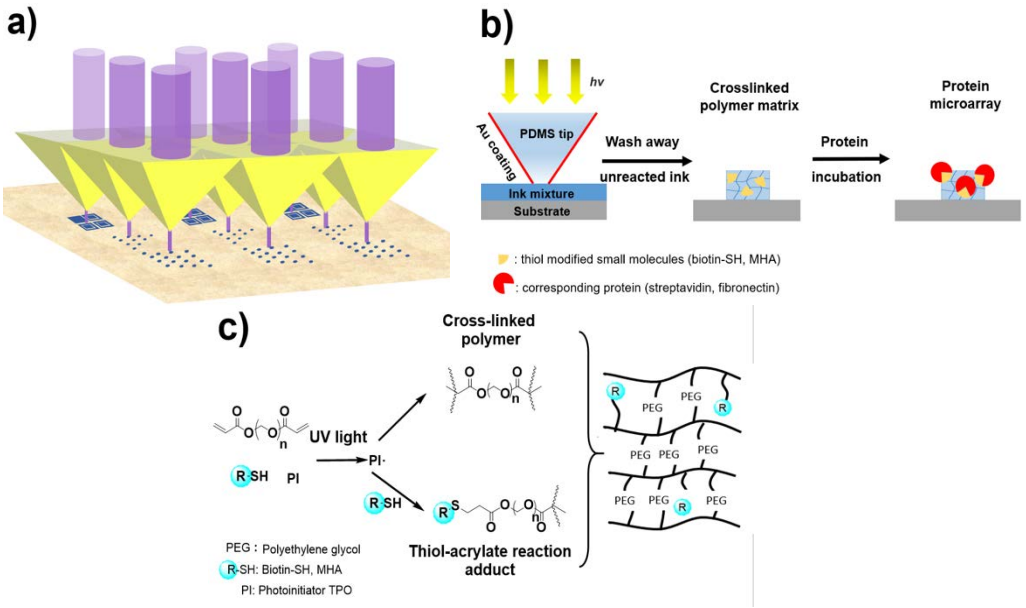

Figure 29. **(a)** Schematic of BPL-controlled, high-resolution printing on a surface. UV light passing through the apertures of the pyramid-like pens locally exposes the pre-polymer ink material, and the photoreaction progress is precisely controlled to form arbitrary patterns. **(b)** Schematic of BPL-controlled photopolymer printing and protein immobilization. **(c)** Reaction scheme of BPL-induced cross-linked network formation. UV light emitted from the tips during BPL induces the cleavage of photoinitiator diphenyl(2,4,6-trimethylbenzoyl) phosphine oxide (TPO) to release radical species for (i) initiating the homopolymerization of poly(ethylene glycol) diacrylate (PEGDA) and forming a cross-linked network as a scaffold, (ii) simultaneously triggering a radical-mediated thiol-acrylate coupling reaction and (iii) incorporating target binding, thiolated molecules (e.g., thiol-PEG-biotin, MHA) into the polymer matrix.

In a typical experiment, a TPO, PEGDA, and a thiol-PEG-biotin photopolymerization system was used and subsequently fluorescently labeled streptavidin was employed to create ultra-high resolution protein patterns. Due to its high stability and binding specificity, thiol-PEG-biotin was implemented as the target-binding species during lithographic printing. Before BPL printing, the gold surface was passivated using poly (ethylene glycol) methyl ether thiol (PEG) to minimize the non-specific binding of proteins (or cells) to the non-patterned areas.[5] A pre-polymer ink composed of TPO, PEGDA, and thiol-PEG-biotin (0.2 g/L, 21.2 g/L, and 1 g/L, respectively) was dissolved in NN-dimethylformamide (DMF) and then spin-coated onto the PEG-treated gold surface to form a uniform pre-polymer layer. The BPL pen array was prepared and mounted on a scanning probe system, equipped with hardware and software that allows advanced control over the patterning process (i.e., contact force in mN), exposure time, light intensity, and feature spacing). Illumination via BPL initiates the photo cross-linking of the PEGDA by repeatedly bringing the pen arrays into contact with the ink material on the surface (405 nm UV light, 90 mW/cm^2, dwell times: 0.2 to 3 s, printing force: 200 to 1,500 mN). After BPL printing, the surfaces were subsequently washed with acetone, ethanol, and Nanopure water to remove unreacted ink.

When an exposure time of 0.5 s was used, uniform 4 × 4 dot features (average diameter of 367 ± 21 nm) were patterned on the TPO, PEGDA, and thiol-PEG-biotin mixture. (**Figure 30a**). This biotin/polymer microarray was incubated in a PBS solution of fluorescently labeled streptavidin (20 µg/mL, 30 minutes), and the resultant protein pattern was evaluated using confocal microscopy (**Figure 30b**). As expected, the amount of attached streptavidin increases as concentration of thiol-PEG-biotin is increased from 0.02 mM to 3.12 mM (in DMF) within the polymer network (as the thiol-PEG-biotin concentration in DMF is increased from 0.02 mM to 3.12 mM).

BPL can be used to spatiotemporally control not only the morphologies of the features composed of polymers and thiolated moieties, but also the attachment of the corresponding binding proteins through the tuning of the UV exposure conditions. Using an ink material composed of TPO, PEGDA, and thiol-PEG-biotin (0.2 g/L, 21.2 g/mL, and 1g/mL in DMF, respectively), 10 × 10 gradient polymer features were printed using exposure times ranging from 0.2 s to 2 s (**Figure**

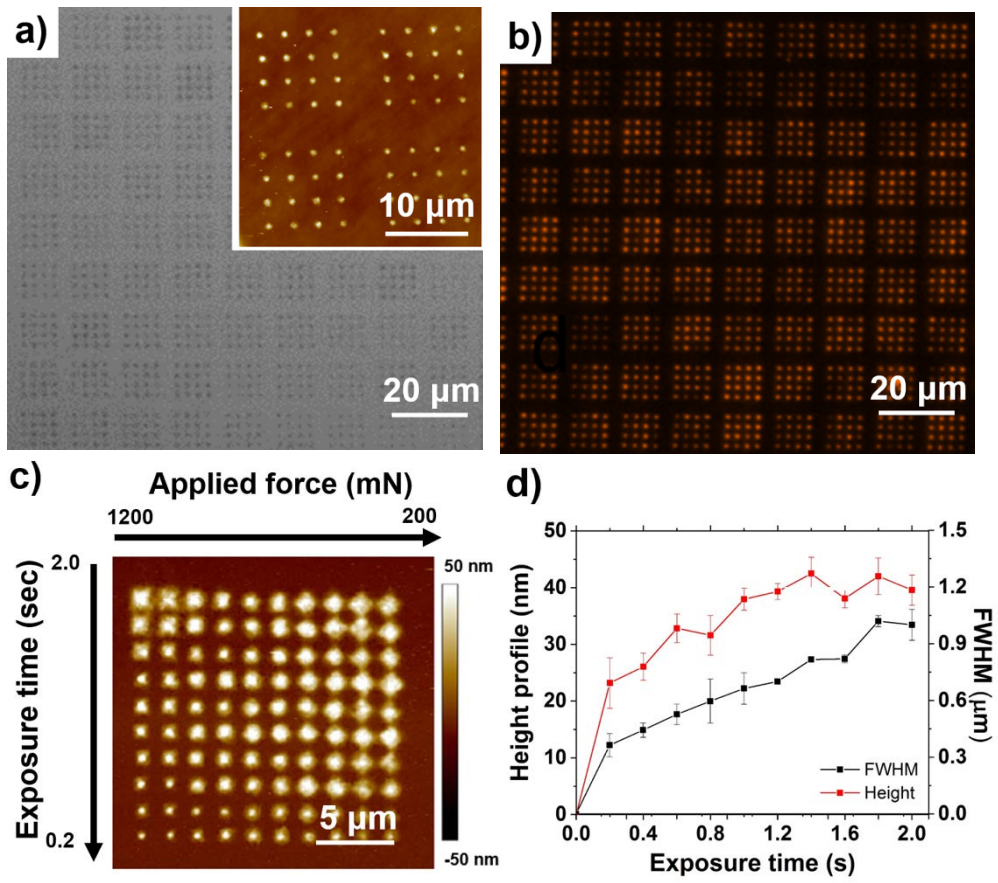

Figure 30. (a) Optical microscopy image of BPL-printed biotin containing cross-linked polymer patterns showing a representative area of ~10,000 duplicates of 4 × 4 dot features, using 0.5 s of 90 mW/cm^2 UV exposure and 800 mN of applied force. The inset shows an AFM image of the polymer pattern, and the average feature diameter was measured to be 367 ± 21 nm. (b) A fluorescence microscopy image of a biotin-containing array treated with fluorescently labeled streptavidin (streptavidin−Cy3), showing uniform immobilization of the protein on a BPL-printed pattern. (c) AFM image of BPL-printed 10 × 10 cross-linked polymer features, using dwell times (y-axis) of 0.2, 0.4, 0.6, 0.8, 1.2, 1.4, 1.6, 1.8, 2.0 s and printing forces of 200, 300, 400, 500, 600, 700, 800, 900, 1000, 1100, 1200 mN. (d) The evolution of the feature height and full width at half maximum (FWHM) of the BPL-printed polymer as a function of exposure time at a printing force of 1,200 mN.

31a). Based on the aforementioned morphology-control experiment (**Figure 30c**), a moderate printing force of 900 mN was applied here to acquire efficient control over the printed features. The normalized fluorescence intensity, calculated as the peak fluorescence divided by the baseline fluorescence, was used to quantify the amount of protein attachment. The normalized fluorescence intensity, calculated as the peak fluorescence divided by the baseline fluorescence, was used to understand the amount of protein attachment. After sufficient solvent wash and fluorescent protein treatment, a gradient of streptavidin patterns was obtained with normalized fluorescence intensity increasing from 2.4 ± 0.2 to 10.0 ± 0.7 with increasing UV exposure time was observed (**Figure 31b**). These data indicate that BPL can be used to precisely control the amount of immobilized protein within each printed feature. This feature makes the presented biopatterning technique attractive and enabling for many applications in functional biochips synthesis, antibody/peptide detection and screening, and cell biological studies.

In addition to biotin/streptavidin arrays, other types of protein nanoscale patterns can also be achieved using the appropriate thiol-binding species in this lithographic system. As a proof-of-concept, rhodamine-labeled fibronectin was immobilized on BPL-printed PEGDA/6-mercaptohexanoic acid (MHA) polymer patterns. First, the surface was passivated with PEG, and then TPO, PEGDA, and MHA (0.2 g/L, 21.2 g/L, and 0.8 g/L, respectively) were mixed as a pre-polymer ink and spin-coated on a gold substrate before BPL printing (force 900 mN, exposure time 0.8 s). After removing the unreacted ink and incubating with fluorescently tagged fibronectin, high-resolution fibronectin features with an average diameter of 810 ± 40 nm were generated and analyzed using confocal microscopy (**Figure 31c**). Fibronectin is an extracellular matrix (ECM) protein that is often used for the immobilization of cells on a surface. Indeed, single cells were attached to the individual micropatterns. However, in some cases, multiple cells attached to the individual micropatterns, and non-specific binding was observed.

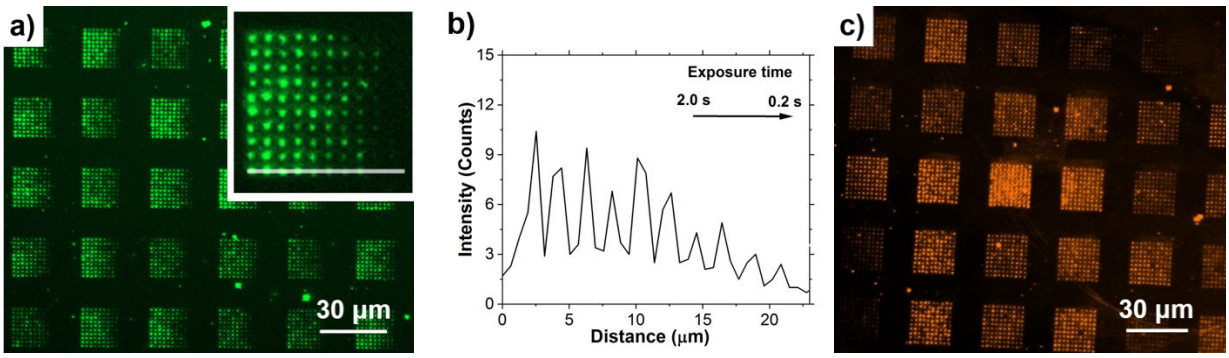

Figure 31. (a) Fluorescence image of a fluorescently labeled streptavidin (Streptavidin−Cy3) array printed on the pattern prepared using BPL with a constant force of 900 mN and illumination times of 0.2, 0.4, 0.6, 0.8, 1.0, 1.2, 1.4, 1.6, 1.8, and 2.0 s (increasing from right to left). The inset shows a 10 × 10 gradient array printed by a single pen. (b) Normalized fluorescence intensity profile of the features printed with different exposure times indicated by the white line in (a). (c) Fluorescence microscopy image of MHA-containing polymer pattern treated with fluorescently labeled fibronectin (rhodamine fibronectin), showing the attachment of fibronectin on the BPL-printed micropattern.

Previous reports describe how polymer pen lithography (PPL) can be used to pattern fibronectin to control focal adhesions and influence stem cell fate.[6] However, PPL cannot be used to modulate the micropattern design created by each pen and adjust protein density between or within the micropatterns as can be done with BPL. Furthermore, other studies point out that the implementation of PEG in biomaterials prolongs the circulation of proteins and peptides without compromising their bioactivity.[7] So, advantageously, this system could be used to control the 3D morphology of a polymer-based fibronectin pattern as well as its mechanical properties, serving as a tool for the preparation of arbitrary bioactive arrays that mimic the cellular microenvironment for the study and control of cell motility, differentiation, and organization.[8]

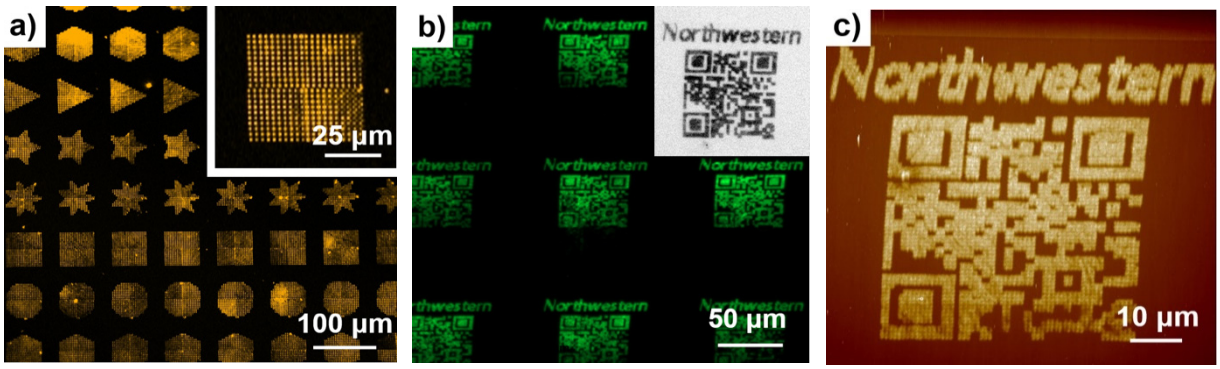

Figure 32. (a) Fluorescence microscopy image of fluorescently labeled streptavidin (streptavidin−Cy3) arrays of varied shapes (e.g., triangle, square, hexagon) printed by BPL. Inset shows a square pattern formed by dot features printed using a single tip. (b) Fluorescence microscopy image of "QR code" patterns generated after treatment with fluorescently labeled streptavidin. Inset shows the optical microscopy image of "QR code" printed by a single tip. (c) AFM image of the polymer pattern printed by an individual tip showing a continuous pattern formed by a pixel size of 830 ± 70 nm.

Conventional contact printing techniques, which are limited by directing cantilevers, are most often used to generate simple dot or line features in a restricted printing area. In contrast, BPL allows one to make arbitrary patterns using massively parallel and individually addressable pens. As a proof-of-concept, fluorescently tagged streptavidin microarrays with different pattern designs (e.g., triangles, squares, and hexagons, consisting of dot features with an average diameter of 750 ± 50 nm) were fabricated using actuated BPL. A pre-polymer ink, composed of TPO, PEGDA, and thiol-PEG-biotin, was photopolymerized within 50 × 50 µm regions using BPL (force 900 mN, dwell time 0.8 s, exposure intensity 72 mW/cm^2). After the removal of the unreacted ink, the system was incubated with Cy3-labeled streptavidin, and the protein patterns were developed (**Figure 32a**). Moreover, the BPL tool's advanced software automatically synchronizes the precise piezo movement of the sample relative to the BPL tip array, projected light pattern at each piezo position, and the light exposure once a desired image to be patterned is uploaded. As a result, BPL allows one to arbitrarily generate continuous features and therefore print micropatterns with more complicated designs. For example, a QR code to the Mirkin group website (https://mirkin-group.northwestern.edu/) with a size of 50 × 50 µm^2 was printed (**Figure 32b**). The resulting pattern was evaluated by AFM, and a continuous polymer pattern was formed with an individual pixel size of 830 ± 70 nm (**Figure 32c**).

Concluding Remarks

The research efforts and results presented here by Northwestern University (Mirkin Group) and TERA-print, LLC are the culmination of a multi-year investment to realize the ability to create arbitrability complicated, spatiotemporally actuated, 2D and 3D 'smart' nanostructures with physical and chemical functionalities dispersed throughout said structures. By using TERA-print's BPL technology, we were able to synthesize various soft-material structures with functionalities that were both nanoscopic in precision and as widespread as the whole mesoscopic structure. By adapting the technology to include a microfluidics sample holder with the ability to precisely control temperature, humidity, and near-UV light exposure, the TERA-print team provided a complete solution to enable TERA-Fab BPL technology to access and functionalize as wide a variety of soft material chemistries as possible,. The NU team used the solutions engineered by TERA-print to explore, modify, and construct 2D and 3D actuated nanostructures, accessing materials ranging from a post-polymerization functionalization method of tethering oligonucleotides to hydrogels, evaluating a photocurable polymeric system which was subsequently utilized to build 2D architectures with submicron precision, and investigating the properties of the photocured material and its application in functional small molecule surface writing was explored. Additionally, the NU team combined cross-linking photopolymerization and thiol-acrylate coupling chemistry to print biomolecule microarrays with ultrahigh resolution, and both teams highlighted the ability to engineer and pattern light-responsive colloidal crystals. Overall, the technical advantages of BPL (high-throughput, nanoscale precision, feature size and geometry modulated by light exposure and, tip-on-substrate force, etc.) were shown to be highly advantageous to synthesize nanostructures with the wide variety of chemical and physical functionalities presented in this report. Critically, the combined research efforts of Northwestern University and TERA-print, LLC have brought the goal of widespread access to facile printing of 2D and 3D 'smart' nanostructures with precisely controlled spatiotemporal functionalities much closer to realization, demonstrating that BPL TERA-Fab technology is not only well-suited to the immediate research challenges addressed in this report, but is integral for further progress to take place in the field of multi-functional nano-fabrication.

References

1. Urban, J. J., Talapin, D. V., Shevchenko, E. V., Kagan, C. R. & Murray, C. B. Synergism in binary nanocrystal superlattices leads to enhanced p-type conductivity in self-assembled PbTe/Ag2Te thin films. *Nature Materials* **6**, 115-121, doi:10.1038/nmat1826 (2007).
2. Auyeung, E. *et al.* Controlling Structure and Porosity in Catalytic Nanoparticle Superlattices with DNA. *Journal of the American Chemical Society* **137**, 1658-1662, doi:10.1021/ja512116p (2015).
3. Chen, J. *et al.* Collective Dipolar Interactions in Self-Assembled Magnetic Binary Nanocrystal Superlattice Membranes. *Nano Letters* **10**, 5103-5108, doi:10.1021/nl103568q (2010).
4. Zhu, J. *et al.* Light-Responsive Colloidal Crystals Engineered with DNA. *Advanced Materials* **32**, 1906600, doi:10.1002/adma.201906600 (2020).
5. Chandradoss, S. D. *et al.* Surface Passivation for Single-molecule Protein Studies. *JoVE*, e50549, doi:10.3791/50549 (2014).

6. Giam, L. R. *et al.* Scanning probe-enabled nanocombinatorics define the relationship between fibronectin feature size and stem cell fate. *Proceedings of the National Academy of Sciences* **109**, 4377, doi:10.1073/pnas.1201086109 (2012).
7. Lu, X., Perera, T. H., Aria, A. B. & Callahan, L. A. S. Polyethylene glycol in spinal cord injury repair: a critical review. *J Exp Pharmacol* **10**, 37-49, doi:10.2147/JEP.S148944 (2018).
8. Wu, J. *et al.* Binding characteristics between polyethylene glycol (PEG) and proteins in aqueous solution. *Journal of Materials Chemistry B* **2**, 2983-2992, doi:10.1039/C4TB00253A (2014).
9. Huo, F. *et al.* Beam pen lithography. *Nature Nanotechnology* **2010**, 637-640, doi:10.1038/nnano.2010.161.

SUPPORTED PERSONNEL

Prof. Chad Mirkin (2% Academic months, 2% summer months, PI, NU)
Dr. Xinpeng Zhang (25%, postdoctoral fellow, NU)
Dr. Alex Anderson (31%, postdoctoral fellow, NU)
Namrata Ramani (50%, graduate student, NU)
EunBi Oh (29%, graduate student, NU)
Dr. Andrey Ivankin (49.91%, TERA-print, CTO)
Dr. Shaowei Ding (24.33%, TERA-print, Research Scientists)
Dr. Kyle Justus (12.32%, TERA-print, Research Scientists)
Dr. Will Hutson (79.84%, TERA-print, Research Engineer)
Jared Magoline (14.63%, TERA-print, Research Scientists)